AD-A179 858 VISID/INVISCID SEPARATED FLOWS(U) MCDONNELL AIRCRAFT CO 1/1
ST LOUIS MO T CEBECI ET AL JUL 86 MDC-J3968
AFWAL-TR-86-3048 F33615-83-C-3026

UNCLASSIFIED F/G 20/4 NL

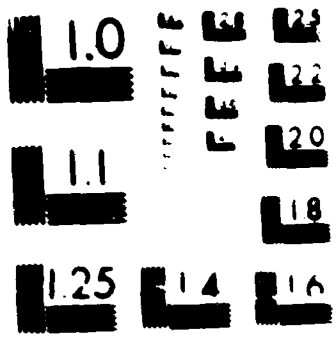
1.0
1.1
1.25
1.4
1.6
1.8
2.0
2.2
2.5

DTIC FILE COPY

AFWAL-TR-86-3048

AD-A179 858

VISCID/INVISCID SEPARATED FLOWS

T. Cebeci
K.C. Chang
R.W. Clark
D.P. Mack
S.M. Schimke

McDonnell Aircraft Company
McDonnell Douglas Corporation
P.O. Box 516
St. Louis, Missouri 63166

DTIC ELECTE APR 28 1987 S D D

JULY 1986

Final Report for Period September 1983 - March 1986

Approved for Public Release; Distribution Is Unlimited

FLIGHT DYNAMICS LABORATORY
AIR FORCE WRIGHT AERONAUTICAL LABS
AIR FORCE SYSTEMS COMMAND
WRIGHT-PATTERSON AIR FORCE BASE, OHIO 45433-6553

87 4

NOTICE

When Government drawings, specifications, or other data are used for any purpose other than in connection with a definitely related Government procurement operation, the United States Government thereby incurs no responsibility nor any obligation whatsoever; and the fact that the Government may have formulated, furnished, or in any way supplied the said drawings, specifications, or other data, is not to be regarded by implication or otherwise as in any manner licensing the holder or any other person or corporation, or conveying any rights or permission to manufacture, use, or sell any patented invention that may in any way be related thereto.

This report has been reviewed by the Office of Public Affairs (ASD/PA) and is releasable to the National Technical Information Service (NTIS). At NTIS, it will be available to the general public, including foreign nations.

This technical report has been reviewed and is approved for publication.

Albert J. Murn
Albert J. Murn
Project Engineer

Bohdan G. Kunciw
Bohdan G. Kunciw, Maj, USAF
Chief, Aerodynamics and Airframe Branch
Aeromechanics Division

FOR THE COMMANDER

DONALD A. DREESBACH, Colonel, USAF
Chief, Aeromechanics Division
Flight Dynamics Laboratory

Copies of this report should not be returned unless return is required by security considerations, contractual obligations, or notice on a specific document.

UNCLASSIFIED

SECURITY CLASSIFICATION OF THIS PAGE

ADA179858

REPORT DOCUMENTATION PAGE

1a. REPORT SECURITY CLASSIFICATION: Unclassified	1b. RESTRICTIVE MARKINGS
2a. SECURITY CLASSIFICATION AUTHORITY	3. DISTRIBUTION/AVAILABILITY OF REPORT: Approved for public release; distribution is unlimited.
2b. DECLASSIFICATION/DOWNGRADING SCHEDULE	
4. PERFORMING ORGANIZATION REPORT NUMBER(S): MDC J3968	5. MONITORING ORGANIZATION REPORT NUMBER(S): AFWAL-TR-86-3048
6a. NAME OF PERFORMING ORGANIZATION: McDonnell Aircraft Company; 6b. OFFICE SYMBOL (If applicable)	7a. NAME OF MONITORING ORGANIZATION: AF Wright Aeronautical Labs (AFWAL/FIMM)
6c. ADDRESS (City, State and ZIP Code): P.O. Box 516, St. Louis, Missouri 63166	7b. ADDRESS (City, State and ZIP Code): Wright-Patterson Air Force Base, Ohio 45433-6553
8a. NAME OF FUNDING/SPONSORING ORGANIZATION; 8b. OFFICE SYMBOL (If applicable)	9. PROCUREMENT INSTRUMENT IDENTIFICATION NUMBER: F33615-83C-3026
8c. ADDRESS (City, State and ZIP Code)	10. SOURCE OF FUNDING NOS.

PROGRAM ELEMENT NO.	PROJECT NO.	TASK NO.	WORK UNIT NO.
62201F	2404	10	81

11. TITLE (Include Security Classification): Viscid/Inviscid Separated Flows

12. PERSONAL AUTHOR(S): T. Cebeci, K.C. Chang, R.W. Clark, D.P. Mack, S.M. Schimke

13a. TYPE OF REPORT	13b. TIME COVERED	14. DATE OF REPORT (Yr., Mo., Day)	15. PAGE COUNT
Final	FROM SEP 83 TO MAR 86	July 1986	88

16. SUPPLEMENTARY NOTATION

17. COSATI CODES		
FIELD	GROUP	SUB. GR.
04	02	
01	03	

18. SUBJECT TERMS (Continue on reverse if necessary and identify by block number): Separated Flow; Viscid/Inviscid Interactions; Interactive Boundary Layer Theory; Wing-Body Geometry; Boundary Layer; Subsonic Flow

19. ABSTRACT (Continue on reverse if necessary and identify by block number)

A method has been developed for calculating subsonic three-dimensional flows over fighter aircraft configurations at flow conditions including separation. The method employs a viscid inviscid interaction approach, with a panel method used for the inviscid analysis and a finite difference boundary layer method for the viscous analysis. The viscid and inviscid analyses are coupled using an interactive technique based on inverse boundary layer theory. This approach allows efficient calculation of flows with large separation regions, including both leading and trailing edge separations.

The method was validated on three fighter aircraft geometries and comparisons with test data are presented.

20. DISTRIBUTION/AVAILABILITY OF ABSTRACT: UNCLASSIFIED/UNLIMITED ☒ SAME AS RPT. ☐ DTIC USERS ☐	21. ABSTRACT SECURITY CLASSIFICATION: Unclassified
22a. NAME OF RESPONSIBLE INDIVIDUAL: Albert J. Murn	22b. TELEPHONE NUMBER (Include Area Code): 513/255-4052; 22c. OFFICE SYMBOL: AFWAL/FIMM

DD FORM 1473, 83 APR EDITION OF 1 JAN 73 IS OBSOLETE

UNCLASSIFIED

SECURITY CLASSIFICATION OF THIS PAGE

FOREWORD

This report was prepared for the United States Air Force by the Douglas Aircraft Company, Long Beach, California, and the McDonnell Aircraft Company, St. Louis, Missouri in partial fulfillment of Contract Number F33615-83-C-3026. This report describes a method for calculating the flowfield about fighter aircraft geometries in the presence of flow separation, and includes comparisons with test data for three fighter configurations.

The contract was under the direction of Mr. Albert J. Murn of the Air Force Flight Dynamics Laboratory, Wright-Patterson Air Force Base, Ohio. His efforts and forbearance are gratefully acknowledged.

TABLE OF CONTENTS

Page

LIST OF ILLUSTRATIONS

SECTION I
INTRODUCTION

In past years aircraft configuration design was accomplished mainly by wind tunnel testing while flow-calculation methods contributed little because they were limited to simple geometries and restricted in the physical processes that they represented. This virtually exclusive reliance on testing had disadvantages which led to less-than-optimum designs. Each potential configuration had to be fabricated as a wind tunnel model with corresponding expense and time delay and, if the tests suggested design changes, the process should have been repeated, though on occasions this could not be done because of the time and expense involved in an iteration cycle. Moreover, tests provide incomplete information in that, for example, static-measurements may be restricted to a small number of locations. Force and moment data are seldom explained in terms of flow phenomena and the extent of separated regions is usually not determined. Finally, there is the necessary scaling from model to full-scale vehicle which can be uncertain so that, for example, separation observed on a model may be different from that encountered in full scale.

Intensive efforts have been pursued for many years to help to overcome the limitations of calculation methods and to develop them to represent accurately the flows over airplane configurations. Regardless of the specific algorithm employed, the cost and especially the elapsed time required to develop a numerical representation of a given configuration is much less than that required for an experimental test. Once such a basic numerical model has been developed, many variations on the design can be investigated computationally and only the most promising selected for wind-tunnel testing. A flow computation method is required to represent the geometry of the airplane and the essential properties of the fluid and, to achieve the objective, limitations of calculation methods have been removed in recent years by the development of new and powerful calculation tools.

There are three possible approaches which can be used for the calculation of the viscous flow over an aircraft configuration. The first approach makes use of the Reynolds-averaged Navier-Stokes equations and various reduced forms including the so-called parabolized and thin-layer Navier-Stokes equations. Significant advances have been made in this area, for example, by Shang and

Scherr [1] who made the first attempt to numerically simulate the flowfield around a complete aircraft by solving the Navier-Stokes equations. To demonstrate the feasibility of their approach, they chose the hypersonic research aircraft X24C-10D for which a detailed experimental database exists. Using a mesh system around 5×10^5 nodes, they performed impressive calculations at an angle of attack of six degrees with a nominal Mach number of 5.95, and indicated areas where future research should concentrate to make this approach more efficient and practical.

The second and third approaches both make use of solutions of inviscid and viscous flow equations coupled by special procedures. The second approach is based on the two-dimensional method developed by Gilmer and Bristow [2] in which an empirical inviscid flow model is used to represent the effects of flow separation [2,3]. A direct boundary-layer calculation is employed up to the point of separation. Downstream of this point, a free surface is introduced to model the separated flow region. The shape and the length of the separation zone are computed by satisfying a constant pressure boundary condition on the surface and very good results have been obtained for airfoils at a wide range of angles of attack including stall.

The third approach, which is referred to as the interactive boundary-layer approach, uses special coupling techniques between inviscid and viscous flows and novel numerical procedures. The particular form developed by Cebeci et al. [4] is very general and allows any inviscid flow method to be coupled with solutions of the boundary-layer equations. For example, in its application to two-dimensional subsonic flows over airfoils, it employs Halsey's inviscid procedure [5] based on the conformal mapping and Fourier analysis techniques and computes the flow over the airfoil and wake. Successive viscous sweeps are performed, after each of which the external inviscid solution is recomputed, until a converged solution is obtained. The boundary-layer method, which is an inverse finite-difference scheme developed by Cebeci [6], uses an algebraic eddy-viscosity formulation due to Cebeci and Smith [7] and is able to compute flows with large regions of separation without numerical problems. In regions of reverse flow, it uses the FLARE approximation [8] in which the streamwise convective term is set equal to zero in the recirculating region. A detailed description of the method and of its application to a range of airfoils at angles of attack up to and including stall is provided in [4]. The results presented in Section 3.1 show that this procedure has removed a major obstacle in that flows with large regions of separation can now be computed accurately.

A comparison between the interactive procedure [4] and a method based on the thin-Navier-Stokes equation has been reported in [9] for the NACA 0012 airfoil. This study demonstrated that the Navier-Stokes approach and the interactive boundary-layer approach gave comparable results up to the stall angle. However, the interactive boundary-layer approach required much less computing time.

The purpose of the present work is to develop a general method for computing three-dimensional flows on wings with leading- and trailing-edge separation. The second and third approaches, described above, have been critically examined to determine the extent to which they can fulfill this purpose. It was considered that the second approach should be more suited to large regions of trailing-edge separation whereas the third approach should be more appropriate for leading-edge separation bubbles. Extensive tests showed that the second approach failed to converge in those situations for which it was intended and, although it was satisfactory for flows with small trailing-edge separation, considerable effort may still be required to overcome its limitations. The third approach on the other hand, has proved to be able to represent leading- and trailing-edge separation without limitations, as discussed further in Section 3.0.

The remainder of this report has been arranged in five sections. In Section 2.0, the inviscid method is briefly described prior to more extensive descriptions of interactive boundary-layer methods based on strip theory and quasi-three-dimensional approximations. The viscous-flow equations, transformations and solution procedure have been described previously in [4] for two-dimensional flows and in [10] for quasi-three-dimensional flows. Results obtained with these procedures are presented in Section 3.0 for several configurations and the relative merits of the two interactive approaches are considered. The computer program, which embodies both methods is described in Section 4.0 and sample input data for the three contract test cases are presented in Section 5.0. The report ends with a summary of the more important conclusions in Section 6.0.

SECTION II

DESCRIPTION OF THE INTERACTIVE BOUNDARY-LAYER METHODS

The method described here combines inviscid flow and inverse boundary layer procedures in an interactive manner which permits the calculation of flows with leading and trailing-edge separation. According to this method, the inviscid method of Section 2.1 is used to compute the flow over the given configuration with a zero normal velocity boundary condition. The resulting pressure distribution serves as a boundary condition for the boundary layer method of Section 2.2 which computes all relevant boundary layer parameters, including a surface blowing distribution to simulate the displacement thickness effect. While the inviscid-flow calculations (see Section 2.1) are performed for the entire configuration, viscous-flow calculations are presently restricted to the wing and make use of strip-theory and quasi three dimensional approximations discussed in Section 2.2.

The viscous effects computed by the boundary-layer method are then used to determine a distribution of normal velocity on the surface. The inviscid flow method is used for a second time with this blowing velocity distribution as a boundary condition and the procedure is repeated until convergence.

2.1 Inviscid Flow Method

The inviscid flow method, which is the first-order surface-source panel method developed by Hess, is capable of computing flow about completely arbitrary configurations. Because of its robustness and its availability, it has been acquired by several dozen facilities around the country and applied not only to aircraft but also to ships, submarines, automobiles, buildings, and topographical features. The three-dimensional body is represented by a set of plane quadrilateral panels, as shown in Fig. 1*. A three-dimensional body consists of lifting and nonlifting portions. A lifting portion, such as a wing or pylon, is characterized by having a well-defined trailing edge, from which issues a trailing vortex wake and along which the Kutta condition is applied. Nonlifting portions of the body lack such trailing edges. Every panel has a constant value of source strength σ. Panels of lifting portions have, in addition, a quadratically varying doublet strength μ. Values of source

---

*Figures begin on page .

density on the panels are independent parameters available for satisfying the boundary condition. The chordwise dipole variation over the panels of a lifting strip (Fig. 1) is assumed in a form that leads to favorable numerics, so that the dipole strength is reduced to a single adjustable parameter - the circulation on that strip. Thus the set of independent dipole parameters equals the number of locations where the Kutta condition is enforced, i.e., at the trailing-edge segment of each strip.

The nature of the Kutta condition adopted by the many panel methods which are currently available varies greatly. The condition adopted by Hess [11] is the physically meaningful condition of equal upper and lower surface pressures at the trailing edge. All other methods make use of other derived conditions, e.g. a prescribed flow direction a short distance downstream, which do not guarantee a pressure match at the trailing edge. For instance, Margason et al. [12] showed that pressure mismatches of up to half of the freestream dynamic pressure could occur from such alternate forms of the Kutta condition. Figure 2, which is taken from [12] shows this clearly. Since we are interested in the computation of flows for which the behavior of the boundary layer at the trailing edge can have a significant effect on the overall flow solution, it is believed that the approach adopted here is more realistic.

The computational procedure is as follows. On each panel a control point is selected where the normal-velocity boundary condition is applied and where velocity and pressure are eventually calculated. Using the well-known point-source potential, the velocity induced by the source density on a panel at a point in space is

$$\vec{v}(\text{panel}) = [\iint_{\text{panel}} \text{grad}(1/r)dS]\sigma(\text{panel}) \tag{2.1}$$

where the constant value of σ has been taken outside the integral whose value therefore depends only on geometry. Suppose N panels are used to define the body, and let σ_j denote the value of source density on the jth panel. The velocity induced by the jth panel at the control point of the ith panel is defined as $\vec{V}_{ij}\sigma_j$, where $\vec{V}_{ij}$ is an integral of the form of Eq. (2.1). The integral may be carried out analytically. Explicit formulas are contained in [11], but they are too lengthy for inclusion here. The corresponding normal velocity at the ith control point is

$$A_{ij}\sigma_j = \vec{n}_i \cdot \vec{V}_{ij}\sigma_j \tag{2.2}$$

where $\vec{n}_i$ is the unit normal vector to the ith panel. Applying the normal velocity boundary condition at all control points then yields the following set of linear algebraic equations:

$$\sum_{j=1}^{N} A_{ij}\sigma_j = -\vec{n}_i \cdot \vec{V}_\infty \tag{2.3}$$

This is the numerical approximation of the integral equation that expresses the zero normal-velocity boundary condition. Once the σ_j have been determined, the disturbance velocities at the control points due to the body are given by

$$\vec{v}_i = \sum_{j=1}^{N} \vec{V}_{ij}\sigma_j \qquad i = 1, 2, \ldots, N \tag{2.4}$$

While the addition of lift in two dimensions causes no significant increase in the complexity of the problem, the problem of three-dimensional lifting flow is not only considerably more complicated than nonlifting flow but requires assumptions that are somewhat arbitrary [11]. The main features are illustrated in Fig. 1. As mentioned above, wings or other lifting portions of the configuration are characterized by having trailing edges from which issue trailing vortex wakes. So-called bound circulation is hypothesized to lie on or within the wing surface, with strength varying in both the chordwise direction and in the direction parallel to the trailing edge ("spanwise" in aerodynamic jargon). The variation of the bound circulation in the chordwise direction is predetermined, while the spanwise variation is adjusted to satisfy a condition of smooth flow off the entire trailing edge, and the trailing vorticity has constant strength in the stream direction and an initial strength at the trailing edge equal to the local "spanwise" derivative of bound circulation strength. The location of the wake once it leaves the trailing edge is initially unknown, which introduces a nonlinearity into the problem. It is customary simply to assume a wake location, because in most problems the calculated results are not sensitive to the details of the wake shape. However, the location can be determined by iterating the calculation if necessary.

With regard to computing effort and cost, the two principal tasks associated with this method are calculation of the N^2 velocities $\vec{V}_{ij}$ and the solution of the set of linear equations, Eq. (2.3). Other portions of the calculation require comparatively negligible computing efforts. In three dimensional applications rather large numbers of panels are employed. Panel numbers over 3000 are common. These are the number of unknowns actually solved for after all symmetries, etc., have been utilized. Accordingly, it is economically important that all possible efficiencies be employed in carrying out the two principal tasks. For the first task this is accomplished by using simple approximate expressions for $\vec{V}_{ij}$ when computing the influence of distant panels [13]. The second task is speeded up by the use of block iterative matrix solutions, as developed by Clark [14]. The source method lends itself particularly well to these efficiencies, without which no three dimensional method is practical.

In updating the external inviscid velocity to account for the boundary layer displacement effects, two approaches can be considered. The first, known as the displacement surface approach, involves modifying the geometry to account for the boundary layer displacement thickness. The second approach is to introduce a blowing velocity on the surface of the original body so that the dividing stream surface of the inviscid flow approximates the displacement thickness computed by the boundary-layer procedure. While both approaches have been applied in our studies, the first approach has been found to be less suitable because it involves the computation of the inviscid flow past a body with a finite opening at the trailing edge. For separated flow, the size of this open trailing edge can become significant and the computation of the inviscid flow past such a body is nonunique unless some additional conditions are imposed along this trailing-edge opening. By adopting the surface blowing approach, the equivalent trailing edge thickness of the dividing stream surface is controlled by the blowing velocity introduced on the wing surface in a physically realistic way without resorting to additional boundary conditions.

The blowing velocity computed by the boundary-layer procedure is applied on the wing surface. However, as pointed out above, the aim is to model the flow past the displacement surface. For flows involving large trailing-edge separation, it has been shown in [4] that it is important to both evaluate the external inviscid pressure distribution and apply the Kutta condition on the displacement surface. In the present method this is achieved by introducing additional off body points corresponding to each control point for which the boundary layer distribution has been computed. These off body points are used both to compute the final pressure distribution and to apply the Kutta condition.

2.2 Interactive Viscous-Flow Method

An accurate prediction of the flowfield over a wing requires the calculation of flow on the surface and in the wake. The airfoil studies conducted in [4] indicate that the wake influence is negligible for airfoils at low angles of attack and that it is sufficient to calculate the flow on the airfoil only. In the case of the NACA 0012 airfoil, for example, the wake effect begins to become important for angles of incidence, α, greater than 10°, and is important at angles of incidence approaching stall, which for this airfoil is around 16° as shown in Fig. 3. The inclusion of the wake effect, which is not considered here, reduces the flow separation on the surface and allows the numerical calculations to be performed with less difficulty. In the present study, we investigate the ability of the interactive boundary-layer scheme to calculate flows with massive separation and perform calculations for configurations at high angles of attack, as discussed in Section 3.0.

2.2.1 Boundary-Layer Equations

The full three-dimensional boundary-layer equations and their boundary conditions may be written as the following nonorthogonal curvilinear coordinate system [10]:

Continuity Equation

$$\frac{\partial}{\partial x}(uh_2 \sin\theta) + \frac{\partial}{\partial z}(wh_1 \sin\theta) + \frac{\partial}{\partial y}(vh_1h_2 \sin\theta) = 0 \qquad (2.5a)$$

x-Momentum Equation

$$\frac{u}{h_1}\frac{\partial u}{\partial x} + \frac{w}{h_2}\frac{\partial u}{\partial z} + v\frac{\partial u}{\partial y} - \cot\theta\, K_1 u^2 + \csc\theta\, K_2 w^2 + K_{12}uw$$

$$= -\frac{\csc^2\theta}{\rho h_1}\frac{\partial p}{\partial x} + \frac{\cot\theta \csc\theta}{\rho h_2}\frac{\partial p}{\partial z} + \frac{\partial}{\partial y}\left(\nu\frac{\partial u}{\partial y} - \overline{u'v'}\right) \qquad (2.5b)$$

z-Momentum Equation

$$\frac{u}{h_1}\frac{\partial w}{\partial x} + \frac{w}{h_2}\frac{\partial w}{\partial z} + v\frac{\partial w}{\partial y} + \csc\theta\, K_1 u^2 - \cot\theta\, K_2 w^2 + K_{21} uw$$

$$= \frac{\cot\theta \csc\theta}{\rho h_1}\frac{\partial p}{\partial x} - \frac{\csc^2\theta}{\rho h_2}\frac{\partial p}{\partial z} + \frac{\partial}{\partial y}\left(\nu\frac{\partial w}{\partial y} - \overline{v'w'}\right) \tag{2.5c}$$

$$y = 0: \quad u,\ v,\ w = 0 \tag{2.6a}$$

$$y = \delta: \quad u = u_e(x,z), \quad w = w_e(x,z) \tag{2.6b}$$

Here x,z denote the coordinate system on the surface of the body and y is the actual distance measured normal to the surface. The boundary-layer equations and boundary conditions for this system according to first-order boundary-layer theory are based on the assumption that the pressure is constant across the shear layer and stress gradients in directions parallel to the surface are negligible compared with those normal to the surface. In the above equations h_1 and h_2 denote the metric coefficients and θ denotes the angle between the coordinate lines and, as a result of first-order boundary-layer theory, they are functions of the surface coordinates x and z only. They can be obtained from the relations which define the three-dimensional body in the Cartesian coordinate system $\bar{x},\bar{y},\bar{z}$ by

$$F(\bar{x},\bar{y},\bar{z}) = 0 \tag{2.7}$$

and those that define the curvilinear coordinate system. Thus the metric coefficients and the angle between θ are given by

$$h_1^2 = \left(\frac{\partial \bar{x}}{\partial x}\right)^2 + \left(\frac{\partial \bar{y}}{\partial x}\right)^2 + \left(\frac{\partial \bar{z}}{\partial x}\right)^2 \tag{2.8a}$$

$$h_2^2 = \left(\frac{\partial \bar{x}}{\partial z}\right)^2 + \left(\frac{\partial \bar{y}}{\partial z}\right)^2 + \left(\frac{\partial \bar{z}}{\partial z}\right)^2 \tag{2.8b}$$

$$\cos\theta = \frac{(\partial\bar{x}/\partial x)(\partial\bar{x}/\partial z) + (\partial\bar{y}/\partial x)(\partial\bar{y}/\partial z) + (\partial\bar{z}/\partial x)(\partial\bar{z}/\partial z)}{h_1 h_2} \tag{2.9}$$

The parameters K_1 and K_2 are known as the geodesic curvatures of the curves z = constant and x = constant, respectively, see Fig. 4, and are given by

$$K_1 = \frac{1}{h_1 h_2 \sin\theta} [\frac{\partial}{\partial x} (h_2 \cos\theta) - \frac{\partial h_1}{\partial z}] \tag{2.10a}$$

$$K_2 = \frac{1}{h_1 h_2 \sin\theta} [\frac{\partial}{\partial z} (h_1 \cos\theta) - \frac{\partial h_2}{\partial x}] \tag{2.10b}$$

The parameters K_{12} and K_{21} are defined by

$$K_{12} = \frac{1}{\sin\theta} [- K_1 - \frac{1}{h_1} \frac{\partial\theta}{\partial x} + \cos\theta \, (K_2 + \frac{1}{h_2} \frac{\partial\theta}{\partial z})] \tag{2.11a}$$

$$K_{21} = \frac{1}{\sin\theta} [- K_2 - \frac{1}{h_2} \frac{\partial\theta}{\partial z} + \cos\theta \, (K_1 + \frac{1}{h_1} \frac{\partial\theta}{\partial x})] \tag{2.11b}$$

The magnitude of the velocity vector u_t in the boundary layer is given by

$$u_t = (u^2 + w^2 + 2uw \cos\theta)^{1/2} \tag{2.12}$$

In the present study we use two reduced forms of the above boundary-layer equations. The first is referred to as the quasi-three-dimensional boundary-layer equations in which the flow variations with respect to z are neglected so that the equations become

$$\frac{\partial}{\partial x} (uh_2 \sin\theta) + \frac{\partial}{\partial y} (vh_1 h_2 \sin\theta) = 0 \tag{2.13a}$$

$$\frac{u}{h_1} \frac{\partial u}{\partial x} + v \frac{\partial u}{\partial y} - K_1 u^2 \cot\theta + K_2 w^2 \csc\theta + K_{12} uw = - \frac{\csc^2\theta}{h_1 \rho} \frac{\partial p}{\partial x} + \frac{\partial}{\partial y} (\nu \frac{\partial u}{\partial y} - \overline{u'v'}) \tag{2.13b}$$

$$\frac{u}{h_1} \frac{\partial w}{\partial x} + v \frac{\partial w}{\partial y} + K_1 u^2 \csc\theta - K_2 w^2 \cot\theta + K_{21} uw = \frac{\csc\theta \cot\theta}{h_1 \rho} \frac{\partial p}{\partial x} + \frac{\partial}{\partial y} (\nu \frac{\partial w}{\partial y} - \overline{u'w'}) \tag{2.13c}$$

The second is referred to as the strip-theory approximation which essentially solves the well-known two-dimensional boundary-layer equations,

$$\frac{\partial u}{\partial x} + \frac{\partial v}{\partial y} = 0 \tag{2.14}$$

$$u \frac{\partial u}{\partial x} + v \frac{\partial u}{\partial y} = u_e \frac{du_e}{dx} + \frac{\partial}{\partial y} (\nu \frac{\partial u}{\partial y} - \overline{u'v'}) \tag{2.15}$$

In this approach, the streamwise external velocity u_e is replaced by the total velocity V defined by

$$V = (u_e^2 + w_e^2 + 2u_e w_e \cos\theta)^{1/2} \qquad (2.16)$$

and is assigned to each spanwise strip.

2.2.2 Interactive Scheme

It is well known that the boundary-layer equations are singular at separation when solved for a prescribed external velocity distribution. They are not singular at separation, however, when the external velocity is computed as part of the solution by, for example, prescribing a displacement thickness: this is known as the inverse problem and leads to solution of the boundary-layer equations with separation.

For flows with separation, the presence of the upstream velocity component introduces a numerical instability into the solution of the boundary-layer equations. Over the years, several approaches have been proposed to overcome this problem. One popular approach, known as the FLARE approximation after the originators, Flugge-Lotz and Reynher [8], neglects the longitudinal convection terms $u(\partial u/\partial x)$ and $u(\partial w/\partial x)$ in the momentum equations (2.5). This approximation is satisfactory provided that the size of the separated region remains small. However, as the size of the recirculation region increases, this approximation becomes less accurate and requires the development of additional procedures to account for the neglected convective terms. One successful scheme, which has been applied to two-dimensional flows, is referred to as the DUIT procedure [15, 16] (Downstream, Upstream Iteration) and requires several sweeps through the recirculation region. With this scheme, the FLARE approach is used to compute a solution within the recirculation region, and then in successive sweeps the $u(\partial u/\partial x)$ term is progressively introduced until it is fully represented. Another successful approach developed by Cebeci [17] makes use of the unsteady boundary-layer equations in which the convective term is introduced into the equations progressively as a function of time. The present method uses only the FLARE approach for both 2-D and quasi-3-D flows, and does not consider the effect of the terms neglected due to this approximation.

In an interactive boundary-layer scheme, a link between a displacement thickness and external flow is provided, and two types of procedures have been developed for this purpose for two-dimensional flows. In the first approach

[18-22], the solutions of the boundary-layer equations are computed initially for a prescribed external velocity to obtain an estimate of the displacement thickness $\delta^*(x)$ distribution, and then in an inverse mode for a specified displacement-thickness distribution $\delta^*(x)$. If this initial calculation encounters separation, $\delta^*(x)$ is extrapolated to the trailing edge. The subsequent boundary-layer calculations are then performed in an inverse mode to compute the blowing velocity needed in the inviscid flow method. In general, this procedure leads to two external velocity distributions, $u_{ev}(x)$ derived from the inverse boundary-layer solution and $u_{ei}(x)$ derived from the updated approximation to the inviscid velocity past the body with viscous effects. A relaxation formula in the form

$$\delta^{*\nu+1}(x) = \delta^{*\nu}(x) \left[1 + \omega \left(\frac{u_{ev}(x)}{u_{ei}(x)} - 1\right)\right], \quad \nu = 0, 1, 2, \ldots \tag{2.17}$$

where ω denotes a relaxation parameter, is then introduced to define an updated displacement thickness distribution and to obtain new solutions of the boundary-layer equations and the inviscid flow equations so that the interactive procedure between inviscid and viscous flow solutions can be iterated until convergence is achieved.

The second approach [23], which is recommended on the grounds of generality and physical basis, treats the external velocity $u_e(x)$ and the displacement thickness $\delta^*(x)$ as unknown quantities. The boundary-layer equations are solved simultaneously in an inverse mode and with successive sweeps over the body surface. For each sweep, the external boundary condition is written as the sum of the inviscid velocity $u_e^o(x)$ over the body, and a perturbation velocity $\delta u_e(x)$, that is,

$$y = \delta, \quad u_e(x) = u_e^o(x) + \delta u_e(x) \tag{2.18}$$

The perturbation velocity δu_e is computed from a local approximation based on a thin airfoil theory in terms of the local blowing velocity, $d/d\sigma\,(u_e\delta^*)$, required to simulate the boundary layer thickness. The perturbation velocity is written as

$$\delta u_e(x) = \frac{1}{\pi} \int_{x_a}^{x_b} \frac{d}{d\sigma} (u_e\delta^*) \frac{d\sigma}{x - \sigma} \tag{2.19}$$

where the interaction region is confined to $[x_a, x_b]$. Introducing a discrete approximation for this integral enables the perturbation velocity to be expressed in terms of the geometric coefficients of the airfoil, as discussed in [4].

This two-dimensional interactive procedure has recently been extended under an AFOSR contract [10] to the quasi-three-dimensional equations referred previously. The relationship between displacement thickness and external velocity needed in the interactive calculations was obtained by generalizing the formulation used for two-dimensional flows. The irrotationality condition, which for an orthogonal system is

$$\frac{\partial}{\partial x}\,[h_2(w_e^o + \delta w_e)] = [\frac{\partial}{\partial z}\,h_1(u_e^o + \delta u_e)] \tag{2.20}$$

was used to provide a relationship between the two velocity components u_e and w_e and shows that the choice of computing the perturbation velocities due to viscous effects is not arbitrary. The assumption that $\delta u_e(x)$ is a function of x alone requires that

$$\frac{\partial}{\partial x}\,(\delta w_e) = 0$$

and that

$$w_e = w_e^o \tag{2.21}$$

In this way the edge boundary conditions for a quasi-three-dimensional boundary-layer flow with interaction are given by Eqs. (2.6) and (2.18).

2.2.3 Turbulence Model

The presence of Reynolds shear stress terms in the boundary-layer equations requires a turbulence model. The algebraic eddy-viscosity ε_m formulation of Cebeci and Smith [7] is used here. According to this formulation for two-dimensional wall boundary-layer flows, ε_m is defined by two separate formulas, given by

$$\varepsilon_m = \begin{cases} \{0.4y[1 - \exp(-y/A)]\}^2 \left|\frac{\partial u}{\partial y}\right| \gamma_{tr} & 0 \le y \le y_c \quad (2.22a) \\[2ex] \alpha \left| \int_0^\infty (u_e - u)dy \right| \gamma_{tr}\gamma & y_c \le y \le \delta \quad (2.22b) \end{cases}$$

where

$$A = 26\nu u_\tau^{-1}, \qquad u_\tau = \left(\frac{\tau_\ell}{\rho}\right)^{1/2}_{max},$$

$$\tau_\ell = \mu \frac{\partial u}{\partial y}, \qquad \gamma = \frac{1}{1 + 5.5(y/\delta)^6} \tag{2.23}$$

The condition used to define y_c is the continuity of the eddy viscosity; from the wall outward Eq. (2.22a) is applied until its value is equal to the one given by Eq. (2.22b).

In Eq. (2.22), γ_{tr} is an intermittency factor which accounts for the transitional region that exists between a laminar and turbulent flow. It is given by

$$\gamma_{tr} = 1 - \exp[-G(x - x_{tr}) \int_{x_{tr}}^{x} \frac{dx}{u_e}] \tag{2.24a}$$

Here x_{tr} is the location of the start of transition. The empirical factor G is

$$G = \frac{1}{1200} \frac{u_e^3}{\nu^2} R_{x_{tr}}^{-1.34} \tag{2.24b}$$

where the transition Reynolds number $R_{x_{tr}} = (u_e x/\nu)_{tr}$ and the transition location x_{tr} is either specified or calculated from the empirical formula of Michel [29]

$$R_{\theta_{tr}} = 1.174 R_{x_{tr}}^{0.46} \left(1 + \frac{22,400}{R_{x_{tr}}}\right) \tag{2.24c}$$

According to the Cebeci Smith model, the parameter α in Eq. (2.22b) is equal to 0.0168 for values of R_θ greater than 5000, and is given by the expression in [24] for R_θ less than 5000. Studies conducted by Head and his associates [25,26] the recent experimental data of Nakayama [27] and Simpson et al. [28] and the numerical studies of Carter [20] indicate that in flows with strong pressure gradient, the value of α should also be changed when R_θ 5000. Head and his associates recommend that α in Eq. (2.22b) be given by

$$\alpha = \alpha_{eq} F(r) \tag{2.25a}$$

where

$$\alpha_{eq} = 0.002094 + 0.02672[1 - \exp(-0.1163G)] \tag{2.25b}$$

$$G = 4.8285\ (\Pi + 1.0717)^{1/2} + 1.8438 \tag{2.25c}$$

$$\Pi = \frac{\delta^*}{\tau_w}\frac{dp}{dx} \tag{2.25d}$$

$$F = \begin{cases} (5 - 4r)/(3 - 2r) & r < 1 \quad (2.25e) \\ \dfrac{1}{2r - 1} & r \geq 1 \quad (2.25f) \end{cases}$$

In Eqs. (2.25e) and (2.25f), r represents the ratio of the local rate of growth of the boundary layer to the rate of growth of the corresponding equilibrium layer.

They also suggested that γ in Eq. (2.23) be replaced by

$$\gamma = \frac{2.0}{1 - \mathrm{erf}[1/2(y/\delta - \beta)]} \tag{2.25g}$$

where β is a function of shape factor H.

Simpson et al. [28] suggest that

$$\alpha = 0.0168/F^{2.5} \tag{2.26a}$$

Here F denotes the ratio of the product of the turbulent energy by normal stresses to that by shear stress evaluated at the location where shear stress is maximum, that is,

$$F = \left\{\frac{(\overline{u'^2} - \overline{v'^2})\ \partial u/\partial x}{\overline{-u'v'}\ (\partial u/\partial y)}\right\}_{(\overline{-u'v'})_{max}} \tag{2.26b}$$

Before Eq. (2.26a) can be used in Eq. (2.26b), an additional relationship between $(\overline{u'^2} - \overline{v'^2})$ and $(\overline{-u'v'})$ at $(\overline{-u'v'})_{max}$ is needed. Here we assume that the ratio in Eq. (2.26b),

$$\beta = \left\{\frac{\overline{u'^2} - \overline{v'^2}}{\overline{-u'v'}}\right\}_{(\overline{-u'v'})_{max}} \tag{2.26c}$$

is a function of $R_T = \tau_w/(\overline{-u'v'})_{max}$ which, according to the data of Nakayama [27], can be represented by

$$\beta = \frac{6}{1 + 2R_T(2 - R_T)} \tag{2.26d}$$

for $R_T < 1.0$. For $R_T \geq 1.0$, we take β to be

$$\beta = \frac{2R_T}{1 + R_T} \tag{2.26e}$$

Introducing the above relationships into the definition of F, we have the following expression for α, according to Eq. (2.26a),

$$\alpha = \frac{0.0168}{[1 - \beta(\partial u/\partial x)/(\partial u/\partial y)]^{2.5}} \tag{2.27}$$

where β is given by Eqs. (2.26d) and (2.26e). This expression is used here although further studies are clearly required to evaluate its range of validity. Work of this nature is in progress.

For three-dimensional flows, the above formulation was generalized as discussed in [16] and in the inner region ε_m is defined by

$$(\varepsilon_m)_i = L^2[(\frac{\partial u}{\partial y})^2 + (\frac{\partial w}{\partial y})^2 + 2(\frac{\partial u}{\partial y})(\frac{\partial w}{\partial y})\cos\theta]^{1/2} \tag{2.28}$$

where

$$L = 0.4y[1 - \exp(-y/A)], \quad A = 26\,\frac{\nu}{u_\tau}, \qquad u_\tau = (\frac{\tau_{tw}}{\rho})^{1/2}$$

$$\tau_{tw} = \mu\,[(\frac{\partial u}{\partial y})_w^2 + (\frac{\partial w}{\partial y})_w^2 + 2(\frac{\partial u}{\partial y})_w(\frac{\partial w}{\partial y})_w\cos\theta]^{1/2} \tag{2.29}$$

In the outer region ε_m is defined by

$$(\varepsilon_m)_o = \alpha\left|\int_0^\infty (u_{te} - u_t)dy\right| \tag{2.30}$$

and α is given by Eq. (2.27).

2.2.4 Transformed Equations

The equations of Section 2.2.1 may be solved in the forms presented or expressed in other forms which are more convenient for accurate solution. For two-dimensional flows, as in [4], we use the Falkner-Skan transformation in the early stages of the flow

$$\eta = \sqrt{u_e/\nu x}\; y, \quad \psi = \sqrt{u_e \nu x}\; f(x,\eta) \tag{2.31}$$

With primes denoting differentiation with respect to η and $b = 1 + \varepsilon_m/\nu$, Eqs. (2.14) and (2.15) and their boundary conditions can be written in the form:

$$(bf'')' + \frac{m+1}{2} ff'' + m[1 - (f')^2] = x(f' \frac{\partial f'}{\partial x} - f'' \frac{\partial f}{\partial x}) \tag{2.32}$$

$$\eta = 0, \qquad f = f' = 0 \tag{2.33a}$$

$$\eta = \eta_e, \qquad f' = 1 \tag{2.33b}$$

Here ψ is the usual definition of the stream function that satisfies the continuity equation,

$$u = \frac{\partial \psi}{\partial y}, \qquad v = -\frac{\partial \psi}{\partial x} \tag{2.34}$$

and m is a dimensionless pressure-gradient parameter,

$$m = \frac{x}{u_e} \frac{du_e}{dx} \tag{2.35}$$

This transformation provides the generation of initial conditions at the stagnation point of the airfoil and allows the calculations to be performed economically and accurately around the leading edge, where the governing equations are being solved for the prescribed external velocity distribution. For interactive boundary-layer calculations, where $u_e(x)$ is not known, a constant reference velocity u_o is used in the transformation

$$Y = \sqrt{u_o/\nu x}\; y, \qquad \psi = \sqrt{u_o \nu x}\; F(x,Y) \tag{2.36}$$

In terms of these new variables, Eqs. (2.14) and (2.15) and their boundary conditions can be written in the form:

$$(bF'')' + \frac{1}{2} FF'' + xe \frac{de}{dx} = x(F' \frac{\partial F'}{\partial x} - F'' \frac{\partial F}{\partial x}) \tag{2.37}$$

$$Y = 0, \qquad F = F' = 0 \tag{2.38a}$$

$$Y = Y_e, \qquad F' = e, \qquad e - \dot{c}_{11} (Y_e e - F) = g_1 \tag{2.38b}$$

where

$$\dot{c}_{11} = c_{11} \sqrt{\nu x/u_o}\,, \qquad e = \frac{u_e}{u_o}$$

Here the parameter g_i, which results from the discrete approximation to Eq. (2.19) is given by

$$g_i = \bar{u}_e^K + \sum_{j=1}^{i-1} c_{ij}(D_j - D_j^K) - c_{ii}D_i^K \tag{2.39}$$

where

$$D = \sqrt{\nu x/u_o}\,(Y_e e - F_e)$$

For quasi-three-dimensional flows, we define

$$x = x, \qquad d\eta = \left(\frac{u_o}{\nu s_1}\right)^{1/2} dy \tag{2.40}$$

Here u_o is a reference velocity and s_1 denotes the length in the longitudinal direction measured from the initial line $x = x^*$. We again introduce the definition of stream function $\psi(x,y)$

$$uh_2 \sin\theta = \frac{\partial\psi}{\partial y}, \qquad vh_1h_2\sin\theta = -\frac{\partial\psi}{\partial x} \tag{2.41)}$$

so that with the definition of eddy viscosity, the quasi-three-dimensional boundary-layer equations given by Eq. (2.13) can be written as [10]

$$(bf'')' + m_1 ff'' + m_3[(f')^2 - e^2] + m_5(f'g' - \bar{w}_e e) + m_4[(g')^2 - (\bar{w}_e)^2]$$
$$= m_9\left(f'\frac{\partial f'}{\partial x} - e\frac{\partial e}{\partial x} - f''\frac{\partial f}{\partial x}\right) \tag{2.42}$$

$$(bg'')' + m_1 fg'' + m_6[(g')^2 - \bar{w}_e^2] + m_7[(f')^2 - e^2)] + m_8(f'g' - \bar{w}_e e)$$

$$= m_9\left(f'\frac{\partial g'}{\partial x} - e\frac{\partial \bar{w}_e}{\partial x} - g''\frac{\partial f}{\partial x}\right) \tag{2.43}$$

where, with $f' = u/u_o$, $g' = w/u_o$, $\bar{w}_e = w_e/u_o$

$$m_1 = \frac{\sqrt{s_1}}{h_1h_2\sin\theta}\frac{\partial}{\partial x}(\sqrt{s_1}\,h_2\sin\theta), \qquad m_3 = K_1 s_1 \cot\theta$$

$$m_4 = -K_2 s_1 \csc\theta, \qquad m_5 = -K_{12}s_1, \qquad m_6 = s_1 K_2 \cot\theta \tag{2.44}$$

$$m_7 = -m_3, \qquad m_8 = -K_{21}s_1, \qquad m_9 = s_1/h_1$$

The boundary conditions become

$$\eta = 0, \qquad f = f' = 0, \qquad g = g' = 0 \tag{2.45a}$$

$$\eta = \eta_e, \qquad f' = e(x), \qquad g' = \bar{w}_e(x) = \bar{w}_e^o \tag{2.45b}$$

$$e(x) = \bar{u}_e^o + \frac{1}{\pi} \int_{x_a}^{x_b} \frac{d\Delta}{d\sigma} \frac{d\sigma}{x - \sigma}$$

where

$$\Delta = \frac{s_1}{\sqrt{R}} (\eta_e e - f_e), \qquad R = \frac{u_o s_1}{\nu} \tag{2.46}$$

2.2.5 Solution Procedure

The numerical solution of the system of equations given in the previous section is obtained with Keller's box method for the standard and interactive methods. This is an efficient, second-order finite-difference method extensively used by Cebeci and his associates for a wide range of flows, as discussed in Bradshaw et al. [16]. The description of the standard method is given in that reference as well as in Cebeci and Bradshaw [29]. The general features of the inverse method which makes use of the Mechul-function formulation are also described for two-dimensional flows in Bradshaw et al. [16] and in [10] for quasi-three-dimensional flows. As in previous two-dimensional studies the FLARE approximation in which the convective term $\partial F'/\partial x$ is set equal to zero in the recirculating region is employed, and no attempt was made to improve the accuracy of the solutions resulting from this approximation.

As in the solution of two-dimensional flows by Keller's method, we write Eq. (2.37) as a first-order system. For this purpose we let

$$F' = u \tag{2.47a}$$

$$u' = v \tag{2.47b}$$

and write Eq. (2.37) as

$$(bv)' + \frac{1}{2} Fv + xe \frac{de}{dx} = x(u \frac{\partial u}{\partial x} - v \frac{\partial F}{\partial x}) \tag{2.47c}$$

Since e is a function of x, only, we write

$$e' = 0 \tag{2.47d}$$

The boundary conditions for the system given by Eqs. (2.47) now can be written as

$$Y = 0, \qquad F = 0, \qquad u = 0 \tag{2.48a}$$

$$Y = Y_e, \qquad u = e, \qquad e - \dot{c}_{11}(Y_e e - F) = g_1 \tag{2.48b}$$

After the finite-difference approximations to Eqs. (2.47) and (2.48) are written, the resulting nonlinear algebraic system is linearized by Newton's method and the linear system is then solved by the block elimination method. For further details, see [29].

SECTION III
RESULTS AND DISCUSSIONS

The interactive boundary-layer procedure described in the previous section has been applied to a number of test cases and the results will be presented here.

Section 3.1 presents the results obtained from the application of the two-dimensional strip theory approach to two wing alone configurations to verify the soundness of the interactive boundary layer technique. Section 3.2 will present the results obtained from the two-dimensional and the quasi-three dimensional methods for three wing-body fighter configurations.

3.1 <u>Wing Alone Configurations</u>

The first configuration considered is an RAE clean wing with a 28° sweep angle for which experimental data has been obtained by Lovell [30]. Figure 5 shows the computed lift curve up to 18° angle of attack. It can be seen that there is good agreement up to about 12°, beyond which the discrepancy increases. This disagreement at the higher angles of attack is due to the three dimensional nature of the flow, and due to the sensitivity of the flow to the transition location. This sensitivity is illustrated by Fig. 6 which shows the variation of the flow solution to the transition location at an angle of attack of 17.5°. Moving the transition location leads to a significant change in the lift separation location and displacement thickness, particularly near the wing tip. Figure 7 shows the results for $\alpha = 18.5°$ with the computed transition location. As can be seen the separation location at this angle of attack occurs at about the midchord location. The size of the leading and trailing edge separation regions at $\alpha = 17.5°$ can be seen from Fig. 8 in which the local skin friction is plotted.

Near the wing tip it can be seen that there is a small leading edge separation, shown by the region of negative skin friction, and that the trailing edge separation is occurring at about 65% local chord.

Figures 9-11 illustrate the results obtained for a NACA 0012 swept wing for which data was obtained by Yip and Shubert [31] for a range of angles of attack. Figure 9 shows the viscous and inviscid lift up to 21.18° from which the effects of the increasing flow separation at higher angles of attack can clearly be seen. Figure 10 shows the computed and experimental pressure distributions for $\alpha = 19.35°$ at two sections, 50% and 85% of semispan, both of which agree very well.

The importance of the transition location is illustrated by Figure 11 which shows the computed separation location, trailing-edge displacement thickness and lift distribution for $\alpha = 21.12°$. Two curves are shown, the solid line was obtained with a computed transition location at about 3% chord on the upper surface. The dashed line was obtained by specifying a transition location closer to the leading edge attachment line on the lower surface. It can be seen that this small movement in the transition location moves the separation location forward from 60% chord to about 30% chord.

3.2 Application to Wing/Body Test Cases

Three wing/body test cases were identified for which there was experimental data available to evaluate the current procedure. The three cases are, an F-15 with a modified wing designed to investigate the role of a leading-edge laminar separation, an Advanced Navy Fighter configuration, and an unmodified F-15. The geometry and input data associated with these test cases is discussed in detail in Section 5 (Figs. 26-30).

The F-15 laminar bubble configuration has been run at a range of angles of attack using both the 2-D and the quasi 3-D boundary-layer procedures. Figure 12 shows the computed lift compared with the experimental data [32]. It can be seen that at lower angles of attack the 2-D and quasi 3-D approaches agree closely, while at higher angles of attack the quasi 3-D boundary-layer procedure agrees better with the experimental data. At lower angles of attack both approaches over-predict the lift, possibly due to an inadequate modelling of the flow over the body.

Figure 13 shows an example of the computed and experimental pressure distributions for $\alpha = 10.75°$ angle of attack at three stations across the span from close to the wing tip to close to the wing root. It can be seen that for this angle of attack there is very little difference between the 2-D and the quasi three dimensional boundary layer methods, and that both give a reasonable approximation to the measured pressures except close to the leading edge.

One further aspect of the present method which has been investigated concerns the use of a panel method for the calculation of compressible flow. A panel method is an incompressible solution procedure and so Mach number effects must be accounted for by means of a compressibility correction. In this case a Goethert correction is applied using the following procedure: the solution to the linearized potential flow equation

$$(1 - M_\infty^2) \frac{\partial^2 \phi}{\partial x^2} + \frac{\partial^2 \phi}{\partial y^2} + \frac{\partial^2 \phi}{\partial z^2} = 0 \qquad (3.1)$$

is obtained, where ϕ is the perturbation in the potential due to the body. Provided that this perturbation velocity is small compared with the freestream velocity equation (3.1) provides a good approximation to the flow. This is true for the flow over thin wings. However, around the leading edge, or on any forward facing surface, this basic assumption is violated.

The compressibility correction for the initial velocity calculation is implemented here by first scaling the y and z coordinates by $\beta = \sqrt{(1 - M_\infty^2)}$. The incompressible flow is then computed about this equivalent body and the computed velocity components are divided by β^2 in the x-direction and β in the y- and z-directions.

For the subsequent updates to the inviscid velocity to account for the viscous effects the same procedure is adopted. However, this calculation involves two additional features over the initial inviscid calculation. The first is the introduction of the blowing velocity required to simulate the displacement thickness and the second is the introduction of off-body points at which the Kutta condition is to be applied and the final velocity computed. In applying the Mach number correction two additional assumptions are therefore necessary. The first is that the blowing velocity is predominantly in the y,z direction so that the blowing velocity applied on the "equivalent incompressible body" can be scaled by β. The second assumption is that the displacement effect of the boundary layer is also predominantly in the y,z direction. Therefore in defining the off-body point location in the transformed plane the displacement thickness is first scaled by β. Since both the displacement thickness and the blowing velocity are most significant near the trailing edge both of these assumptions are valid.

It should be pointed out that the interactive viscous calculation is performed entirely in the physical plane. The Mach number correction outlined above is used to provide the compressible external velocity distribution.

While the compressibility correction will provide a good approximation at lower angles of attack, it becomes less accurate at higher angles of attack when the flow can become supercritical and shock waves can form through the leading edge region. Figure 14 shows the inviscid computed pressure distribution at the mid-semispan location computed by the present panel method and by the transonic full-potential wing/body code developed by Chen et al. [33] at α = 6.84°, 10.75° and 12.95° for M = 0.6. At the lower angle of attack the two procedures agree well except close to the leading edge where the transonic code predicts a higher suction peak. However, at α = 12.95° the transonic method predicts a shock wave and a larger difference in the pressure distribution through this region is predicted.

The second wing/body test case which has been considered is the Advanced Navy Fighter (ANF) for which experimental data is available [34]. This configuration was tested experimentally both with and without a canard. Figure 15 shows the computed and experimental lift distribution for this configuration without the canard and Figure 16 shows the viscous and inviscid pressure distribution compared with experimental data at α = 7.7° across the span. It can be seen that there is good agreement. The only other pressure data for this particular configuration is for α = 22° at which angle the data shows the presence of a shock wave near the leading edge suction peak. Due to the limitations of the compressibility correction outlined above this case has not been pursued. The effect of the canard is shown in Figure 17, in which the computed viscous lift distribution is shown with and without the canard. This case was run with the canard at zero deflection angle for which there was no experimental data, and the viscous effects were computed only on the main wing.

The final configuration which has been investigated is an unmodified F-15 wing/body for which experimental data was obtained by Anderson [35]. Figure 18 shows the computed and experimental lift curves from which it can be seen that there is good agreement up to 8.66° angle of attack. Figure 19 shows the computed pressure distribution for 8.66° which is in good agreement with the experimental data.

SECTION IV
PROGRAM DESCRIPTION

The method developed here calculates the viscous flow over a lifting body through the use of an interactive boundary-layer technique in which a three-dimensional panel method is coupled with a finite-difference boundary-layer method. Two distinct boundary-layer procedures have been adopted, the first of which uses a two-dimensional strip theory approach while the second is a quasi-three-dimensional boundary-layer method.

The structure of the code is illustrated in Figure 20, which gives a schematic flow chart of the code. There are three major computational modules required, namely the inviscid panel method, the two-dimensional boundary-layer routines and the quasi-three-dimensional boundary-layer routines. The communication between the potential flow code and the boundary-layer routines is handled through the use of external disk storage.

For a given flow condition the inviscid solution is first computed and the pressure distribution over the wing is saved. If the 2-D boundary-layer mode is selected, this data is separated into strips, and an interactive boundary-layer calculation is performed independently for the upper and lower parts of each lifting strip using the method outlined in Section 2.2.5. Each of these boundary-layer calculations require a number of iterative sweeps over each surface in order to match the current external velocity distribution, given by Eqs. (2.18) and (2.19), with that computed by the boundary-layer equations, (2.47) and (2.48). Once these inner iterations have been completed and the corresponding displacement thickness and blowing velocity has been computed these data are transferred back to the inviscid flow code and the external velocity distribution is updated to incorporate the viscous effects. One complete iteration between the viscous and inviscid codes is referred to as a cycle. Several such cycles are usually performed in order to obtain a fully converged solution in which the computed viscous and inviscid solutions match one another. The precise number of cycles performed is governed either by an input parameter which specifies the maximum number of cycles, or else by a convergence check which is based on the maximum change in a displacement thickness parameter form one cycle to the next. Typically up to 5 cycles may be required for a fully converged solution.

A similar procedure is employed for the quasi three-dimensional boundary layer method with interface routines handling the transfer of the data between the viscous and the inviscid codes. In this case the data required is more extensive than that required for the two-dimensional boundary layer calculation since surface coordinates and curvatures are required for the complete surface. Therefore, the interface program accesses the velocity data produced by the inviscid calculations, and computes a dividing line separating the upper and lower portions of the wing flowfield. For each surface, a boundary-layer grid is now defined and the geometric surface curvatures and the velocity components are interpolated onto the boundary-layer grid. The quasi three-dimensional boundary-layer procedure now iterates over each surface in a similar fashion to the two-dimensional approach in which the perturbed inviscid velocity is matched with that computed by the boundary-layer equations, (2.42) - (2.46). The computed displacement thickness and blowing velocity is then transferred back to the potential flow code for the next viscous/inviscid cycle.

After a converged solution has been obtained for the first specified angle of attack, the process is repeated for the next angle of attack. However, rather than start the calculation using the purely inviscid potential flow solution, the blowing velocity and displacement thickness computed for the previous angle of attack are used for boundary conditions in the first inviscid flow solution. Therefore, when running multiple angles of attack, the angles should be specified in increasing order. In this way the number of cycles required for a converged solution is reduced, particularly at higher angles of attack when boundary-layer separation can lead to fairly large displacement thicknesses. To take further advantage of this fact, the program may be executed in a restart mode in which data stored by a previous run may be input as a starting solution for the next angle of attack to be computed. After each run, the following two datasets may therefore be saved for use in a subsequent run:

Unit #33 This stores the blowing velocity and the displacement thickness data.

and

Unit #47 This unit stores the geometric coefficients of the airfoil appearing in the interaction formula used in the quasi three-dimensional boundary layer method.

or

Unit #51 - This unit stores the geometric coefficients of the airfoil appearing in the interaction formula used in the two-dimensional boundary-layer method.

The user can therefore run a range of angles of attack either by specifying all of the angles of attack in one single run, or else as a series of separate runs which make use of the restart capability.

4.1 Input Data Description

4.1.1 Body Geometry

The input to this program consists of the coordinates of a number of points that define the surface of a three-dimensional configuration on which the flow is to be computed. For the purpose of organizing these points for computation, each point is assigned a pair of integers, m and n. These integers need not be input, but their use must be understood to insure the correctness of the input and to facilitate the interpretation of the output.

For each point, n identifies the "column" of points to which it belongs, while m identifies its position in the "column," i.e, the "row." The first point of a "column" always has m = 1. To insure that the program will compute outward normal vectors, the following condition must be satisfied by the input points. If an observer is located in the flow and is oriented so that locally he sees points on the surface with m values increasing upward, he must also see n values increasing toward the right. Examples of correct and incorrect input are shown in Figure 21. In this figure the flowfield lies above the paper, while the interior of the body lies below the paper. Occasionally, it happens that despite all care a body is input incorrectly. If the entire body is input incorrectly - not some sections correctly and some incorrectly - the difficulty can be remedied by changing the sign of one coordinate of all the input points. This trick will give an input body of the proper shape at perhaps a peculiar location. Otherwise, the input will have to be done over.

The body surface is divided into sections, which may be actual physical divisions or may be selected for convenience. A section is defined as consisting of a group of at least two n-lines. Within each section the n-lines are input in order of increasing n. On each n-line the points are input in order of increasing m. All n-lines in a section must have the same number of points, but this may vary from section to section. The first n-line of the first section is n = 1. From then on the n-lines may be thought of as numbered consecutively through all sections, i.e., the numbering is not begun over at the beginning of each section. Panels will be formed that are associated with points on every n-line except those that are last in their respective sections. Points on these latter n-lines are used only to form panels associated with points on the next lowest n-lines.

To illustrate this procedure, consider the plan view of a body shown in Figure 22. This body has been divided into four sections, as shown in the figure. The first section contains four n-lines, n = 1, 2, 3, 4; the second, five n-lines, n = 5, 6, 7, 8, 9; the third three n-lines, n = 10, 11, 12; and the fourth three n-lines; n = 13, 14, 15. The number of points on each n-line are:

Section =	1	2	3	4
M =	4	7	4	2

Notice that the line n = 4 has only four points, the points m = 1, 2, 3, 4 and the m-grid of Section 1, which is listed in the figure along the n = 1 line. The lines n = 4 and n = 5 are physically identical. Some of the points on the two lines are physically identical but correspond to different values of m. This is of no consequence. In this scheme sections are completely independent. No elements are computed corresponding to points on lines n = 4, 9, 12, 15.

There is no restriction that the m and n lines of different sections have to be roughly parallel. The arrangement shown in Figure 23 is permissible.

As discussed in Section 2.1, the body is divided into lifting and nonlifting sections. The arrangement of the input requires that all lifting sections precede nonlifting sections with a one-point-per-card format of (3F10.5,2I1) with a maximum of 2000 panels and 100 strips defining the configuration. This data is input to the program through Unit #29. Also, since the boundary-layer calculations can be made for only one lifting section, this section must precede any other lifting sections. The two integers that follow each set of coordinates are the status flag and label flag, respectively, that is

STATUS FLAG	LABEL FLAG
2 - new section	1 - lifting body, or 0 - nonlifting body
1 - new N-line	(these flags are needed only when STATUS FLAG = 2)
0 - same N-line	
3 - end of input for the whole body	

4.1.2 Namelist Block Input

There are two namelist blocks that contain two groups of input data.

Namelist Name A:

This namelist block consists of all the control flags and flow conditions required to control the interactive viscous calculation.

Variables	Remarks
LIFT3D	Control flag for the execution of the potential-flow program. = 0 Skip the initial potential flow and execution will start with the boundary-layer code. = 1 Use the potential flow program for every cycle. (default is 1)
IBL3D	Control flag for executing a boundary-layer program. = 0 Use the two-dimensional boundary-layer program. = 1 Use the quasi-three-dimensional boundary-layer program. (default is 0)
KINKNO	Total number of "kink" stations input ("kink" station means a discontinuity in the planform of the first lifting section). (default is 0, maximum is 5)
MS	Station numbers where "kink" occurs in the planform. The order of these "kink" stations should be in the same order as the spanwise stations input to the Neumann program. They are also part of the input spanwise stations. (default is 0)
MLINE(i)	Number of defining chordwise points on each N-line of the i-th lifting section.
NLINE(i)	Number of defining spanwise points on each M-line of the i-th lifting section.
MAXCYC	Maximum number of interaction cycles. (default is 0)

Variables	Remarks
MAXANG	Number of angles of attack to be calculated. (default is 1, maximum is 10)
IPNTGM	Optional (debug) print flag for the interfacing program. = 0 No intermediate print. = 1 With intermediate print. (default is 0)
IPNTNU	Optional (debug) print flag for the potential flow program. = 0 No intermediate print. = 1 With intermediate print. (default is 0)
IPNTB3	Optional (debug) print flag for the quasi-three-dimensional boundary layer program. = 0 No intermediate print. = 1 With intermediate print. (default is 0)
DBMAX	Maximum difference in circulation values generated from potential flow solution for convergence. (default is 0.01)
ALPHAI	Input angles of attack values. Total number input = MAXANG. (default is 0.0)
AMACH	Input Mach number. (default is 0.0)

Namelist Name B:

Namelist B contains the geometric variables and control flags which pertain to the potential flow calculation.

Variables	Remarks
BOV2	The semi-span value of the lifting body. (default is 1.0)
IAUTOW	Automatic wake generation flag: = 1 Program generates bisector wake. = 2 Program generates flat wake, i.e. wake panel is parallel to the x-axis. = 0 User input wake panels. (default is 1)
IPCV	Chordwise vorticity flag. = 0 Constant vorticity used. = 1 Parabolic vorticity used. (default is 0)

Variables	Remarks
	NOTE: This flag controls the form of the predetermined chordwise bound-vorticity variation discussed in Section 2.1. For wings with cusped or thin trailing edges, the constant variation may lead to unrealistic variations in the pressure close to the trailing edge. In such cases, the parabolic variation should be used. Otherwise the constant chordwise option should be used.
ITERAT	Matrix Solution flag. = 0 (direct solution for 350 panels or less, otherwise use iterative solution). = 1 Iterative solution. = 2 Direct solution. (default is 1) Note: Iterative solution must be used when viscous calculations are made.
IVNSP	Nonuniform Flow/Specified Normal Velocity flag. = 0 No nonuniform flow or blowing velocity. = 1 Nonuniform Flow Specified. In the case onset flow velocity components at every control point must be input on Unit 33 in 3F10.6 card image format. Otherwise velocity components are computed from freestream flow direction. = 2 Nonzero normal velocity condition is specified on some section or sections. If this option is used, then Unit 33 must contain the following data: 1st record: "SECTION k" Subsequent records: required normal velocity (FORMAT 1F10.6) with 1 record for each control point in the k-th section. These cards are repeated for each section for which nonzero boundary condition is satisfied. NOTE: These options are only available for a purely inviscid calculation.
LIFSEC	Number of lifting sections input. NOTE: Boundary-layer calculations can be made for the first lifting body only.
LINEAR	Spanwise vorticity flag. = 0 Constant vorticity used. = 1 Linear vorticity used. If selected, the variables, NLINE1 and NLINEN must be input. (default is 0) NOTE: This flag controls the variation of spanwise vorticity across a given lifting strip. The level on each strip is determined by the Kutta condition as discussed in Section 2.1.

Variables	Remarks
NLINE1(i)	Condition for the first N-line of the i-th lifting section. = 1 The first N-line is the wing tip. = 4 The first N-line belongs to an extra strip or is next to a symmetry plane.
NLINEN(i)	Condition for the last N-line of the i-th lifting section. = 1 The last N-line is the wing tip. = 4 The last N-line belongs to an extra strip or next to a symmetry plane.
LIST	Geometry formation flag. = 0 Complete potential flow calculation modes. = 1 Calculation stop after geometry formation (default is 0)
NOFF	Off-body point flag. = 0 No off-body point input. = 1 Off-body point input. (default is 0) NOTE: Off-body points are points in the flow at which the velocity and pressure are to be computed. If this option is used, the off-body coordinates must be supplied on Unit 32 using 3F10.6 card image format.
NSYM1	First plane of symmetry flag. = 0 No symmetry. = 1 One plane of symmetry (about the x-z plane). (default is 1)
NSYM2	Second plane of symmetry flag. = 0 No second plane of symmetry used. = 1 Symmetry about the y-z plane (NSYM1 must also be = 1). (default is 0)
ORIGNX ORIGNY ORIGNZ	The x,y,z coordinates of the input moment origin (default is 0, 0, 0).
NSORCE(i)	Number of on-body panels per strip for the i-th lifting section.
NWAKE(i)	Total number of wake panels input for the i-th lifting section. (If IAUTOW $\neq$ 0, NWAKE $\equiv$ 1)
NSTRIP(i)	Total number of strips in the i-th lifting section.
IXFLAG(i)	Extra strip option input for the i-th lifting section. = 0 No extra strip. = 1 First strip is an extra strip. = 2 First and last strips are extra strips. = 3 Last strip is an extra strip.

Variables	Remarks
	NOTE: An extra strip is a strip of panels on a lifting section which carries a vorticity distribution but on which no boundary conditions are satisfied. Such a strip is used for instance at an intersection between a wing and a fuselage in order to provide a more accurate carry-over of the wing lift across the fuselage. In this case the extra strip is internal to the fuselage, and it extends from the wing root to the fuselage centerline. Further details of the use of extra strips is discussed by Hess [36].
REFCHD	Reference chord value. (This is needed for the calculation of the lift coefficient.) (default is 1.0)
RFAREA	Reference area value. (This is needed for the calculation of the lift coefficient.) (default is 1.0)

4.1.3 Boundary-Layer Calculation Data Input

(a) Card number 1
Format (6F10.0)

Card Column	Variables		Remarks
1-10	RCx10^{-6}		Reynolds number based on CREF.
11-20	CREF		Reference length. In the same physical units that are used for the input geometry. NOTE: This need not be the same value as REFCHD used above. CREF is only used to calculate the local Reynolds number in terms of the input coordinates. e.g. If the geometry is specified in inches, and the Reynolds number/ft is input, then CREF would be 12.
31-40	FRSTAT	= 1.0	Option for using a previous angle of attack solution as an initial estimate for the current angle of attack calculation.
		= 0.0	Option not used (or the initial run).
41-50	FPRNT	= 1.0	Detailed boundary-layer print.
		= 0.0	No boundary-layer print.

(b) Card Number 2
Format (6F10.0)

Card Column	Variables	Remarks
1-10	FNBLU	Number of boundary layer stations at which calculations are made on the upper surface of the first lifting body (max = 100).
11-20	FTRIU	Transition input flag = 0 Transition location specified across the span. See Cards 3 and 4. = 1 Transition calculated by the program at pressure peak. = 2 Transition calculated by the program using Michel's criteria.
21-30	FSWPU	Number of iteration sweeps to be made for the upper surface. (FSWPU = 10.0 is recommended)
31-40	FNTRU	Number of transition locations to be specified. (if FTRIU = 0)

(c) Card number 3 (needed only if FTRIU = 0).
Format (6F10.0)

Card Column	Variables	Remarks
1-10	YTRN	Spanwise location, in the input geometry system, where transition will be specified (this location does <u>not</u> have to correspond to the coordinates used to define the geometry).
11-20	YTRN+1	
	.	
	.	
	.	
51-60	YTRN+5	

(Repeat this card if necessary until i = FNTRU.)

(d) Card number 4 (needed only if FTRIU = 0).
Format (6F10.0)

Card Column	Variables	Remarks
1-10	XCTRN	x/c chordwise location of specified transition.

11-20 XCTRN+1

.

.

.

51-60 XCTRN+5

(Repeat this card if necessary until i = FNTRU.)

The following cards, numbers 5, 6 and 7, have the same format as cards 2, 3 and 4 and the variables have the same meaning but correspond to the lower surface.

(e) Card number 5
Format (6F10.0)

Variables FNBLL, FTRIL, FSWPL, FNTRL

FSWPL = 5.0 is recommended.

(f) Card number 6
Format (6F10.0)

Variable YTRN

(g) Card number 7
Format (6F10.0)

Variable XCTRN

Note that the chordwise location of specified transition must be preceded by a minus sign when it is being input on the airfoil lower surface.

The cards in this section, (a) through (g), are to be repeated for each angle of attack calculated.

4.2 <u>Output Data Description</u>

4.2.1 Summary

Potential Flow

The following data are printed for the potential flow calculation:

1. Input flags.

II. Panel formation.

III. Matrix solution (by iteration method).

IV. Solution summary. This includes:

lift coefficient, drag coefficient, pitch, roll, yaw and n values for each lifting and nonlifting section, plus the same set of data for the whole configuration.

V. Final cycle. For every panel, the following data are printed:

. panel number
. control point coordinates - x_o, y_o, z_o
. inviscid velocities - v_x, v_y, v_z
. inviscid total velocity V_T and viscous corrected pressure coefficient Cp
. displacement thickness - DELS
. shape factor - H
. skin friction - CF.

4.2.2 Format

A test case consisting of one lifting and four nonlifting sections with a total of 221 panels, Figure 24, was created to present a sample of the program output, and a listing of this geometry (input through Unit #29) is presented in Table 1. Two angles of attack were calculated with the transition locations on the lifting section computed by the program. The namelist block input for this case is:

```
  REPORT TEST CASE,TRANS. CALC., 2DSTRIP BL, M=0.6, ALPHAS
&A  LIFT3D=1,IBL3D=0,
 MAXCYC=2,NLINE=5,MLINE=21,
 MAXANG=2,ALPHAI(1)=1.3,ALPHAI(2)=3.4,
 AMACH=0.6,&END
&B BOV2=12.955,IAUTOW=2,NSYM1=1,LIFSEC=1,REFCHD=8.2912,
 LINEAR=0,IXFLAG(1)=3,IPCV=1,
 RFAREA=95.904,NSORCE=20,NSTRIP=4,NWAKE=1,&END
7.0        12.0       0.0        0.0
70.0       2.0        10.0
51.0       2.0        5.0
7.0        12.0       0.0        0.0
70.0       2.0        10.0
51.0       2.0        5.0
```

For conciseness, the output presented here will be the pertinent information for the first angle of attack only and is shown in Figure 25.

Table 1. Input geometry data for the sample test case.

x	y	z	x	y	z	x	y	z
29.320007	12.950000	5.669997221	22.049988	5.6999998	5.478327200	25.103775	0.0000000	6.985788300
29.248184	12.950000	5.659527600	21.486954	5.6999998	5.458943400	26.737854	0.0000000	6.692972200
29.039001	12.950000	5.642725900	21.298386	5.6999998	5.502729400	28.032578	0.0000000	6.436945900
28.712479	12.950000	5.627047500	21.491623	5.6999998	5.590855600	28.858948	0.0000000	6.247252500
28.301193	12.950000	5.604246100	22.046387	5.6999998	5.692218800	29.139999	0.0000000	6.169997200
27.848039	12.950000	5.568881300	22.921051	5.6999998	5.774380700	1.4399996	0.0000000	6.159999820
27.390981	12.950000	5.529635300	24.025009	5.6999998	5.855646100	1.4399996	0.0064315	6.161227200
26.979996	12.950000	5.503606700	25.251343	5.6999998	5.891611400	1.4399996	0.0096837	6.160487200
26.653732	12.950000	5.482195900	26.478624	5.6999998	5.850277900	1.4399996	0.0104338	6.157036800
26.444412	12.950000	5.467638400	27.582291	5.6999998	5.776900300	1.4399996	0.0103374	6.151741000
26.371002	12.950000	5.482908200	28.461868	5.6999998	5.728014000	1.4399996	0.0085511	6.149518000
26.441806	12.950000	5.511903600	29.026505	5.6999998	5.690294300	1.4399996	0.0027379	6.150368700
26.650253	12.950000	5.537014000	29.220001	5.6999998	5.669997200	1.4399996	-0.0001927	6.149361600
26.975800	12.950000	5.569729600	29.161774	1.6310434	5.669997210	1.4399996	-0.0004819	6.145678500
27.385544	12.950000	5.614847200	28.907547	1.6285334	5.653652200	1.4399996	0.0000000	6.139999400
27.840240	12.950000	5.660013200	28.172806	1.6335659	5.600514400	3.0000000	0.0000000	6.899999610
28.296280	12.950000	5.681705500	27.029526	1.6679520	5.521410000	3.0000000	0.1928538	6.868820300
28.708923	12.950000	5.683177000	25.588623	1.7761669	5.490619700	3.0000000	0.3631767	6.767053600
29.036896	12.950000	5.675870900	23.986252	1.8357840	5.538683900	3.0000000	0.4916574	6.616421700
29.247543	12.950000	5.669478500	22.388657	1.9419851	5.619744300	3.0000000	0.5607882	6.435597400
29.320007	12.950000	5.669997200	20.949631	2.0539112	5.696937600	3.0000000	0.5604406	6.237468700
29.270004	9.3299999	5.669997210	19.806320	2.1326818	5.759267600	3.0000000	0.4959082	6.053067200
29.137955	9.3299999	5.658049600	19.071396	2.1750240	5.786211000	3.0000000	0.3600985	5.914361000
28.758011	9.3299999	5.606512100	18.846466	2.2000370	5.877244000	3.0000000	0.1880037	5.816710300
28.162079	9.3299999	5.569171900	19.097687	2.1932545	5.996942500	3.0000000	0.0000000	5.759999300
27.409607	9.3299999	5.558603700	19.818451	2.1308517	6.136426900	6.6000004	0.0000000	6.000000010
26.576279	9.3299999	5.522551500	20.959732	2.0326290	6.215392100	6.6000004	0.3757620	7.875558900
25.743439	9.3299999	5.469905900	22.402405	1.9267807	6.247961100	6.6000004	0.6720765	7.607360800
24.991823	9.3299999	5.443327900	24.003601	1.8365239	6.225601200	6.6000004	0.9096854	7.281573300
24.394516	9.3299999	5.426945700	25.601135	1.7746887	6.115730300	6.6000004	1.0701628	6.911097600
24.012192	9.3299999	5.395672800	27.038620	1.6883613	5.961447700	6.6000004	1.1407099	6.517292000
23.888367	9.3299999	5.438118900	28.180145	1.6216841	5.824655500	6.6000004	1.0307589	6.135311100
24.009415	9.3299999	5.507829700	28.911484	1.6258926	5.714633300	6.6000004	0.7527732	5.845423700
24.391281	9.3299999	5.547428100	29.161774	1.6310434	5.669997200	6.6000004	0.3936298	5.667017900
24.986647	9.3299999	5.597860300	29.139999	0.0000000	6.169997210	6.6000004	0.0000000	5.579999900
25.734604	9.3299999	5.667744100	28.848022	0.0000000	6.168208100	6.6000004	0.0000000	6.000000020
26.566864	9.3299999	5.750865900	28.003937	0.0000000	6.146680800	6.6000004	0.3796224	7.883428700
27.400864	9.3299999	5.741601900	26.688950	0.0000000	6.150129300	6.6000004	0.6668429	7.606372800
28.154190	9.3299999	5.711964600	25.034119	0.0000000	6.235967600	6.6000004	0.9006196	7.278782800
28.753342	9.3299999	5.696475000	23.206055	0.0000000	6.412736900	6.6000004	1.0639114	6.909449600
29.138046	9.3299999	5.680374100	21.384949	0.0000000	6.657525100	6.6000004	1.1430740	6.518009200
29.270004	9.3299999	5.669997200	19.750641	0.0000000	6.928585100	6.6000004	1.0284891	6.137653400
29.220001	5.6999998	5.669997210	18.454025	0.0000000	7.150182700	6.6000004	0.7542607	5.843463900
29.026016	5.6999998	5.651124000	17.620010	0.0000000	7.282521200	6.6000004	0.3924263	5.672342300
28.466064	5.6999998	5.587138200	17.362259	0.0000000	7.422036200	6.6000004	0.0000000	5.579999900
27.591843	5.6999998	5.509122800	17.644577	0.0000000	7.553010000	9.0400000	0.0000000	9.399999610
26.486252	5.6999998	5.478968600	18.488068	0.0000000	7.602229100	9.0400000	0.5151625	9.148937200
25.260284	5.6999998	5.480446800	19.803375	0.0000000	7.556008300	9.0400000	0.7953402	8.646261200
24.033768	5.6999998	5.476083800	21.457535	0.0000000	7.437680200	9.0400000	0.7559274	8.067444800
22.927994	5.6999998	5.478483300	23.286606	0.0000000	7.253735500	9.0400000	1.1665621	7.672409100

Table 1. Continued

x	y	z	x	y	z	x	y	z
8.0400000	1.3772738	7.142297700	18.828384	2.2364789	6.462138300	35.999969	1.1518841	6.365452600
8.0400000	1.3488974	6.571766900	18.828660	2.1972866	5.858491100	35.999969	1.4077408	6.017142300
8.0400000	1.0454197	6.085439700	20.898666	0.0000000	8.928970310	35.999969	1.5362034	7.606899900
8.0400000	0.5897094	5.763486900	20.905899	0.5430155	8.889450100	35.999969	1.5333567	7.173847200
8.0400000	0.0000000	5.659998900	20.905583	1.0725965	8.772514300	35.999985	1.4977627	6.743378600
11.470000	0.0000000	9.439999610	20.903854	1.6052437	8.677392000	35.999969	1.3129396	6.353323000
11.470000	0.5272306	9.172776200	20.906998	2.0392551	8.391488100	13.239998	2.4958245	6.089368820
11.470000	0.7217981	8.626779600	20.896912	2.0498791	7.846530900	13.239998	1.8680210	5.985590200
11.470000	1.1584234	8.287037800	20.887115	2.0407487	7.302287100	13.239998	1.2355471	5.953220400
11.470000	1.4484529	7.763385800	20.884354	2.0329008	6.757774400	13.239998	0.6313735	5.758119700
11.470000	1.4818241	7.156081100	20.892029	2.0380592	6.213587600	13.240000	0.0000000	5.699997900
11.470000	1.4360714	6.551931400	23.898637	0.0000000	9.001497310	16.428421	2.3336849	5.938537610
11.470000	1.1543350	6.030721700	23.902847	0.5091249	8.985810500	16.429657	1.7531338	5.831500100
11.470000	0.6007650	5.783112600	23.901566	1.0143394	8.898937400	16.428345	1.1574640	5.780499500
11.470000	0.0000000	5.699998900	23.901718	1.4768286	8.687146200	16.428558	0.5921336	5.612080600
13.240000	0.0000000	9.159999610	23.892563	1.7295752	8.254428900	16.428741	0.0000000	5.531056400
13.240000	0.4588436	8.860602400	23.894165	1.8317699	7.755288200	18.828660	2.1972866	5.856490110
13.240000	0.9617693	8.596923800	23.885254	1.8213902	7.245484400	18.832535	1.7481203	5.612126400
13.240000	1.4046688	8.214414600	23.885834	1.8420534	6.735670100	18.829605	1.1604424	5.576710700
13.240000	1.5412626	7.633884400	23.893600	1.8425722	6.225677500	18.831253	0.5821130	5.486088600
13.240000	1.5878000	7.038955700	26.970062	0.0000000	8.950943910	18.831085	0.0000000	5.408371900
13.240000	1.4770479	6.451713600	26.974182	0.4979586	8.905910500	20.886703	2.0584173	5.698275610
13.240000	1.1558962	5.957092300	26.972397	0.9651402	8.728383100	20.879913	1.7316999	5.396406200
13.240000	0.5905445	5.769768800	26.985439	1.3427353	8.403904900	20.876480	1.1529741	5.371751800
13.240000	0.0000000	5.679999400	26.957245	1.5826340	7.965964300	20.881332	0.5750989	5.334808300
13.240000	0.0000000	9.180000320	26.959717	1.6738930	7.473424900	20.878632	0.0000000	5.280242900
13.239998	0.5253173	8.854889900	26.957230	1.6788139	6.973434400	23.872177	1.8409662	5.543289210
13.239998	1.0979691	8.571403500	26.959366	1.6910200	6.472663900	23.855942	1.4630432	5.435104400
13.239998	1.5787401	8.185799600	26.969768	1.6907654	5.971776900	23.855820	0.9678683	5.445723500
13.239998	2.2372141	8.191214600	28.432983	0.0000000	8.923834810	23.850540	0.4829558	5.552112600
13.239998	2.7671642	7.936422300	28.435516	0.5035268	8.839376400	23.849945	0.0000000	5.480190300
13.239998	2.8483087	7.282396300	28.433823	0.9718443	8.640609700	26.953262	1.6929741	5.520196910
13.239998	2.8114061	6.634428000	28.426285	1.3321495	8.282444000	26.940323	1.4043455	5.558596600
13.239998	2.4954042	6.089308700	28.420990	1.5627708	7.827078800	26.936279	0.9289543	5.868654400
16.429108	0.0000000	8.939050710	28.423691	1.6276817	7.321527500	26.933533	0.4746038	5.671554600
16.428986	0.6114895	8.895422000	28.423798	1.6208820	6.810544000	26.933487	0.0000000	5.606169700
16.427983	1.1782858	8.682560000	28.428085	1.6278219	6.299611100	28.438095	1.6290388	5.623371110
16.434341	1.6870451	8.361007700	28.442627	1.6164026	5.789165500	28.421432	1.3282881	5.639211700
16.428437	2.2952356	8.290433900	30.761002	0.0000000	8.918388410	28.416946	0.8805089	5.775707200
16.432297	2.4785501	7.730806400	30.761002	0.4970595	8.827903700	28.416656	0.4509697	5.730981600
16.428482	2.4784088	7.118317600	30.761002	0.9552400	8.622685400	28.417343	0.0000000	5.657381100
16.425522	2.4915514	6.505960500	30.761017	1.3085413	8.265527700	30.773056	1.6295404	5.824080510
16.428421	2.3335943	5.938472700	30.761002	1.5700121	7.834810900	30.773056	1.2827339	5.800822300
18.830946	0.0000000	8.939308210	30.761017	1.6472712	7.338638300	30.773056	0.6504359	5.897216800
18.830780	0.6015922	8.857445700	30.761002	1.6413708	6.833274800	30.773071	0.4332541	5.781866100
18.829712	1.1878748	8.701623900	30.761002	1.6388779	6.327983900	30.773056	0.0000000	5.716668100
18.835739	1.7537479	8.524406400	30.761002	1.6295509	5.822973300	35.999969	1.3129187	6.353290610
18.825607	2.2591143	8.284925500	36.000000	0.0000000	8.890000310	35.999969	1.0792589	6.037482300
18.832809	2.2711515	7.675120400	35.999969	0.4268687	8.821646700	35.999969	0.7593449	5.810174900
18.830536	2.2706423	7.067986500	35.999969	0.8200570	8.642345400	35.999969	0.3865908	5.681399300
						36.000000	0.0000000	5.619998000

4.3 External Units

There are a total of 50 external units required although they are not simultaneously used. A list of the unit numbers and types follows:

1. Direct access data sets:

   Unit #20 - 400 records, each 200 words long - potential flow velocity

   Unit #61 - 3280 records, each 990 words long - used for quasi-3-D boundary-layer program

   Unit #62 - 41 records, each 990 words long - used for quasi-3-D boundary-layer program

2. Sequential data sets: This includes units 3, 4, 5, 8, 9, 10, 11, 12, 13, 14, 15, 16, 17, 18, 19, 22, 23, 24, 25, 26, 27, 28, 29, 30, 31, 32, 33, 34, 35, 36, 38, 39, 40, 41, 42, 43, 44, 45, 56, 47, 51, 63, 64, 65, 66, 67.

   Unit #29 is the geometry data set for the input body. These datasets are used both for the inviscid velocity calculation and for the communication between the viscous and the inviscid parts of the calculation.

3. Datasets required to be saved:

   Unit #34 - This unit contains the inviscid velocities and control points.

   Unit #33 - This unit contains the blowing velocities and the displacement thickness values for viscous/inviscid interactive runs.

   Unit #51 - This unit contains some input data to the 2-D boundary-layer program.

   Unit #47 - This unit contains the blowing velocities from the 3-D boundary-layer program.

4.4 CRAY JCL

An example of the JCL required for the execution of the program on CRAY using the two-dimensional strip theory boundary-layer procedure, follows. Example 1 is for an initial calculation with the appropriate data saved for subsequent runs and example 2 shows how the previously saved data is used to make additional calculations.

Example 1

```
JOB,JN=xxxxx  ,T=900,MFL=2000000.
ACCOUNT,US=xxxxxx  ,UPW= xxxxx ,AC=xxxxxxxx  .
*.
COPYF,I=$IN,O=INPUT. COPY INPUT FILE
REWIND,DN=INPUT.
*.
COPYF,I=$IN,O=GEOM.  COPY INPUT FILE
REWIND,DN=GEOM.
*.
ACCESS,DN=KCMCAIR,PDN=KCMCAIRCRAY,ID=OBJLIB.
STATIC,LEVEL=NEW.
BUILD,I=0,L=0,OBL=KCMCAIR,B=0,NBL=MCARBIN,NODIR.   CREATE SEQUENTIAL BIN
*.
ASSIGN,DN=INPUT,A=FT05.   ALLOCATE APPROPRIATE FILES
ASSIGN,DN=$OUT,A=FT06.
ASSIGN,DN=GEOM,A=FT29.
ASSIGN,DN=FILE34,A=FT34.
ASSIGN,DN=FILE33,A=FT33.
ASSIGN,DN=FILE51,A=FT51.
*.
MODE,FI=DISABLE.
*.
SEGLDR,CMD='BIN=MCARBIN'.   LINK BINARIES
SABD.  EXECUTE LOAD MODULE
*.                                                           saved for
SAVE,DN=FILE34,PDN=INVELNEW.  SAVE OUTPUT DATASET FOR THE NEXT CAL.  future
SAVE,DN=FILE33,PDN=BLOW2DNEW.                                runs
SAVE,DN=FILE51,PDN=BL2DINPNEW.
*.
EXIT.
/EOF
F15 WITH LAMINAR BUBBLE WING, MULTIPLE ALPHAS, M=0.6
 &A LIFT3D=1,IBL3D=0,MAXCYC=2,MLINE=51,NLINE=14,
  MAXANG=2,ALPHAI(1)=6.95,ALPHAI(2)=8.95,AMACH(1)=0.60,
  AMACH(2)=0.6,&END
 &B BOV2=13.008,IAUTOW=2,NSYM1=1,LIFSEC=1,NSTRIP=13,            input
  IXFLAG(1)=3,NSORCE=50,NWAKE=1,RFAREA=96.7,REFCHD=8.325,&END   data set
 6.022      8.325      0.0       0.0
 61.0       2.0        10.0      0.0
 51.0       2.0        5.0       0.0
 6.022      8.325      1.0       0.0
 61.0       2.0        10.0      0.0
 51.0       2.0        5.0       0.0
/EOF
 32.966003 13.008000 5.949856821
 32.924698 13.008000 5.950995400
 32.863266 13.008000 5.952991500
 32.782425 13.008000 5.956209200
 32.683380 13.008000 5.959699600
 32.567581 13.008000 5.961723300
     .         .          .                                  geometry
     .         .          .                                  data set
     .         .          .
 43.000000 1.3186102 5.600000400
 43.000000 0.5522600 5.600000400
 43.000000 0.1862400 5.600000400
 43.000000 0.0000000 5.600000400
/EOF
```

Example 2

```
JOB,JN=xxxxxx ,T=1200,MFL=2400000.
ACCOUNT,US=xxxxxxx ,UPW=xxxxxxx,AC=xxxxxxxxx .
*.
COPYF,I=$IN,O=INPUT. COPY INPUT FILE
REWIND,DN=INPUT.
*.
COPYF,I=$IN,O=GEOM.  COPY INPUT FILE
REWIND,DN=GEOM.
*.  ACCESS PERMANENT DATASETS
ACCESS,DN=KCMCAIR,PDN=KCMCAIRCRAY,ID=OBJLIB.
ACCESS,DN=DUMMY34,PDN=INVELNEW.                                   data from
ACCESS,DN=DUMMY33,PDN=BLOW2DNEW.                                  previous
ACCESS,DN=DUMMY51,PDN=BL2DINPNEW.                                 run
*.                    COPY DATASETS
*.                    COPY FILE34
REWIND,DN=DUMMY34.
COPYR,I=DUMMY34,O=FILE34,NR.
REWIND,DN=FILE34.
*.                    COPY FILE33
REWIND,DN=DUMMY33.
COPYR,I=DUMMY33,O=FILE33,NR.
REWIND,DN=FILE33.
*.                    COPY FILE51
REWIND,DN=DUMMY51.
COPYR,I=DUMMY51,O=FILE51,NR.
REWIND,DN=FILE51.
*.
STATIC,LEVEL=NEW.
BUILD,I=0,L=0,OBL=KCMCAIR,B=0,NBL=MCARBIN,NODIR.   CREATE SEQUENTIAL BIN
*.
ASSIGN,DN=INPUT,A=FT05.   ALLOCATE APPROPRIATE FILES
ASSIGN,DN=$OUT,A=FT06.
ASSIGN,DN=GEOM,A=FT29.
ASSIGN,DN=FILE34,A=FT34.
ASSIGN,DN=FILE33,A=FT33.
ASSIGN,DN=FILE51,A=FT51.
*.
MODE,FI=DISABLE.
*.
SEGLDR,CMD='BIN=MCARBIN'.   LINK BINARIES
$ABD.   EXECUTE LOAD MODULE
*.                                                                saved for
SAVE,DN=FILE34,PDN=INVELNEW.   SAVE OUTPUT DATASET FOR THE NEXT CAL.  future
SAVE,DN=FILE33,PDN=BLOW2DNEW.                                     runs
SAVE,DN=FILE51,PDN=BL2DINPNEW.
*.
EXIT.
/EOF
F15 WITH LAMINAR BUBBLE WING, MULTIPLE ALPHAS, M=0.6
 &A LIFT3D=1,IBL3D=0,MAXCYC=2,MLINE=51,NLINE=14,
  MAXANG=2,ALPHAI(1)=7.95,ALPHAI(2)=8.95,AMACH(1)=0.60,
  AMACH(2)=0.6,&END
 &B BOV2=13.008,IAUTOW=2,NSYM1=1,LIFSEC=1,NSTRIP=13,
  IXFLAG(1)=3,NSORCE=50,NWAKE=1,RFAREA=96.7,REFCHD=8.325,&END     input
 6.022      8.325      1.0        0.0                             data set
 61.0       2.0        10.0       0.0
 51.0       2.0        5.0        0.0
 6.022      8.325      1.0        0.0
 61.0       2.0        10.0       0.0
 51.0       2.0        5.0        0.0
/EOF
 32.966003 13.008000 5.949856821
 32.924698 13.008000 5.950995400
 32.863266 13.008000 5.952991500
 32.782425 13.008000 5.956209200                                  geometry
      .         .         .                                       data set
      .         .         .
      .         .         .

 43.000000 0.5522600 5.600000400
 43.000000 0.1862400 5.600000400
 43.000000 0.0000000 5.600000400
/EOF
```

SECTION V
TEST CASES

Three test cases were investigated: (1) F-15 with laminar bubble wing, (2) Advanced Navy Fighter (ANF), and (3) unmodified F-15.

5.1 Test Case 1 - F-15 with Laminar Bubble Wing

The coordinates of the geometry for test case 1 are given in model scale (4.7%) in inches. 1084 panels defined this configuration with 600 of them describing the wing, as shown in Figure 26. All of the calculations use the symmetry option of the program so that the given number of panels are for only half the configuration.

Inviscid and viscous calculations for Case 1 were made to compare with test data [32] at a Mach number ≈0.6, Rc ≈ 8.5 x 10^6/ft and a range of angle of attack from 6.84° through 15.83°. Viscous solutions were calculated by both the two-dimensional strip theory boundary layer and the quasi-three-dimensional boundary-layer procedures, and the location of transition was calculated by the program using Michel's criterion.

The input required to execute the two-dimensional strip theory boundary-layer procedure for case 1 was:

1. A data set, Unit 29, Format (3F10.0, 2I1), containing the x,y,z coordinates of the geometry, and

2. A data set, Unit 5, containing the flags, geometry and flow parameters, and boundary-layer parameters.

```
F15 - LAMINAR BUBBLE WING, A=6.84, M=0.6, TRANS. CALC.
 &A LIFT3D=1,IBL3D=0,MAXCYC=2,MLINE=51,NLINE=14,
  MAXANG=1,ALPHAI(1)=6.84,AMACH=0.60,&END
 &B BOV2=13.008,IAUTOW=2,NSYM1=1,LIFSEC=1,NSTRIP=13,
  NSORCE=50,NWAKE=1, RFAREA=96.7,REFCHD=8.325,&END
 6.022       8.325      0.0        0.0
 81.0        2.0        10.0
 51.0        2.0        5.0
```

If more calculations are desired for additional, higher angles of attack, the results of the calculations of a lower angle of attack may be used for the initial guess for these calculations. The data saved on units 33 and 51 from the first calculation is now used as input for the additional calculations and the namelist block input will appear as:

```
F15 WITH LAMINAR BUBBLE WING, MULTIPLE ALPHAS, M=0.6
 &A LIFT3D=1,IBL3D=0,MAXCYC=2,MLINE=51,NLINE=14,
  MAXANG=2,ALPHAI(1)=10.75,ALPHAI(2)=12.95,
  AMACH=0.6,&END
 &B BOY2=13.008,IAUTOW=2,NSYM1=1,LIFSEC=1,NSTRIP=13,
  NSORCE=50,NWAKE=1, RFAREA=96.7,REFCHD=8.325,&END
 6.022      8.325      1.0        0.0
 61.0       2.0        10.0
 51.0       2.0        5.0
 6.022      8.325      1.0        0.0
 61.0       2.0        10.0
 51.0       2.0        5.0
```

To execute the program using the quasi-three-dimensional boundary-layer procedure, the input is identical to that of the two-dimensional strip theory boundary-layer procedure with the exception of the following flags in Namelist A: IBL3D = 1, INTF = 1.

5.2 Test Case 2 - Advanced Navy Fighter (ANF)

Geometry data for the Advanced Navy Fighter consisted of 6% model scale coordinates given in inches. The configuration (Figure 27) was defined by approximately 1200 panels which provided for 360 panels to describe the wing and 192 panels to describe the canard. Since the boundary-layer effects can be calculated on only one lifting section, this configuration was first run without the canard (Figure 27a) and the results were compared with experiment (Figures 15 and 16). Calculations with the canard on (Figure 27b) were then made and the effect was compared with the canard off case (Figure 17).

Because the wing is mounted so low on the fuselage the wing extra strip would protrude through the fuselage if it were defined as a continuation of the wing to the centerline as is usually done. Therefore the extra strip was tilted "up" so that it fell completely inside the fuselage so as not to change the fuselage geometry, See Figure 28.

Calculations for test case 2 were made for $M = 0.5988$, $R_L = 7.0\times10^6$/ft, $C_L = 0.45$ and $\alpha = 7.7182°$ to compare pressure data given in Reference 34. Viscous solutions were obtained with the strip theory boundary-layer procedure being used to calculate the viscous effects. As in test case 1, the transition location was calculated by the program using Michel's criterion. The namelist block input for this case was:

```
 ANF. NO CANARD.,TRANS. CALC., 2DSTRIP BL, M=0.6
&A  LIFT3D=0,IBL3D=0,
 MAXCYC=2,NLINE=8,MLINE=51,
 MAXANG=1,ALPHAI(1)=7.7182,AMACH=0.6,&END
&B BOV2=12.955,IAUTOW=2,NSYM1=1,LIFSEC=1,REFCHD=8.2912,
 LINEAR=0,IXFLAG(1)=3,IPCV=1,
 RFAREA=95.904,NSORCE=50,NSTRIP=7,NWAKE=1,&END
7.0        12.0       0.0        0.0
70.0       2.0        10.0
51.0       2.0        5.0
```

A series of calculations at various angles of attack were made to compare the calculated and experimental lift coefficients for the canard-off case. These calculations were repeated for the configuration with the canard to compare the calculated effect of the canard. The namelist block input for the configuration with canard for multiple angles of attack was:

```
 ANF. CANARD.,TRANS. CALC., 2DSTRIP BL, M=0.6, MULT. ALPHAS
&A  LIFT3D=1,IBL3D=0,
 MAXCYC=2,NLINE=8,MLINE=51,
 MAXANG=6,ALPHAI(1)=1.3,ALPHAI(2)=3.4,ALPHAI(3)=4.7,
 ALPHAI(4)=6.0,ALPHAI(5)=7.7182,ALPHAI(6)=9.2,AMACH=0.6,&END
&B BOV2=12.955,IAUTOW=2,NSYM1=1,LIFSEC=2,REFCHD=8.2912,
 LINEAR=0,IXFLAG(1)=3,IXFLAG(2)=3,IPCV=1,RFAREA=95.904,
 NSORCE(1)=50,NSORCE(2)=48,NSTRIP(1)=7,NSTRIP(2)=5,NWAKE(1)=1,
 NWAKE(2)=1,&END
7.0        12.0       0.0        0.0
70.0       2.0        10.0
51.0       2.0        5.0
7.0        12.0       0.0        0.0
70.0       2.0        10.0
51.0       2.0        5.0
7.0        12.0       0.0        0.0
70.0       2.0        10.0
51.0       2.0        5.0
7.0        12.0       0.0        0.0
70.0       2.0        10.0
51.0       2.0        5.0
7.0        12.0       0.0        0.0
70.0       2.0        10.0
51.0       2.0        5.0
7.0        12.0       0.0        0.0
70.0       2.0        10.0
51.0       2.0        5.0
```

5.3 Test Case 3 - Unmodified F-15

The unmodified F-15 geometry coordinates were full scale in inches. This configuration [35] was defined by 981 panels, 450 of which described the wing (Fig. 29). The wing is mounted high on the fuselage and as in the case of the Advanced Navy fighter configuration, the extra strip had to be tilted, in this case "down", so as not to protrude through the top of the nacelle. Figure 30 shows the arrangement of the panels on the wing used in the calculations of test case 3. The measured data was obtained with a sting-mounted fuselage/wing configuration which included the vertical tail. The computed results, however, were for a configuration without the vertical tail.

Viscous and inviscid calculations were made for this configuration to compare with experiment [35] at $M = 0.6$, $R_L/ft = 5.78 \times 10^6$ for a range of angle of attack, $2.21° \leq \alpha \leq 8.66°$. The two-dimensional strip theory boundary-layer procedure was used in the interaction calculation to compute the viscous results. The namelist block input for test case 3 follows:

```
NEW F15 CONFIGURATION, M=0.8, STRIP2D BL, TRANSITION INPUT
&A LIFT3D=1,IBL3D=0,
 MAXCYC=2,NLINE=11,MLINE=61,
 MAXANG=2,ALPHAI(1)=4.36,ALPHAI(2)=6.51,
 AMACH=0.6,KINKNO=1,MS=6,&END
&B BOY2=256.20,IAUTOW=2,NSYM1=1,LIFSEC=1,
 IXFLAG(1)=3,IPCY=1,REFCHD=191.23,RFAREA=43776.,NSORCE=60,
 NSTRIP=10,NWAKE=1,&END
4.33       191.23     0.0        0.0
71.0       0.0        10.0       6.0
254.0      220.0      185.0      150.0      115.0      80.0
0.05       0.05       0.05       0.05       0.05       0.05
61.0       0.0        5.0        6.0
254.0      220.0      185.0      150.0      115.0      80.0
-0.05      -0.05      -0.05      -0.05      -0.05      -0.05
4.33       191.23     1.0        0.0
71.0       0.0        10.0       6.0
254.0      220.0      185.0      150.0      115.0      80.0
0.05       0.05       0.05       0.05       0.05       0.05
61.0       0.0        5.0        6.0
254.0      220.0      185.0      150.0      115.0      80.0
-0.05      -0.05      -0.05      -0.05      -0.05      -0.05
```

SECTION VI
CONCLUSIONS AND RECOMMENDATIONS

An interactive viscous/inviscid procedure has been developed for the computation of viscous flow over 3-D wing/body configurations. The method developed makes use of a three-dimensional surface-source panel method developed by Hess [11] and an inverse finite-difference boundary-layer procedure of [6].

Two alternative boundary-layer formulations have been considered, the first is a two-dimensional strip theory implementation [4] and the second [10] is a quasi-three-dimensional boundary-layer method. These procedures have been coupled with the external potential flow calculation via an interface routine which handles the necessary interpolation and transfer of data between the viscous and the inviscid parts of the calculation.

The present method is able to compute flows with both leading- and trailing-edge separations. In most of the cases considered here, the calculations were performed by computing transition by an empirical formula, which, at higher angles of attack, resulted in a separated region as much as 35% upstream of the trailing edge. However, at the conditions approaching stall, a small change in transition location led to regions of massive flow separation on the wing, which the present method handled without any numerical difficulties.

The studies conducted here indicate that at lower angles of attack there is very little difference between the results computed by either of the two boundary-layer procedures. However, at higher angles of attack, for which there are significant regions of flow separation, the quasi-three-dimensional boundary-layer procedure has been found to provide a useful improvement in the results when compared with the experimental data.

The inviscid method used here is general and can be applied to complex aircraft configurations. The viscous effects, however, are limited to the wing alone with some approximations. For example, the use of either two-dimensional strip theory or the quasi-three-dimensional boundary-layer approximation is satisfactory at low to medium angles of attack. At higher angles of attack, the flow becomes "more" three dimensional and the calculations should use the complete equations. Furthermore, the effect of the viscous wakes neglected in the solution procedure also becomes important at higher angles of attack and needs to be included in the solution procedure.

The viscous capabilities of the present computer code can also be extended to the other components of the airplane configurations to include, for example, multiple lifting sections, as well as the fuselage and other nonlifting components.

SECTION VII
REFERENCES

1. J. S. Shang, and S. J. Scherr, Navier-Stokes Solution of the Flow Field Around a Complete Aircraft. AIAA Paper 85-1509, 1985.

2. B. R. Gilmer, and D. R. Bristow, "Analysis of Stalled Airfoils by Simultaneous Perturbations to Viscous and Inviscid Equations." AIAA J. 20, 1982, pp. 1160-1166.

3. G. Maskew, and F. A. Dvorak, "Investigation of Separation Models for the Prediction of $C_{L\,max}$." J. Am. Helicopter Soc. 23, 1978, pp. [illegible]

4. T. Cebeci, R. W. Clark, K. C. Chang, N. D. Halsey, and K. Lee, "Airfoils with Separation and the Resulting Wakes," J. Fluid Mechanics, 163, 1986, pp. 323-347.

5. N. D. Halsey, "Potential Flow Analysis of Multielement Airfoils Using Conformal Mapping," AIAA J. 17, 1979, pp. 1281-1288.

6. T. Cebeci, Separated Flows and Their Representation by Boundary Layer Equations, Mech. Engg. Dept. Rept. ONR CR215-234-2, California State University, Long Beach, 1976.

7. T. Cebeci, and A.M.O. Smith, Analysis of Turbulent Boundary Layers, Academic Press, N.Y., 1974.

8. T. A. Reyhner, and I. Flugge-Lotz, "The Interaction of a Shock Wave with a Laminar Boundary Layer," Int. J. on Nonlinear Mech. [illegible] 173-199.

9. U. Mehta, K. C. Chang, and T. Cebeci, "Relative Advantages [illegible] and Thin Navier Stokes Procedures." In Numerical and Physical Aspects of Aerodynamic Flows III (Ed. T. Cebeci) Springer-Verlag [illegible] TM 86778.)

10. T. Cebeci, K. Kaups, and A. A. Khattab, Studies of Interactive Procedures for Three-Dimensional Flows. Pt. I, Separation and Reattachment Near the Leading Edge of a Thin Wing. Douglas Aircraft Co. Rept. MDC J3835, 1985.

11. J. L. Hess, "The Problem of Three Dimensional Lifting Flow and Its Solution by Means of Surface Singularity Distribution," Comp. Meth. in Appl. Mech. and Engg. 4, 1974.

12. R. J. Margason, S. O. Kjelgaard, W. L. Sellers, III, C. E. K. Morris, Jr., K. B. Walkley, and E. W. Shields, Subsonic Panel Methods - A Comparison of Several Production Codes. AIAA Paper No. 85-280, 1985.

13. J. L. Hess, and A. M. O. Smith, "Calculation of Nonlifting Potential Flow About Arbitrary Three Dimensional Bodies," J. Ship Research, Vol. 8, No. 2, 1964. (An expanded version is given in Douglas Aircraft Company Report No. ES 40622, 1962.)

14. R. W. Clark, A New Iterative Matrix Solution Procedure for Three-Dimenisonal Panel Methods, AIAA Paper No. 85-0176, 1985.

15. P. G. William, "A Reverse Flow Computation in the Theory of Self Induced Separation," Proc. 4th Int. Conf. Numer. Meth. Fluid Mech., Lecture Notes in Phys. 35, 1975, p. 445.

16. P. Bradshaw, T. Cebeci, and J. H. Whitelaw, Engineering Calculation Methods for Turbulent Flow, Academic Press, London, 1981.

17. T. Cebeci, "Calculation of Unsteady Two-Dimensional Laminar and Turbulent Boundary Layers with Fluctuations in External Velocity," Proc. Royal Soc. London, Series A 355, 1977, pp. 225 238.

18. J. C. LeBalleur, "Couplage Visqueux Non Visquex: Methode Numerique et Applications Aux Ecoulements Bidimensionnels Transsonique Set Supersoniques," Le Recherche Aerospatiale, No. 1978 2, 1978, pp. 65 76.

19. J. E. Carter, A New Boundary Layer Inviscid Iteration Technique for Separated Flow, AIAA Paper 79 1450, 1979.

20. J. E. Carter, Viscous-Inviscid Interaction Technique for Separated Flow, AIAA Paper 81-1241, 1981.

21. J. E. Carter, and V. N. Vasta, Analysis of Airfoil Leading-Edge Separation Bubbles, NASA Contractor Rept. 165935, Contract NAS1-16585, 1982.

22. J. C. LeBalleur, "Numerical Viscid-Inviscid Interaction in Steady and Unsteady Flows," In Numerical and Physical Aspects of Aerodynamic Flows II (Ed. T. Cebeci), Springer-Verlag, N.Y., 1984.

23. A. E. P. Veldman, "New Quasi-Simultaneous Method to Calculate Interacting Boundary Layers," AIAA J. 19, 1981, p. 769.

24. T. Cebeci, and P. Bradshaw, Momentum Transfer in Boundary Layers, McGraw-Hill/Hemisphere, 1977.

25. M. J. Nituch, S. Sjolander, and M. R. Head, "An Improved Version of the Cebeci-Smith Eddy-Viscosity Model," Aero. Quarterly XXIX, 1978.

26. M. R. Head, "Eddy Viscosity in Turbulent Boundary Layers," Aero. Quarterly XXVII, 1976.

27. A. Nakayama, Measurements in the Boundary Layer and Wake of Two Airfoil Models, Douglas Aircraft Co. Rept. MDC J2403, 1982.

28. R. L. Simpson, Y. T. Chew, and B. G. Shivaprasad, "The Structure of a Separating Turbulent Boundary Layer. Pt. 1, Mean Flow and Reynolds Stresses," J. Fluid Mech. 113, 1981, p. 23.

29. T. Cebeci, and P. Bradshaw, Physical and Computational Aspects of Convective Heat and Momentum Transfer, Springer-Verlag, New York, 1984.

30. D. A. Lovell, A Wind Tunnel Investigation of the Effects of Flap Span and Deflection Angle, Wing Planform and a Body on the High Lift Performance of a 28° Swept Wing, RAE CP 1372, 1977.

31. L. P. Yip, and G. L. Shubert, Pressure Distributions on a 1- by 3-Meter Semispan Wing at Sweep Angles from 0° to 40° in Subsonic Flow, NASA TN D-8307, 1976.

32. K. E. Tatum, and J. Pavelka, Wind Tunnel Pressure Distribution Test Results of Short Laminar Separation Bubble Wing Design, PSWT Test 409, Rept. No. MDC A5983, 1979.

33. L. T. Chen, J. C. Vassberg, and C. C. Peavey, A Transonic Wing-Body Flowfield Calculation with Improved Grid Topology and Shock Point Operators, AIAA Paper 84-2155, 1984.

34. J. S. Althuis, Close Coupled Canard-Wing Interactions on Panel Loads Series I, McDonnell Douglas Corp. Preliminary Report MDC IR0184, 1985.

35. R. M. Anderson, Wind Tunnel Test on the 4.7 Percent Scale F-15 Model in the McDonnell Douglas Polysonic Wind Tunnel, Tests PSWT 281 and 286, Vol. I and II. McDonnell Douglas Corp. Report MDC A0974, 1971.

36. J. L. Hess, Calculation of Potential Flow about Arbitrary Three-Dimensional Lifting Bodies, McDonnell Douglas Corp. Report No. MDC J5679-01, 1972.

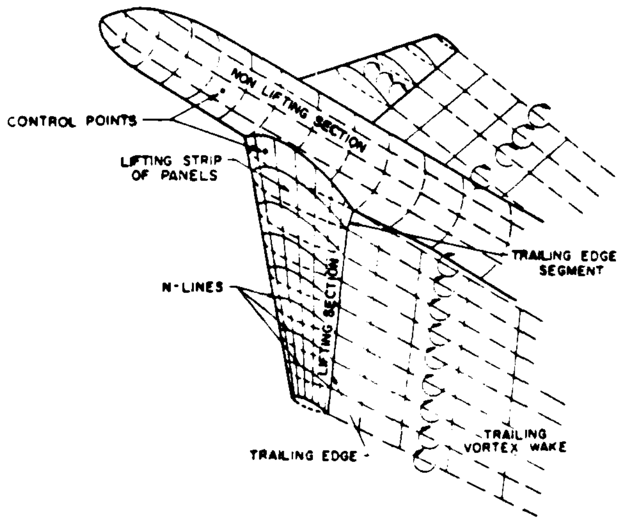

Figure 1. Wing/body configuration.

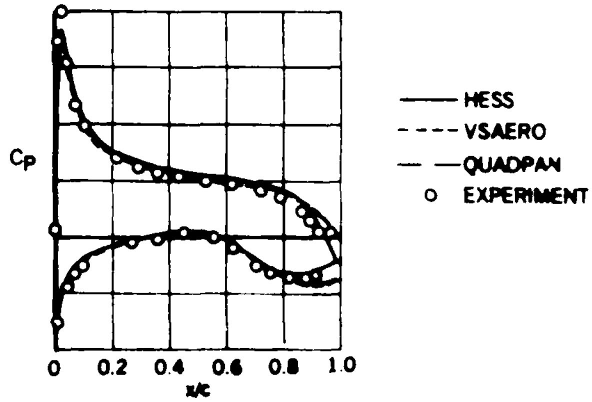

Figure 2. Effect of alternate Kutta conditions.

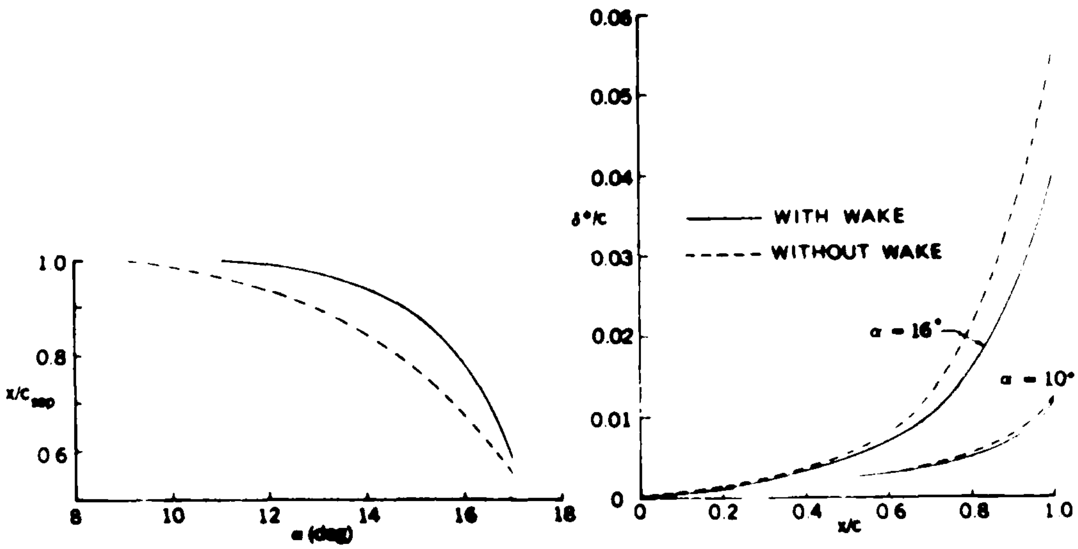

Figure 3. Effect of wake on the separation region and displacement thickness for the NACA 0012 airfoil, $R_c = 6.0 \times 10^6$.

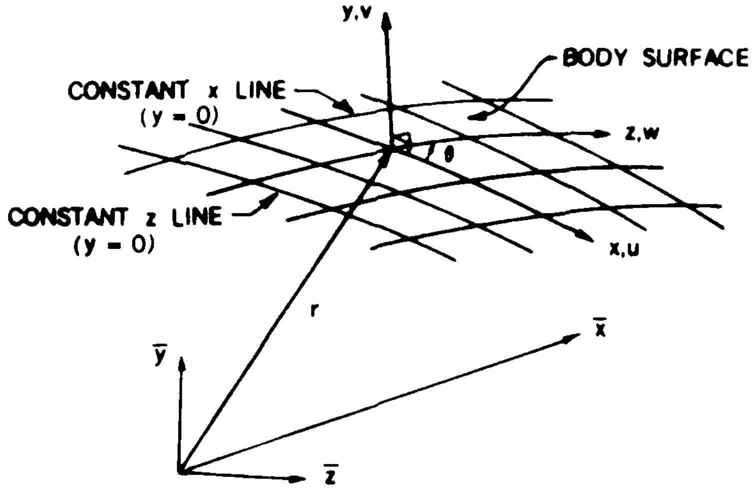

Figure 4. Notation for nonorthogonal curvilinear coordinate system on the body surface. Note that x and z are not orthogonal to each other but y is to x and z.

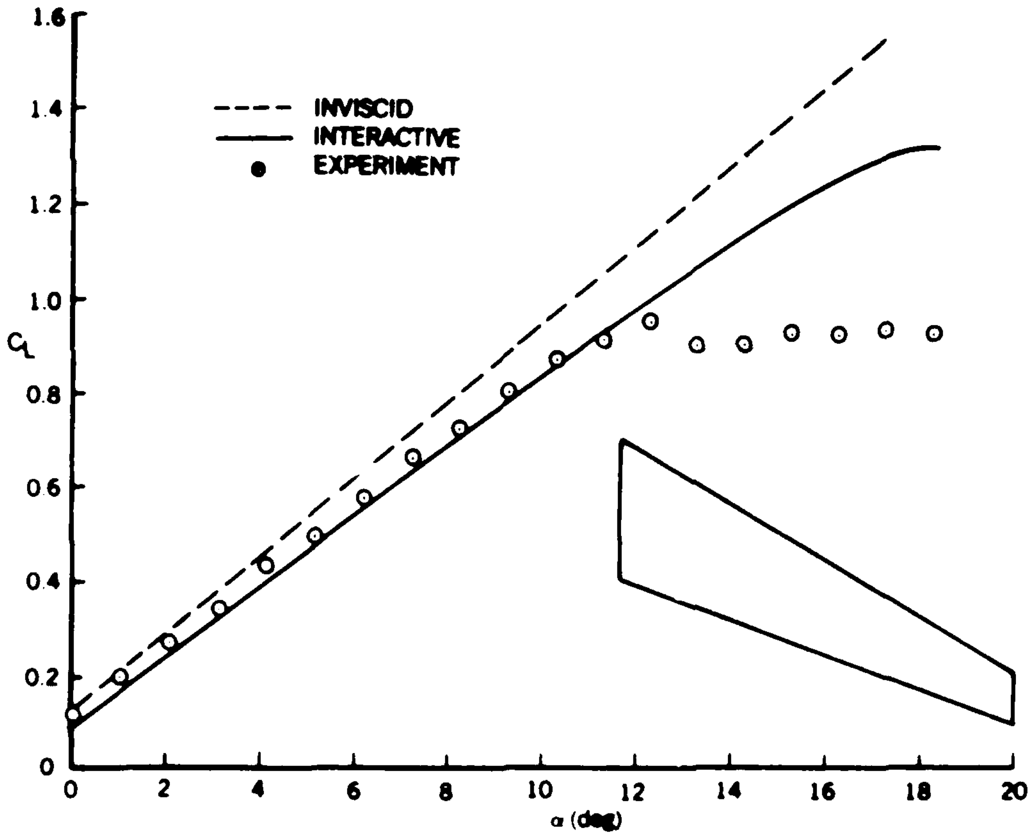

Figure 5. Comparison of computed and experimental lift curves for the RAE wing.

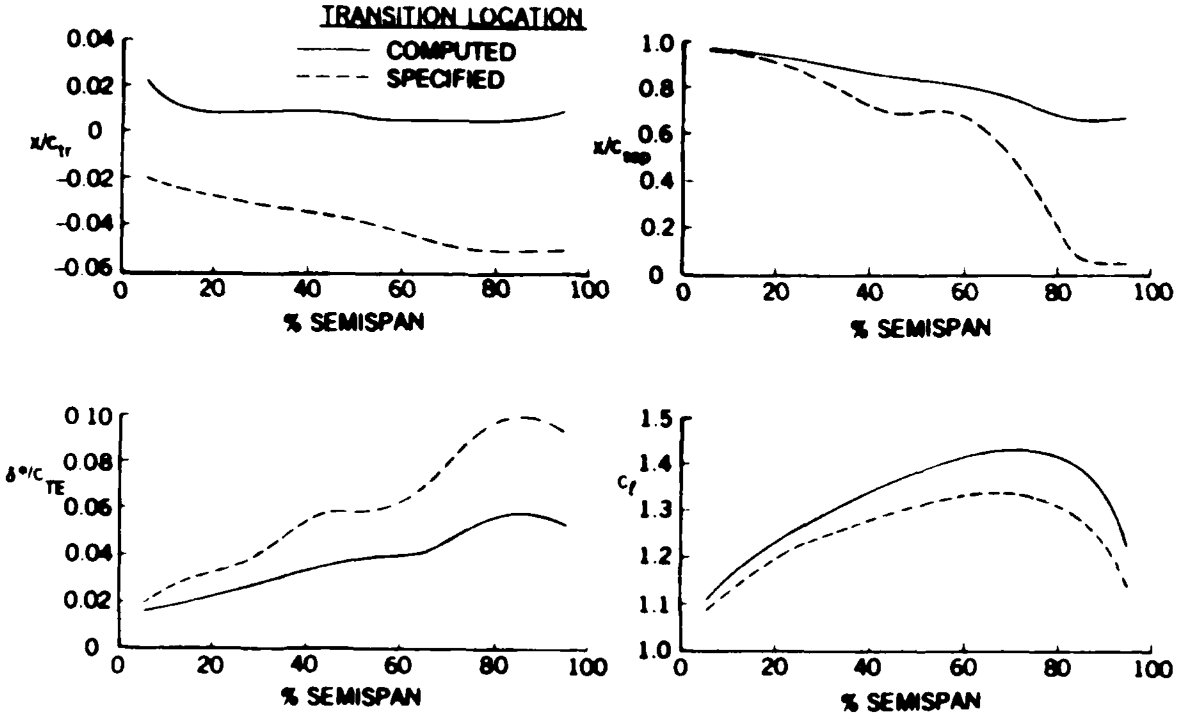

Figure 6. Effect of transition location on flow separation, displacement thickness and lift distribution for the RAE wing, α = 17.5°.

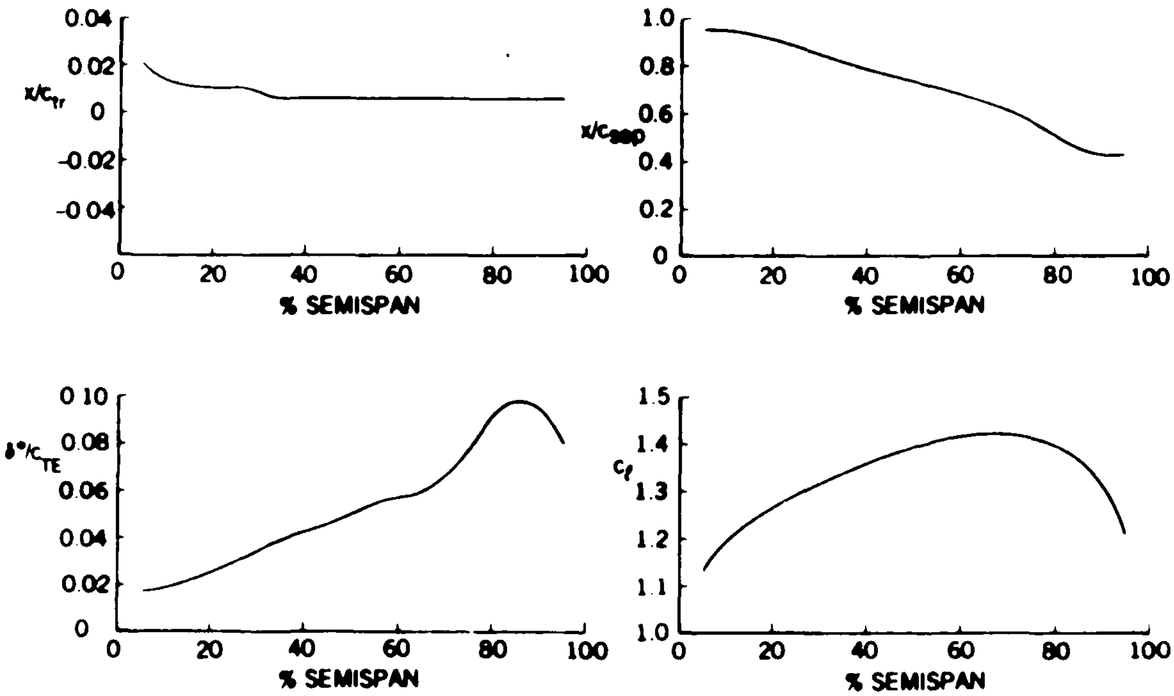

Figure 7. Computed transition location, flow separation, displacement thickness and lift distribution for the RAE wing, α = 18.5°.

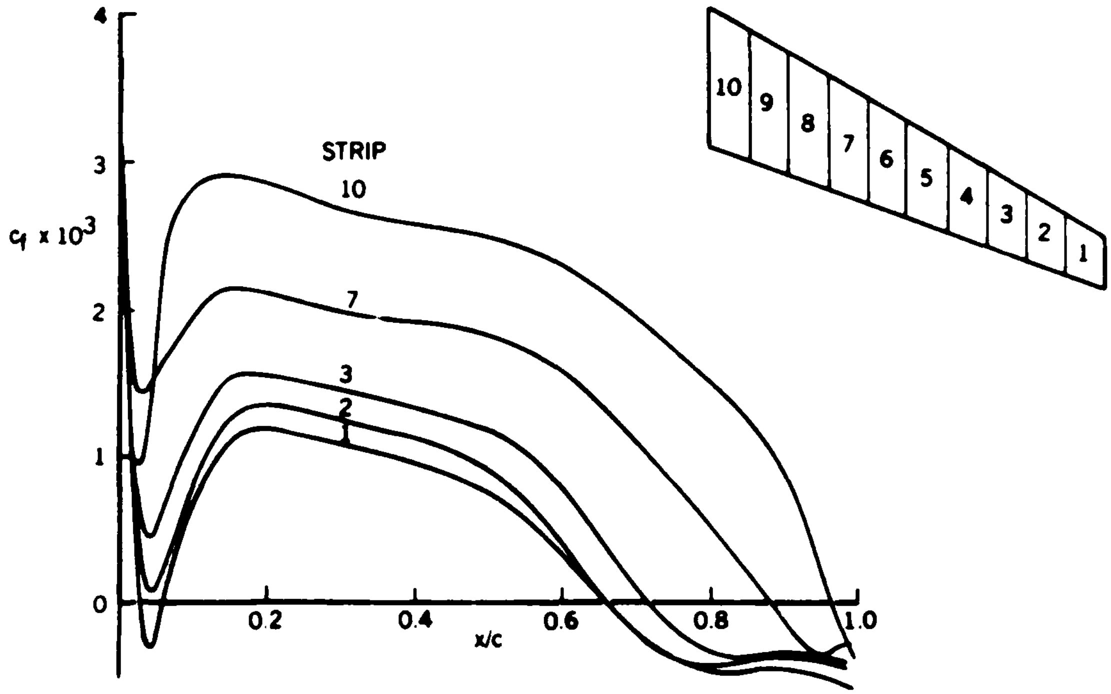

Figure 8. Leading and trailing edge separation location for the RAE wing, α = 17.5°.

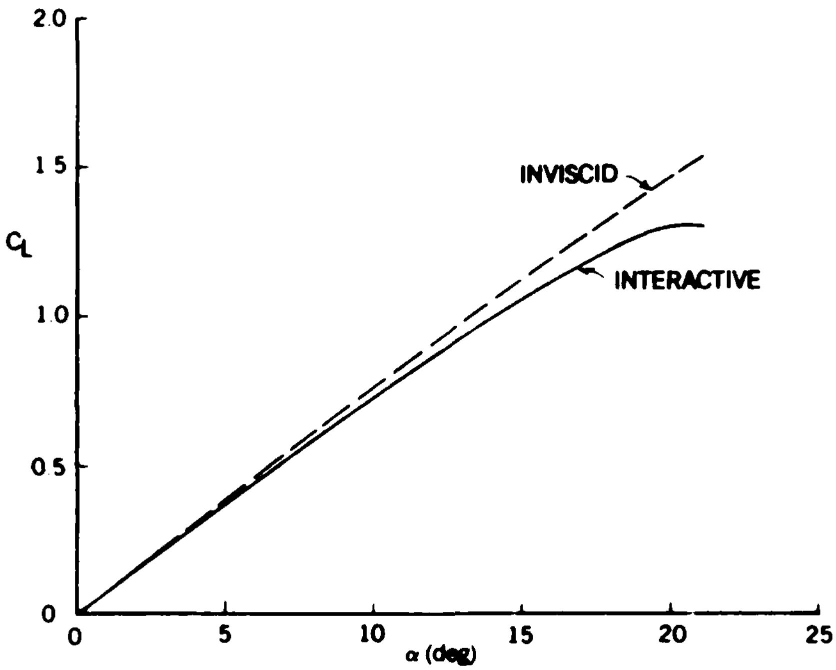

Figure 9. Computed viscous and inviscid lift curve for the NACA 0012 swept wing.

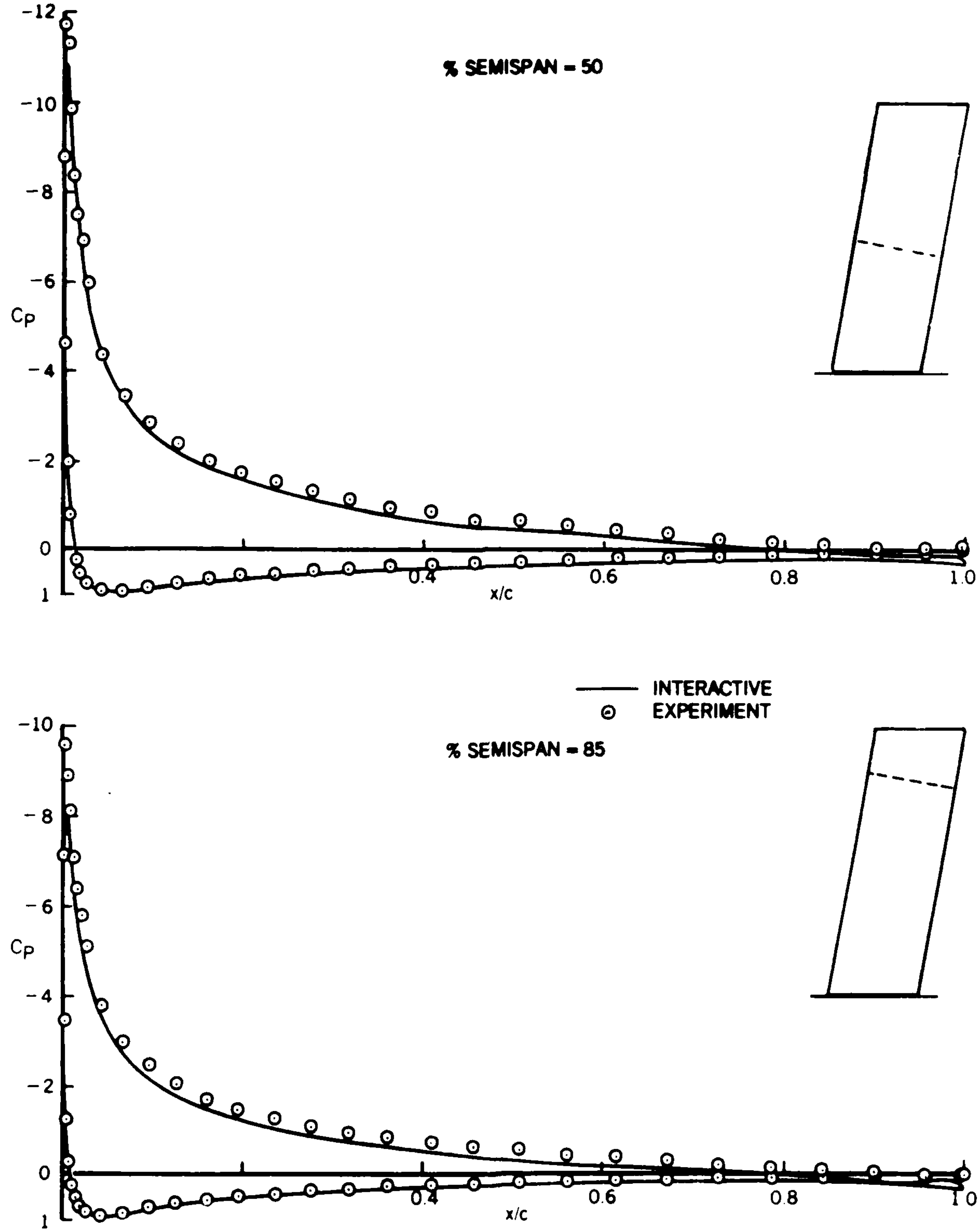

Figure 10. Comparison of calculated and experimental pressure distribution on the NACA 0012 swept wing, $\alpha = 19.35°$.

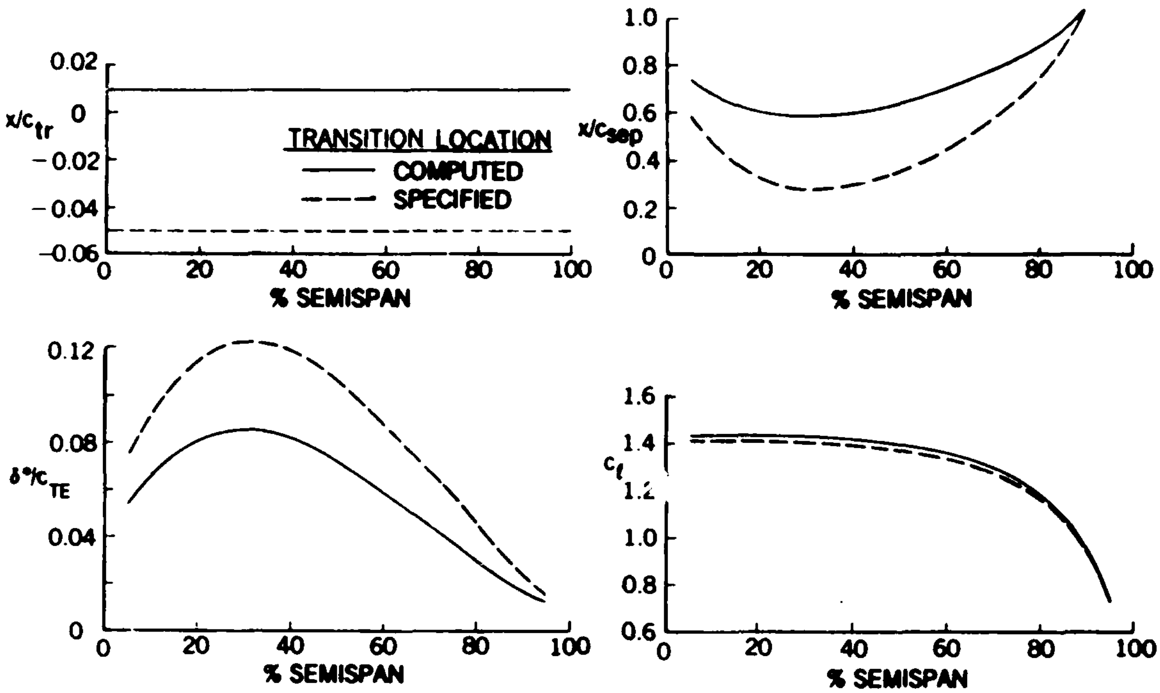

Figure 11. Effect of transition location on flow separation, displacement thickness and lift distribution for the NACA 0012 swept wing, $\alpha = 21.12°$.

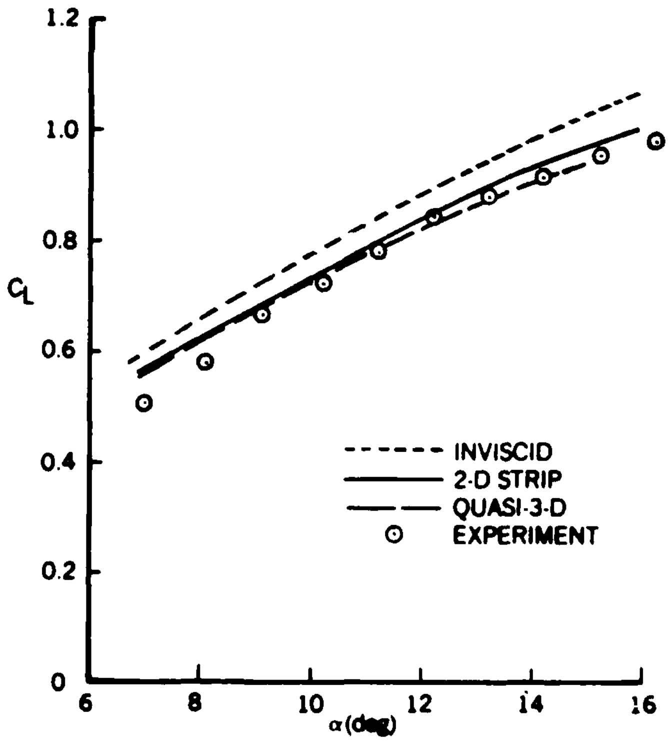

Figure 12. Comparison of 2-D strip theory and quasi-3-D methods for the F-15 fighter with laminar bubble wing.

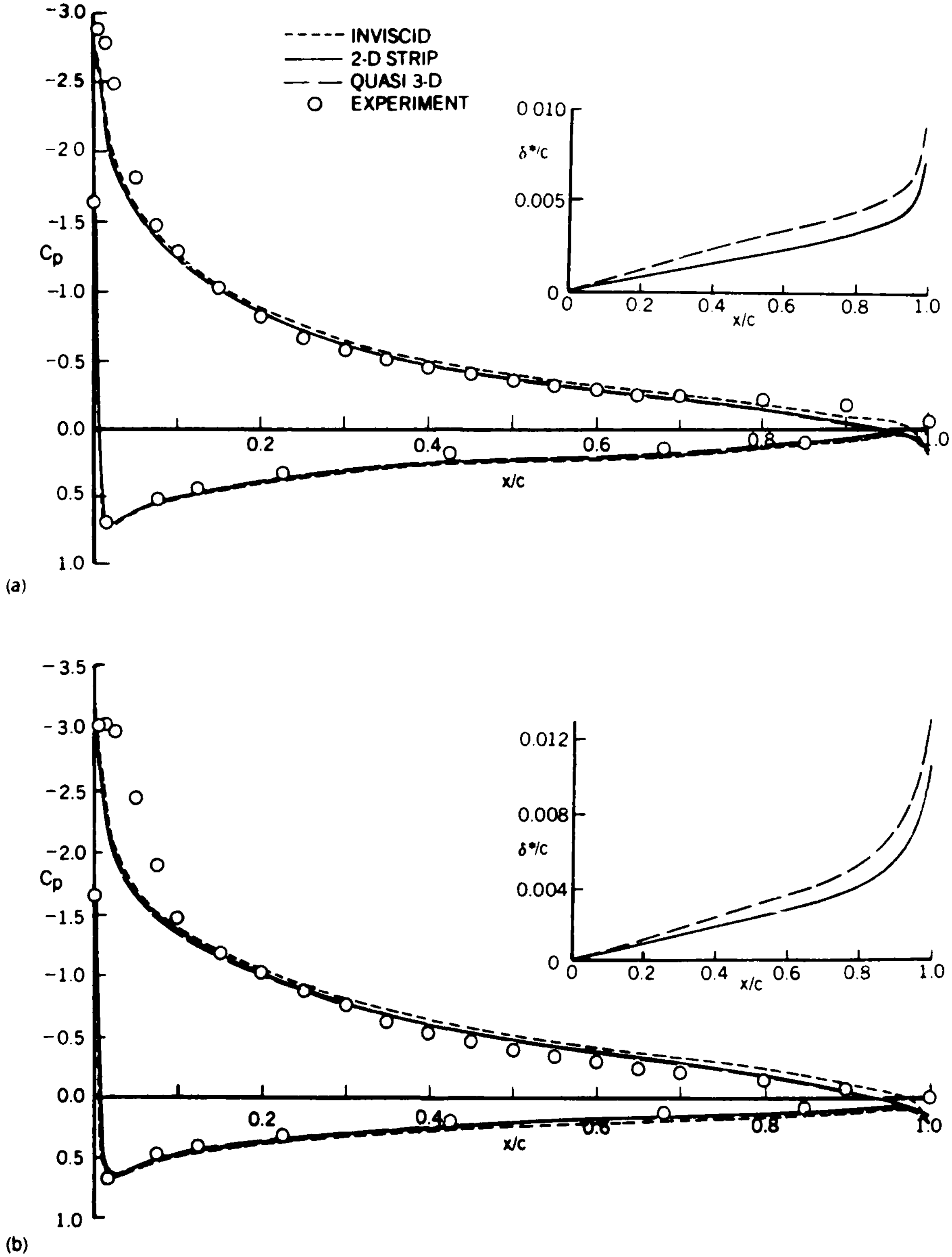

Figure 13. Comparison of the calculated and experimental pressure distribution for the F-15 with laminar bubble wing, α = 10.75°. Insert shows the chordwise variation of displacement thickness as calculated by the 2-D strip theory and the quasi-three-dimensional boundary-layer methods. (a) 38% semispan. (b) 58% semispan.

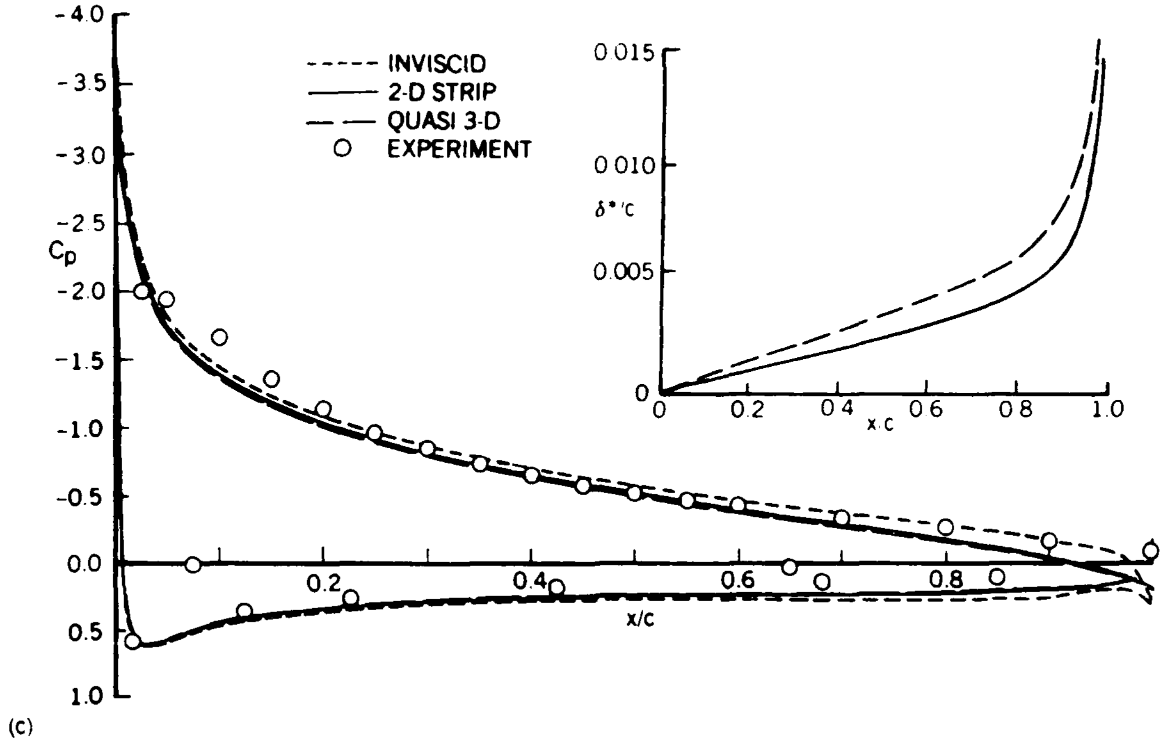

Figure 13. (Continued) (c) 88% semispan.

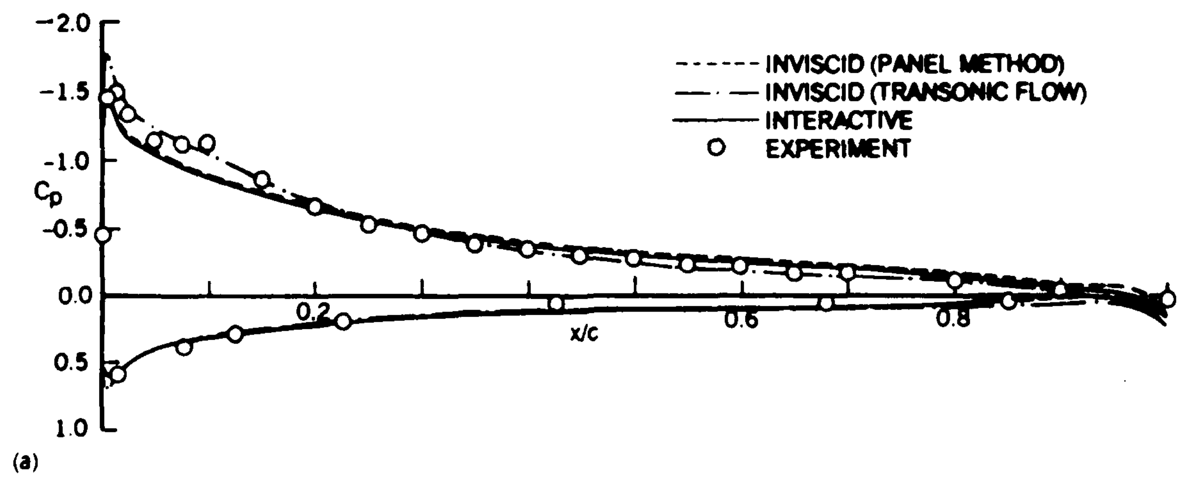

Figure 14. Comparison of the mid-semispan pressure distribution obtained by the panel method and the transonic flow method for the F-15 with laminar bubble wing, M = 0.6. (a) α = 6.84°.

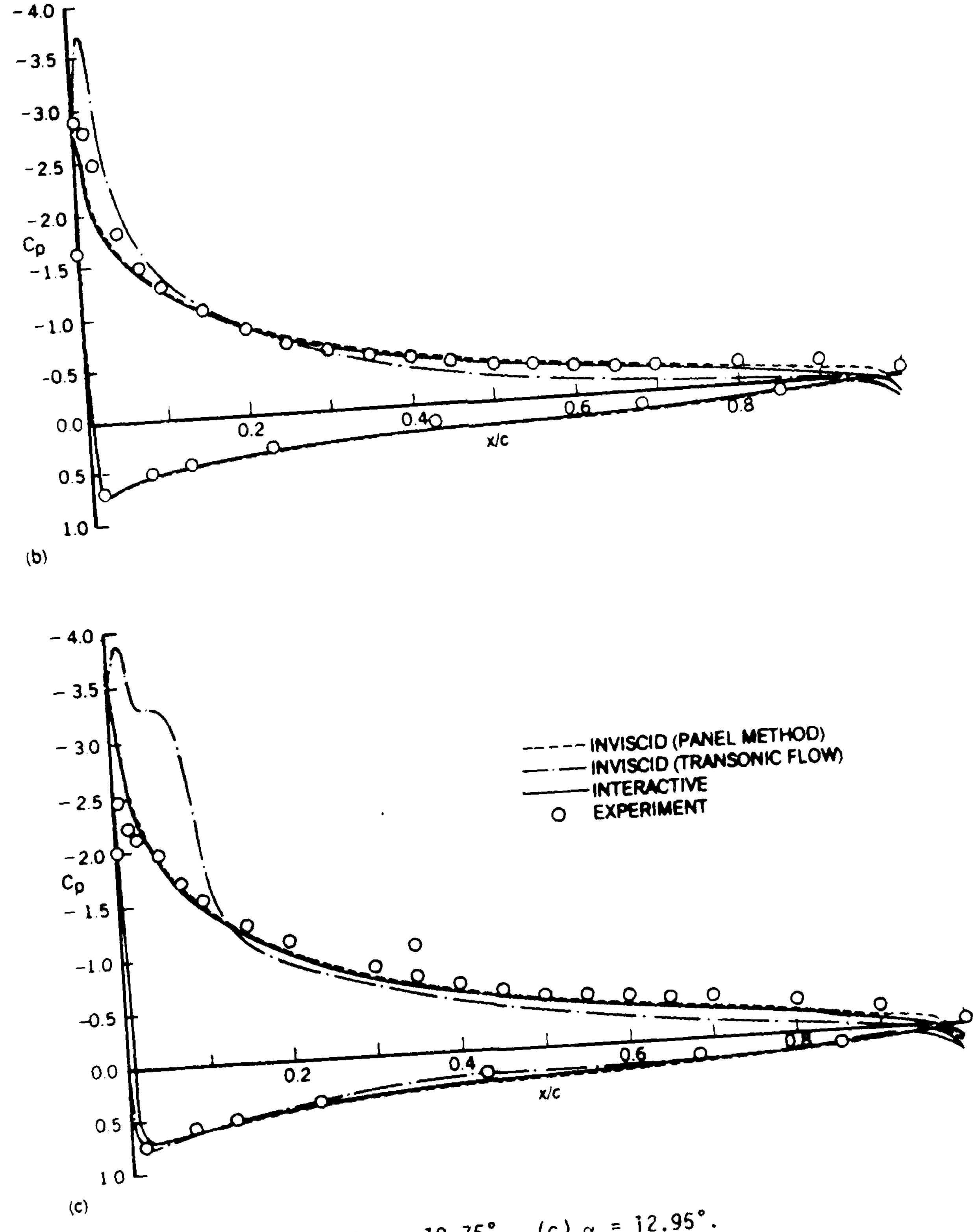

Figure 14. (Continued) (b) α = 10.75°. (c) α = 12.95°.

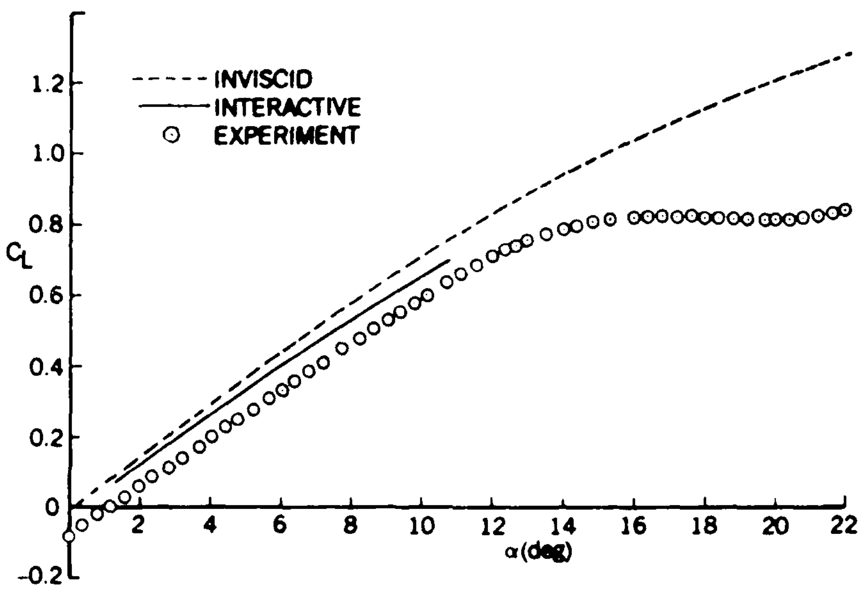

Figure 15. Comparison of computed and experimental lift curves for the ANF wing/body configuration.

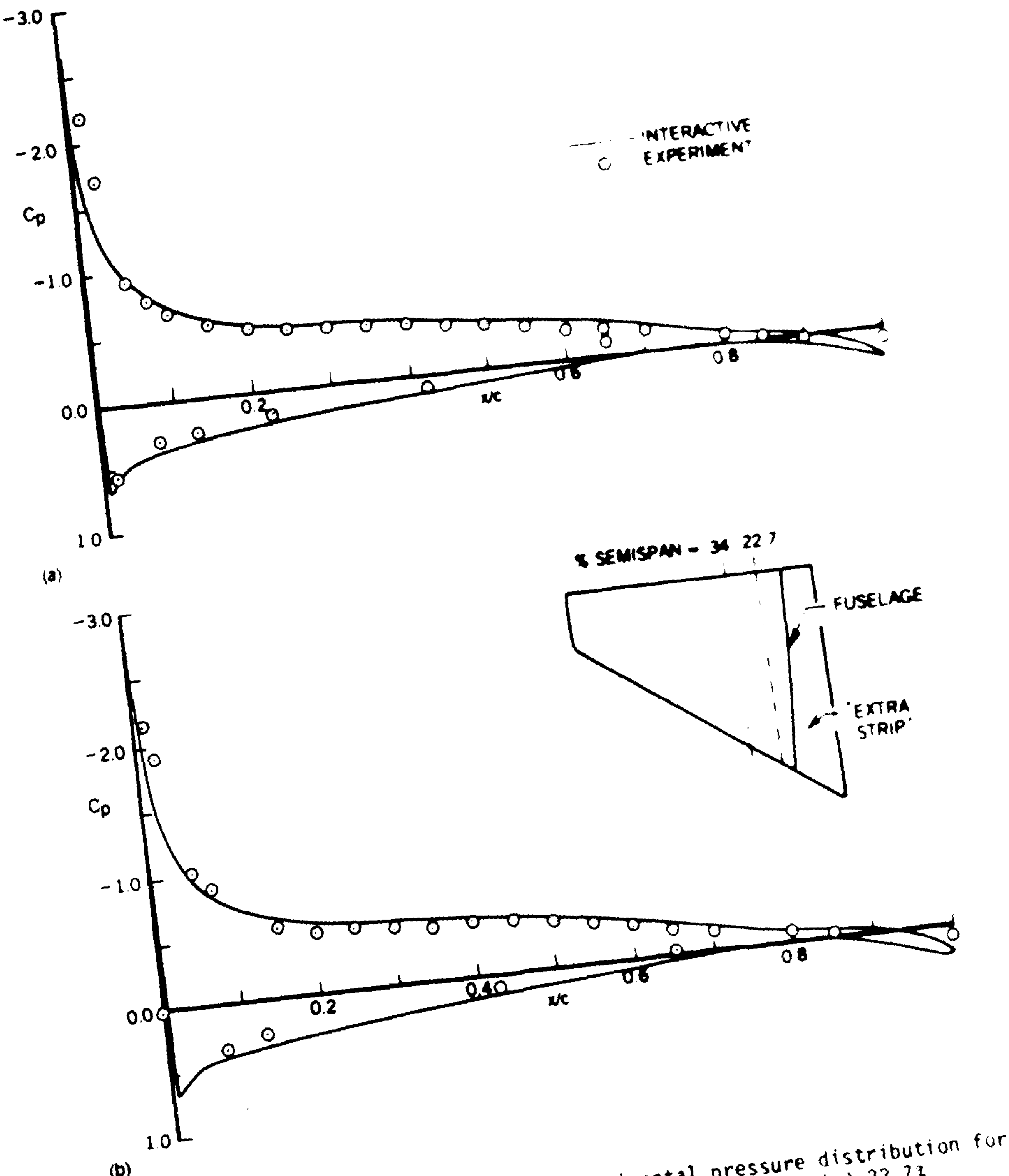

Figure 16. Comparison of computed and experimental pressure distribution for ANF wing/body configuration, $\alpha = 7.7°$, $M = 0.6$. (a) 22.7% semispan. (b) 34.5% semispan.

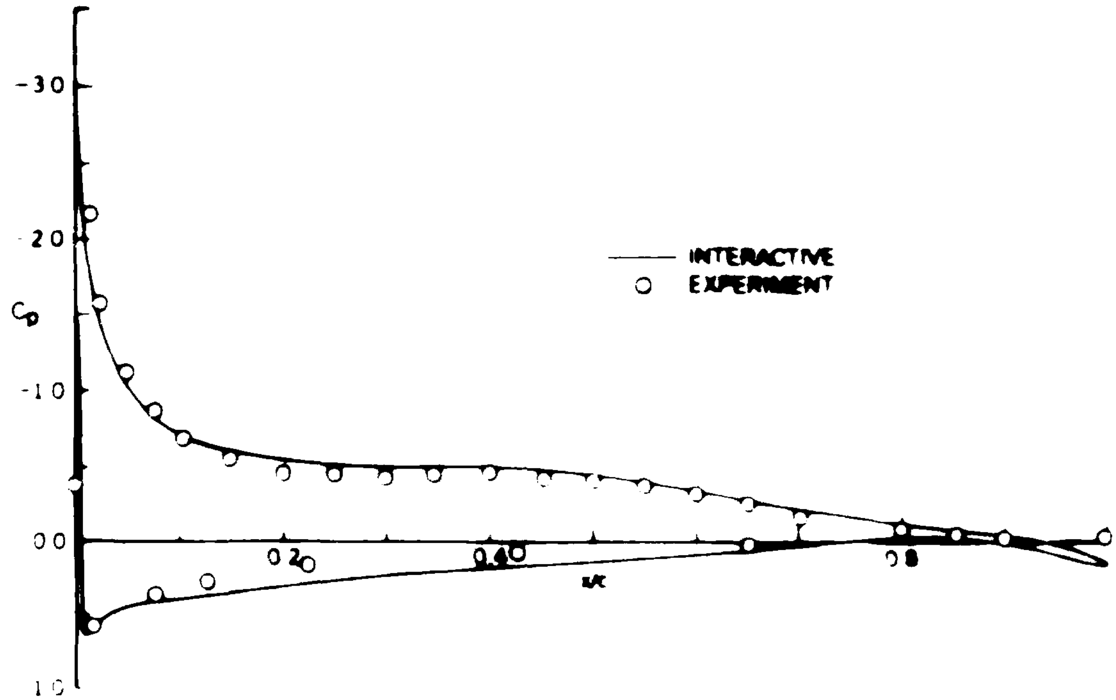
-3.0
-2.0
Cp
-1.0
0.0
0.2
0.4
x/c
0.8
1.0
INTERACTIVE
EXPERIMENT

c

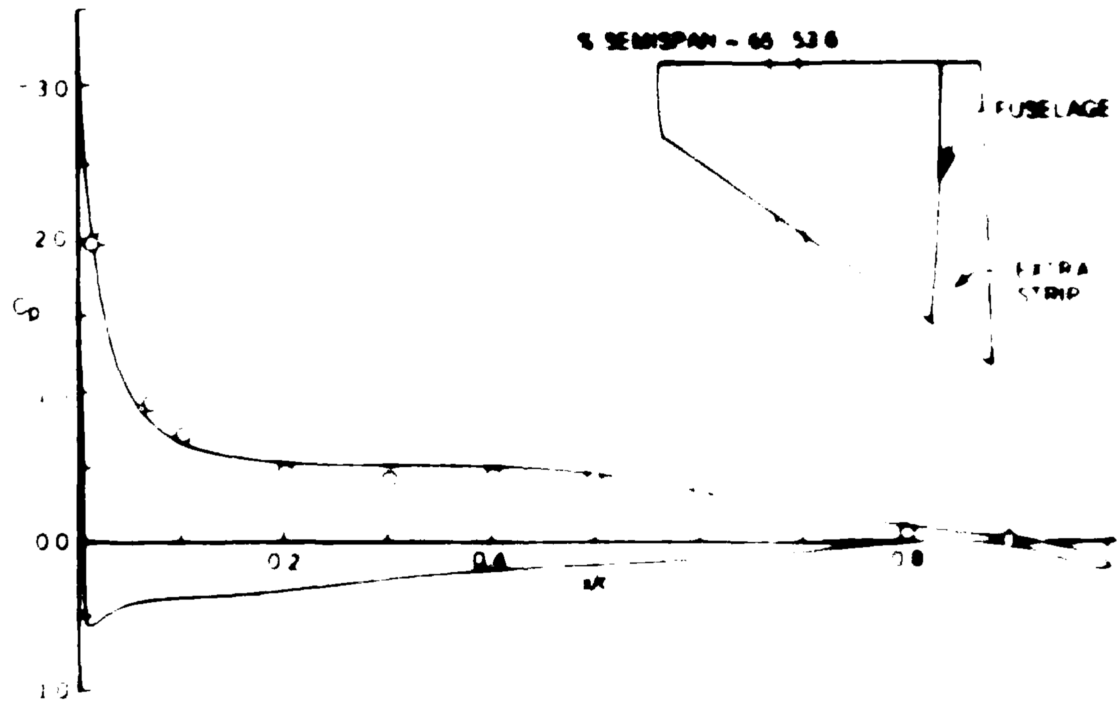
% SEMISPAN = 66 53.6
FUSELAGE
-3.0
2.0
Cp
0.0
0.2
0.4
x/c
1.0

d

Figure

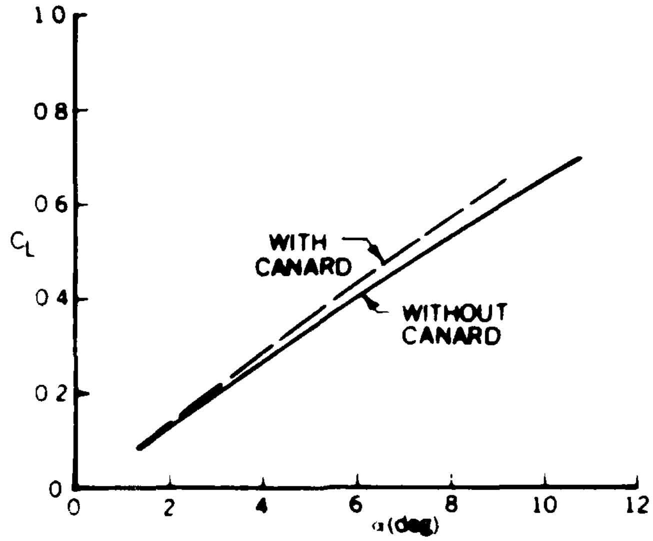

Figure . Effect of canard on the calculated lift curve of the ANF wing/body configuration, M = 0.6.

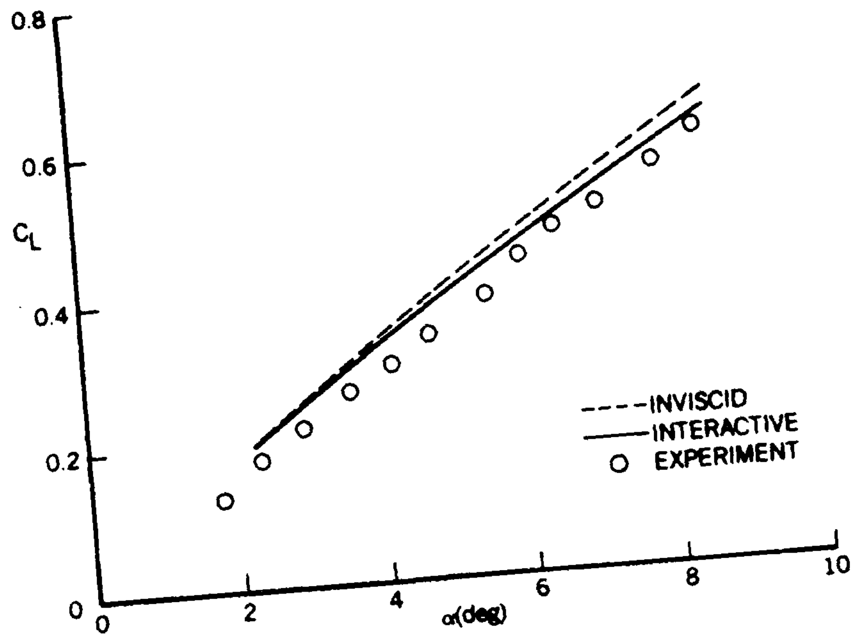

Figure 18. Comparison of computed and experimental lift curves for the unmodified F-15.

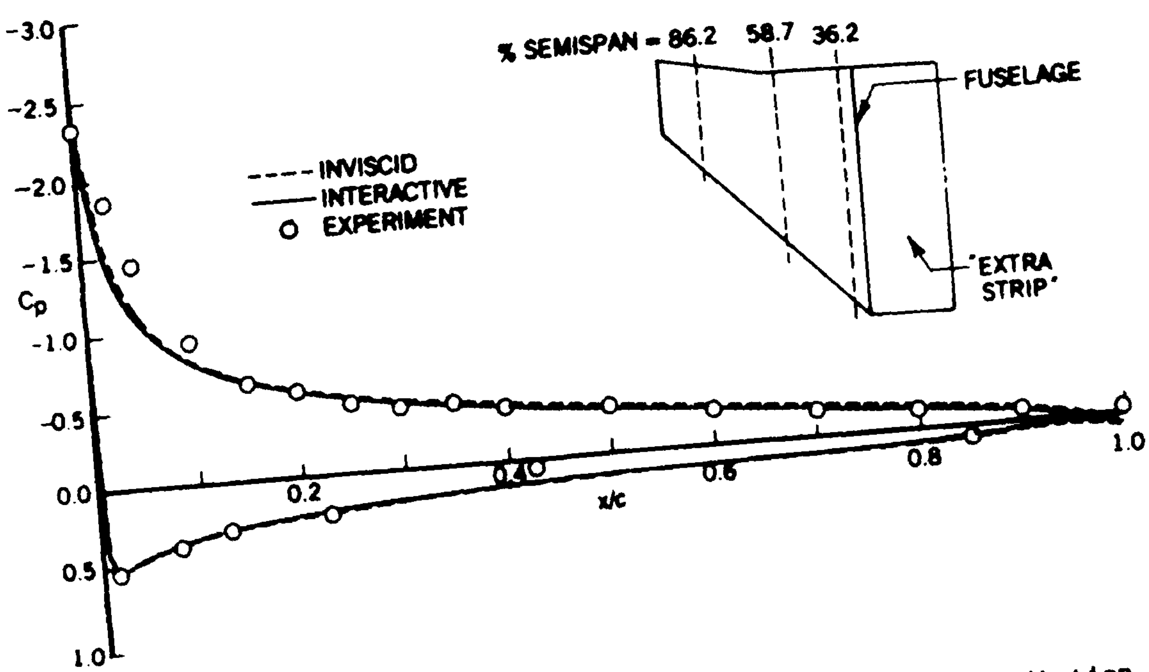

Figure 19. Comparison of computed and experimental pressure distribution for the unmodified F-15, α = 8.66°, (a) 36.2% semispan.

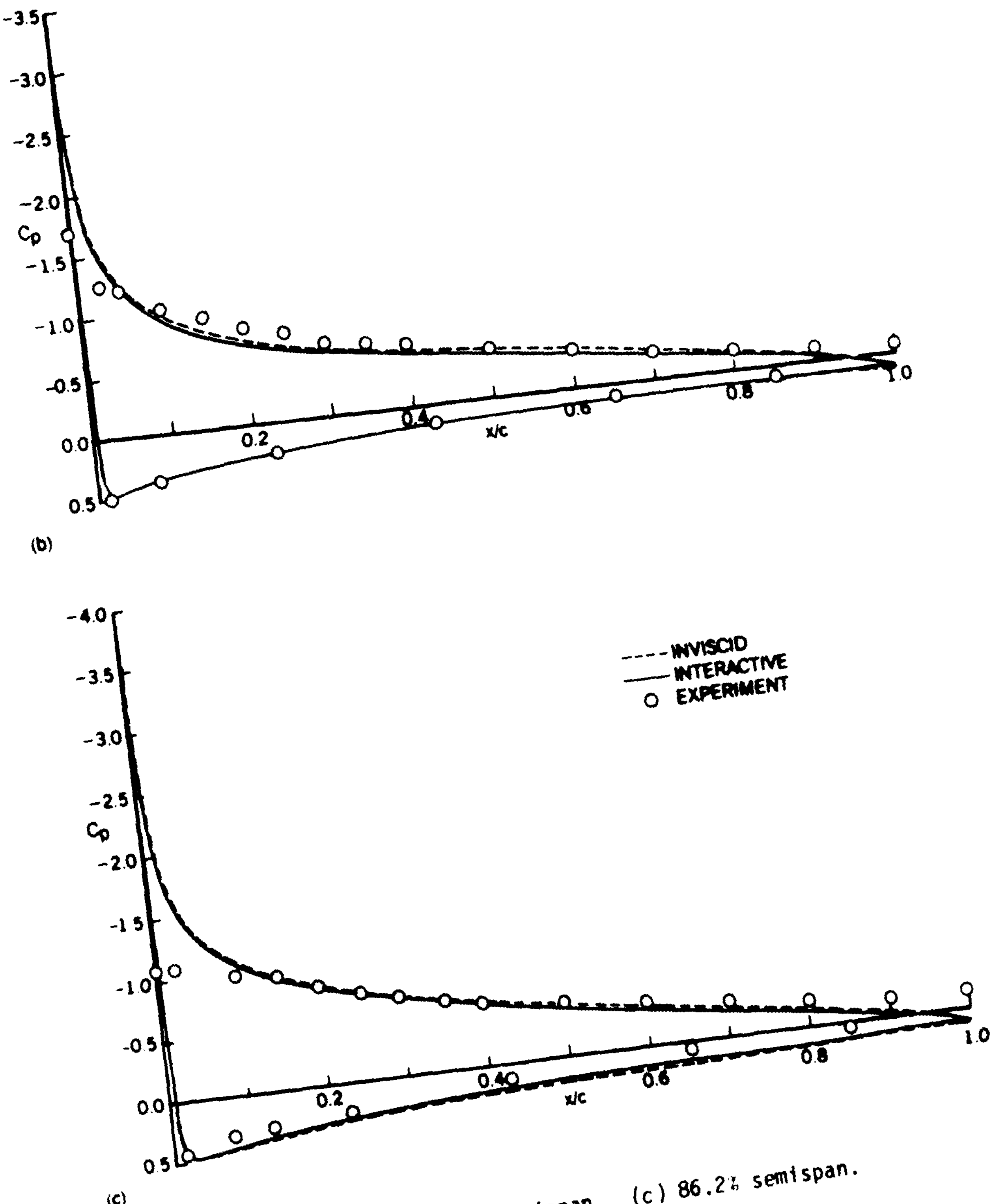

Figure 19. (Continued) (b) 58.7% semispan. (c) 86.2% semispan.

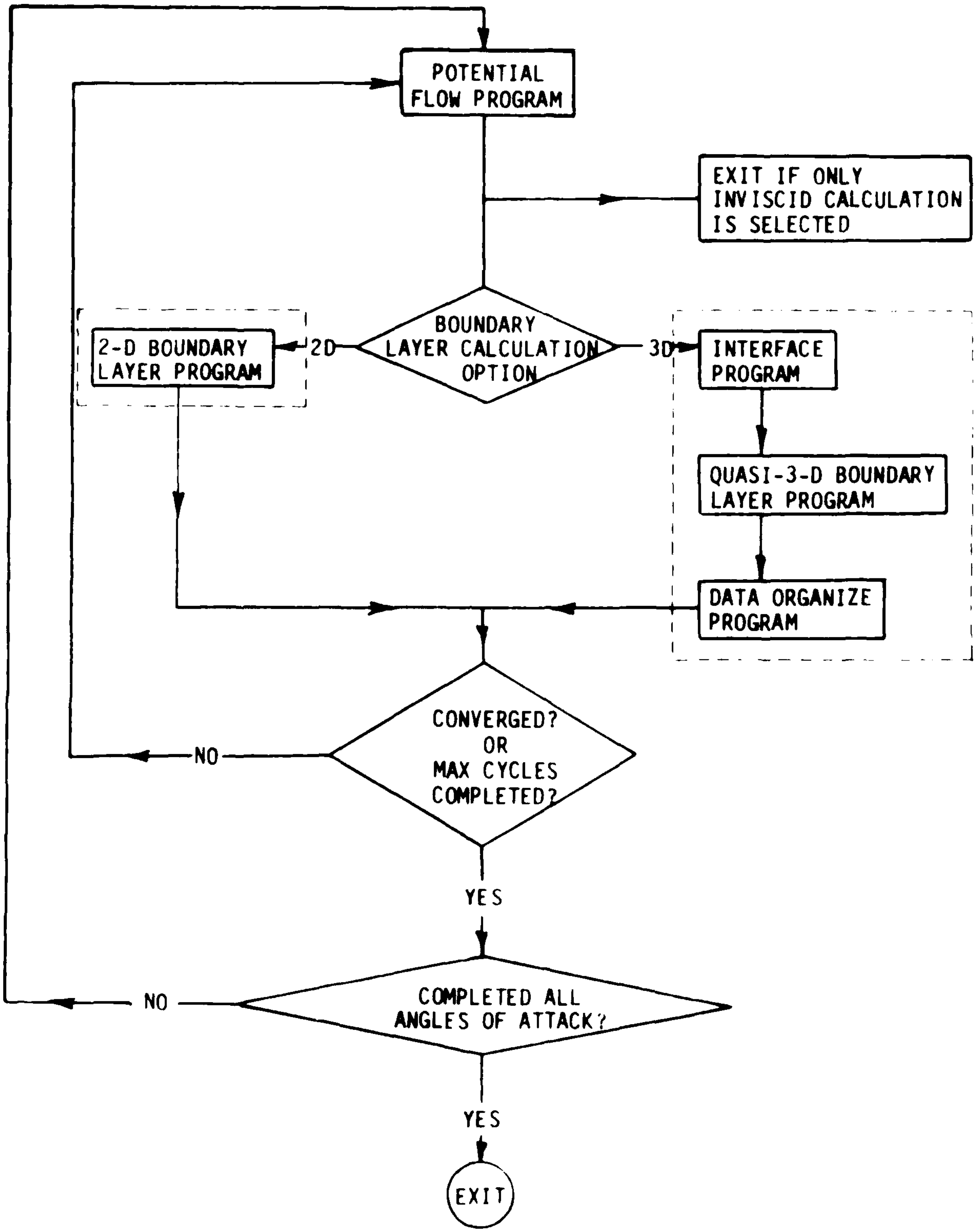

Figure 20. Flow structure of three-dimensional viscous/inviscid interaction program.

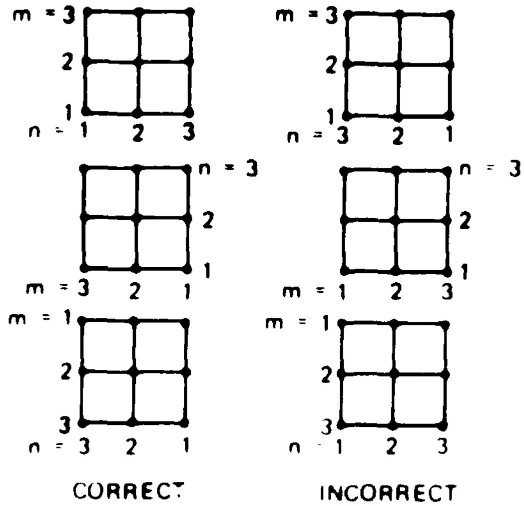

Figure 21. Examples of correct and incorrect input.

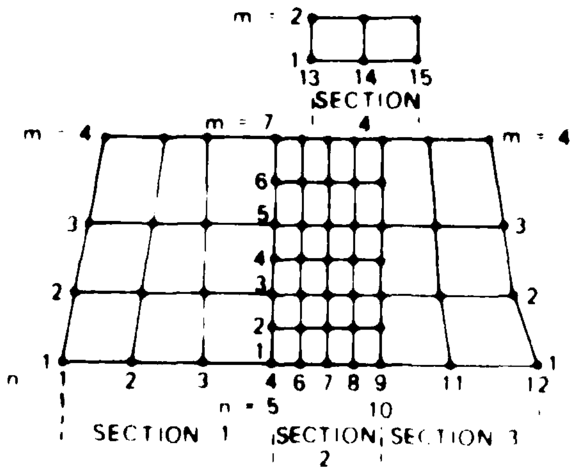

Figure 22. Plan view of the input points on a body divided into sections.

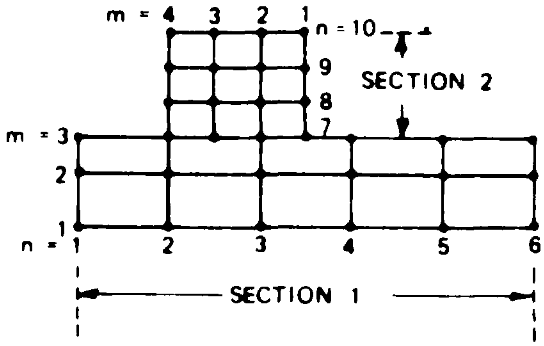

Figure 23. Another possible division into sections.

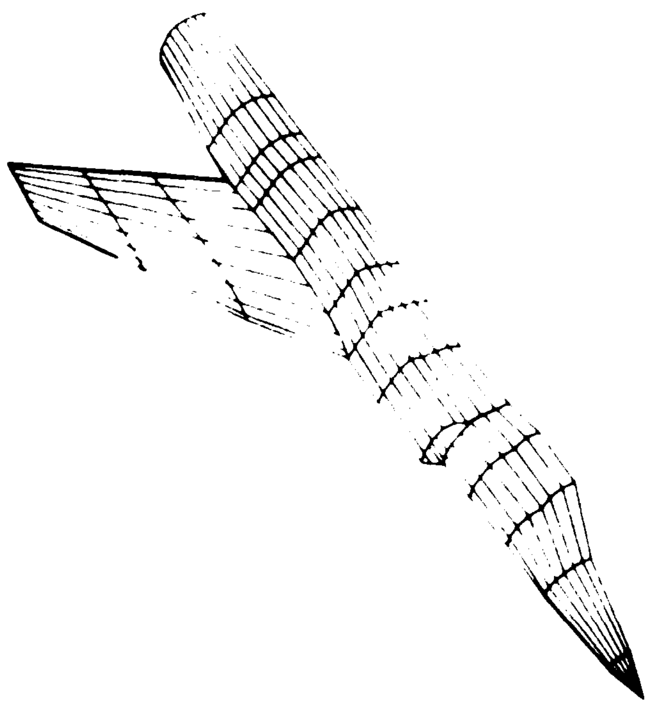

Figure 24. Arrangement of panels for the sample test case.

```
PAGE    1                          3-D VISCOUS-INVISCID INTERACTIVE PROGRAM                          TUESDAY,   APR 15, 1986

CASE TITLE:     REPORT TEST CASE,TRANS. CALC., 2DSTRIP BL, M=0.6, ALPHAS                        ALPHA =   1.30 MACH = 0.6000
PAGE TITLE:  USER INPUT DATA                                                                     VISCOUS/INVISCID CYCLE NO.   0
------------------------------------------------------------------------------------------------------------------------------

  CASE TITLE :    REPORT TEST CASE,TRANS. CALC., 2DSTRIP BL, M=0.6, ALPHAS
  ------------

  NAMELIST "A" INPUT DATA :
  -------------------------

  IBL3D  =   0  IPNTB3 =   0  IPNTGM =   0  IPNTNU =   0  KINKNO =   0
  LIFT3D =   1  MAXANG =   2  MAXCYC =   2  MLINE  =  21  NLINE  =   5
  ALPHAI =     1.300000     3.400000
  AMACH  =     0.600000

  NAMELIST "B" INPUT DATA :
  -------------------------

  IAUTOW =   2  IPCV   =   1  ITERAT =   1  IVNSP  =   0  LIFSEC =   1
  LINEAR =   0  LIST   =   0  NOFF   =   0  NSYM1  =   1  NSYM2  =   0
  IXFLAG =     3    0    0    0    0    0    0    0    0    0    0    0    0    0    0    0    0    0    0    0
  NLINE1 =     0    0    0    0    0    0    0    0    0    0    0    0    0    0    0    0    0    0    0    0
  NLINEN =     0    0    0    0    0    0    0    0    0    0    0    0    0    0    0    0    0    0    0    0
  NSTRIP =     4    0    0    0    0    0    0    0    0    0    0    0    0    0    0    0    0    0    0    0
  NSORCE =    20    0    0    0    0    0    0    0    0    0    0    0    0    0    0    0    0    0    0    0
  NWAKE  =     1    0    0    0    0    0    0    0    0    0    0    0    0    0    0    0    0    0    0    0
  BOV2   =    12.955000  ORIGNX =      0.0        ORIGNY =      0.0       ORIGNZ =      0.0
  REFCHD =     8.291200  RFAREA =     95.904007

  BOUNDARY LAYER INPUT DATA :
  ---------------------------

  AL2D   =     0.000000  RC     =  0.70000E+07  RSTART =      0.0       VGP    =      1.125353
  ETAE   =     8.000000  DETA1  =     0.015775

  UPPER SURFACE DATA :
  NB     =  70  ITR    =   2  ISWP   =  10  NTRN   =   0

  LOWER SURFACE DATA :
  NB     =  51  ITR    =   2  ISWP   =   5  NTRN   =   0

  START COMPUTING ALPHA =      1.300
```

Figure 25. Output from the sample test case.

```
PAGE    2                 3-D VISCOUS-INVISCID INTERACTIVE PROGRAM                        TUESDAY,   APR 15, 1986
                          ----------------------------------------
CASE TITLE:     REPORT TEST CASE,TRANS. CALC., 2DSTRIP BL, M=0.6, ALPHAS          ALPHA =   1.30 MACH = 0.6000
PAGE TITLE:  INPUT DATA                                                         VISCOUS/INVISCID CYCLE NO.   0
---------------------------------------------------------------------------------------------------------------

                                     INPUT FLAGS
                                     -----------

                                     ICYCLE =  0
                                     BOV2   =         12.95500
                                     C1VAL  =          0.0
                                     HGND   =          0.0
                                     IAUTOW =  2
                                     IBLFIT =  1
                                     ICONT  =  1
                                     ICONV  =  1
                                     IOUT   =  0
                                     IPCV   =  1
                                     ITERAT =  1
                                     KUTTA  =  0
                                     IVNSP  =  0
                                     LIFSEC =  1
                                     LINEAR =  0
                                     LIST   =  0
                                     MAXCYC =  2
                                     MPR    =  0
                                     NLR    =  0
                                     NOFF   =  0
                                     NSYM1  =  1
                                     NSYM2  =  0
                                     ORIGNX =          0.0
                                     ORIGNY =          0.0
                                     ORIGNZ =          0.0
                                     RFAREA =         95.90401
                                     REFCHD =          8.29120
                                     RMACH  =          0.60000

                        RUN MODE =  0  ( 0=INITIAL RUN. 1=BLOWING RUN.)

                                     NSORCE =  20
                                     NWAKE  =   1
                                     NSTRIP =   4
                                     IXFLAG =   3

                        INPUT UNIFORM ONSET FLOWS IN DEGS AND COMPONENTS

              ( 1)  DEG --   1.299999  COMPONENTS --     0.999743    0.0          0.022687

                       INPUT MACH NO. =     0.600000  BETA =  0.800000E+00

                                     ------------- * -------------
```

Figure 25. (Continued) Output from the sample case.

CASE TITLE REPORT TEST CASE,TRANS CALC , 2DSTRIP BL, M=0.6, ALPHAS ALPHA = 1.30 MACH = 0.6000
PAGE TITLE INPUT PANEL CORNER POINTS AND COMPUTED PANEL QUANTITIES VISCOUS/INVISCID CYCLE NO. 0

PNL NO	IV	IU	EX	XA	YA	ZA	XB	YB	ZB	NX	NY	NZ	AVERAGE PROJ.DIST	MAXIMUM DIAGONAL	PROJECTED AREA
SEC 1.TYP=LIFT				29.32001	12.95000	5.67000	29.27000	9.33000	5.67000						
1	1	1		29.24818	12.95000	5.65953	29.13795	9.33000	5.65805	0.10929	-0.00222	-0.99401	0.001278	3.624596	0.37137
2		2		29.03900	12.95000	5.64273	28.75801	9.33000	5.60651	0.11523	-0.00105	-0.99334	0.003709	3.653433	1.07383
3		3		28.71248	12.95000	5.62705	28.16208	9.33000	5.56917	0.05738	0.00639	-0.99833	0.001543	3.725430	1.67248
4		4		28.30119	12.95000	5.60425	27.40961	9.33000	5.55680	0.03021	0.00852	-0.99951	0.005184	3.847998	2.10782
5		5		27.84604	12.95000	5.56869	26.57628	9.33000	5.52255	0.05410	-0.00324	-0.99853	0.005439	4.010833	2.33594
6		6		27.39096	12.95000	5.52954	25.74344	9.33000	5.46991	0.07109	-0.01408	0.99737	0.003351	4.187514	2.33741
7		7		26.98000	12.95000	5.50361	24.99162	9.33000	5.44333	0.04511	-0.00611	-0.99896	0.003680	4.343831	2.10698
8		8		26.65373	12.95000	5.48220	24.39452	9.33000	5.42695	0.04090	-0.00805	-0.99913	0.004027	4.449197	1.67299
9		9		26.44441	12.95000	5.46784	24.01219	9.33000	5.39567	0.07686	-0.03227	-0.99652	0.000889	4.482141	1.07461
10		10		26.37100	12.95000	5.48291	23.88837	9.33000	5.43812	-0.27423	0.20135	-0.94035	0.002981	4.431656	0.38034
11		11		26.44160	12.95000	5.51190	24.00941	9.33000	5.50783	-0.43796	0.29157	0.85040	0.003127	4.430559	0.40875
12		12		26.65025	12.95000	5.53701	24.39128	9.33000	5.54743	-0.10865	0.07127	0.99152	0.001114	4.480996	1.07802
13		13		26.97580	12.95000	5.56973	24.98685	9.33000	5.59786	-0.08975	0.05795	0.99428	0.001655	4.447989	1.67683
14		14		27.38554	12.95000	5.61485	25.73460	9.33000	5.68774	-0.11555	0.07192	0.99070	0.001324	4.342628	2.11475
15		15		27.84024	12.95000	5.66001	26.56686	9.33000	5.75087	-0.08371	0.05631	0.99490	0.003436	4.187966	2.34150
16		16		28.29628	12.95000	5.68171	27.40086	9.33000	5.74160	-0.00963	0.02370	0.99967	0.008647	4.012593	2.33662
17		17		28.70892	12.95000	5.68318	28.15419	9.33000	5.71196	0.02415	0.00741	0.99968	0.005717	3.849562	2.11149
18		18		29.03690	12.95000	5.67587	28.75334	9.33000	5.69648	0.02458	0.00397	0.99969	0.000378	3.726239	1.67861
19		19		29.24754	12.95000	5.66948	29.13805	9.33000	5.68037	0.03776	0.00230	0.99928	0.000781	3.653674	1.07835
20		20		29.32001	12.95000	5.67000	29.27000	9.33000	5.67000	0.04816	0.00044	0.99884	0.002004	3.624587	0.37073
21		21	H	29.39252	12.95000	5.67000	29.40248	9.33000	5.67000	0.0	0.0	1.00000	0.0	3.622074	0.37102
				29.27000	9.33000	5.67000	29.22000	5.70000	5.67000						
22	2	1		29.13795	9.33000	5.65805	29.02602	5.70000	5.65112	0.09411	-0.00115	-0.99556	0.000266	3.638230	0.59441
23		2		28.75801	9.33000	5.60651	28.46606	5.70000	5.58714	0.12199	-0.00319	-0.99253	0.002400	3.692335	1.71883
24		3		28.16208	9.33000	5.56917	27.59184	5.70000	5.50912	0.07822	0.00162	-0.99693	0.004696	3.813978	2.67675
25		4		27.40961	9.33000	5.55680	26.48625	5.70000	5.47897	0.02288	0.01428	-0.99964	0.002424	3.999170	3.37360
26		5		26.57628	9.33000	5.52255	25.26028	5.70000	5.48045	0.01591	0.01161	-0.99981	0.010493	4.219386	3.73916
27		6		25.74344	9.33000	5.46991	24.03377	5.70000	5.47608	0.02767	-0.00659	-0.99960	0.014789	4.432336	3.74083
28		7		24.99162	9.33000	5.44333	22.92799	5.70000	5.47648	0.01409	-0.01274	-0.99982	0.007990	4.593949	3.37264
29		8		24.39452	9.33000	5.42695	22.04999	5.70000	5.47933	0.00918	-0.01735	-0.99981	0.005450	4.672458	2.67814
30		9		24.01219	9.33000	5.39567	21.48695	5.70000	5.45894	0.05449	-0.05243	-0.99714	0.005177	4.651081	1.72121
31		10		23.88837	9.33000	5.43812	21.29839	5.70000	5.50273	-0.26231	0.16808	-0.95023	0.003924	4.533655	0.59741
32		11		24.00941	9.33000	5.50783	21.49162	5.70000	5.59086	-0.42567	0.31672	0.84764	0.003785	4.530722	0.67371
33		12		24.39128	9.33000	5.54743	22.04639	5.70000	5.69222	-0.14757	0.12961	0.98052	0.008763	4.646369	1.73498
34		13		24.98685	9.33000	5.59786	22.92105	5.70000	5.77438	-0.08939	0.09817	0.99115	0.001625	4.672473	2.69231
35		14		25.73460	9.33000	5.68774	24.02501	5.70000	5.85565	-0.09162	0.09467	0.99128	0.010295	4.593665	3.39129
36		15		26.56686	9.33000	5.75087	25.25134	5.70000	5.89181	-0.04808	0.06244	0.99689	0.011455	4.432856	3.74899
37		16		27.40086	9.33000	5.74160	26.47662	5.70000	5.85028	0.02465	0.02676	0.99934	0.005650	4.221378	3.74025
38		17		28.15419	9.33000	5.71196	27.58229	5.70000	5.77690	0.05532	0.01247	0.99839	0.006043	4.001312	3.37981
39		18		28.75334	9.33000	5.69648	28.46187	5.70000	5.72801	0.04349	0.00810	0.99902	0.005292	3.815083	2.68679
40		19		29.13805	9.33000	5.68037	29.02650	5.70000	5.69029	0.05660	0.00256	0.99839	0.002849	3.692742	1.72593
41		20		29.27000	9.33000	5.67000	29.22000	5.70000	5.67000	0.09383	-0.00073	0.99559	0.001024	3.638208	0.59340
42		21	H	29.40248	9.33000	5.67000	29.41472	5.70000	5.67000	0.0	0.0	1.00000	0.0	3.634578	0.59385
				29.22000	5.70000	5.67000	29.16177	1.63104	5.67000						
43	3	1		29.02602	5.70000	5.65112	28.90755	1.62853	5.65365	0.07834	-0.00201	-0.99692	0.001809	4.083470	0.91498

Figure 25. (Continued) Output from the sample case.

PAGE 4 3-D VISCOUS-INVISCID INTERACTIVE PROGRAM TUESDAY, APR 15, 1986

CASE TITLE REPORT TEST CASE,TRANS CALC., 2DSTRIP BL, M=0.6, ALPHAS ALPHA = 1.30 MACH = 0.6000
PAGE TITLE INPUT PANEL CORNER POINTS AND COMPUTED PANEL QUANTITIES VISCOUS/INVISCID CYCLE NO. 0

PNL NO	IV	IU	E X	|<---------- D E F I N I N G XA	YA	ZA	N - L I N E S XB	YB	---------->| ZB	|<---- N O R M A L S NX	NY	--- >| NZ	AVERAGE PROJ.DIST	MAXIMUM DIAGONAL	PROJECTE AREA
44		2		28.46606	5.70000	5.58714	28.17281	1.63357	5.60051	0.09007	-0.00650	-0.99591	0.006644	4.155313	2.64594
45		3		27.59184	5.70000	5.50912	27.02953	1.68795	5.52141	0.07733	-0.01136	-0.99694	0.005085	4.262078	4.10008
46		4		26.48625	5.70000	5.47897	25.58682	1.77617	5.49062	0.02365	-0.00737	-0.99969	0.001998	4.406711	5.09187
47		5		25.26028	5.70000	5.48045	23.98625	1.83578	5.53868	-0.01761	-0.00406	-0.99984	0.010056	4.602991	5.53808
48		6		24.03377	5.70000	5.47608	22.38866	1.94199	5.61974	-0.02774	-0.01585	-0.99949	0.019194	4.732355	5.46672
49		7		22.92799	5.70000	5.47648	20.94963	2.05391	5.69694	-0.03193	-0.03350	-0.99893	0.017456	4.781501	4.82229
50		8		22.04999	5.70000	5.47933	19.80632	2.13268	5.75927	-0.03411	-0.04928	-0.99820	0.013554	4.749308	3.73834
51		9		21.48695	5.70000	5.45894	19.07140	2.17502	5.78621	-0.00766	-0.08031	-0.99674	0.012314	4.625520	2.36084
52		10		21.29839	5.70000	5.50273	18.84647	2.20004	5.87724	-0.30168	0.11448	-0.94651	0.007721	4.404711	0.80284
53		11		21.49162	5.70000	5.59086	19.09769	2.19325	5.99694	-0.38998	0.36394	0.84585	0.000404	4.396436	0.93019
54		12		22.04639	5.70000	5.69222	19.81845	2.13085	6.13643	-0.17003	0.22631	0.95910	0.001449	4.592165	2.42994
55		13		22.92105	5.70000	5.77438	20.95973	2.03263	6.21539	-0.07081	0.16140	0.98434	0.009470	4.743588	3.81329
56		14		24.02501	5.70000	5.85565	22.40240	1.92678	6.24798	-0.03891	0.12971	0.99079	0.018784	4.793959	4.88158
57		15		25.25134	5.70000	5.89181	24.00360	1.83852	6.22560	-0.00188	0.09538	0.99544	0.016850	4.741836	5.48845
58		16		26.47662	5.70000	5.85028	25.60114	1.77469	6.11573	0.05485	0.06174	0.99658	0.012906	4.601089	5.54991
59		17		27.58229	5.70000	5.77690	27.03862	1.68638	5.96145	0.09048	0.04023	0.99509	0.013508	4.410319	5.10722
60		18		28.46187	5.70000	5.72801	28.18015	1.62168	5.82466	0.09225	0.02518	0.99542	0.016240	4.265160	4.12453
61		19		29.02650	5.70000	5.69029	28.91148	1.62589	5.71483	0.11308	0.00926	0.99354	0.013185	4.167491	2.66030
62		20		29.22000	5.70000	5.67000	29.16177	1.63104	5.67000	0.14522	-0.00011	0.98940	0.004006	4.086027	0.91352
63		21	M	29.41472	5.70000	5.67000	29.41631	1.63104	5.67000	0.0	0.0	1.00000	0.0	4.076810	0.91398
				29.16177	1.63104	5.67000	29.14000	0.0	6.17000						
64	4	1	*	28.90755	1.62853	5.65365	28.84802	0.0	6.16821	0.03304	-0.29778	-0.95406	0.003971	1.734078	0.46668
65		2	*	28.17281	1.63357	5.60051	28.00394	0.0	6.14668	0.04389	-0.31171	-0.94916	0.008309	1.926676	1.35720
66		3	*	27.02953	1.68795	5.52141	26.68895	0.0	6.15013	0.02153	-0.33633	-0.94150	0.015783	2.275011	2.17747
67		4	*	25.58682	1.77617	5.49062	25.03412	0.0	6.23597	-0.02688	-0.36258	-0.93156	0.017741	2.710762	2.90402
68		5	*	23.98625	1.83578	5.53868	23.20605	0.0	6.41274	-0.06703	-0.38749	-0.91943	0.019998	3.111118	3.39134
69		6	*	22.38866	1.94199	5.61974	21.38495	0.0	6.65753	-0.09914	-0.41166	-0.90593	0.020614	3.376589	3.62136
70		7	*	20.94963	2.05391	5.69694	19.75064	0.0	6.92859	-0.11689	-0.44096	-0.88988	0.025084	3.530232	3.52737
71		8	*	19.80632	2.13268	5.75927	18.45403	0.0	7.15018	-0.11683	-0.47512	-0.87213	0.020892	3.545797	2.99242
72		9	*	19.07140	2.17502	5.78621	17.62001	0.0	7.28252	-0.10056	-0.50794	-0.85550	0.014675	3.414163	2.01416
73		10	*	18.84647	2.20004	5.87724	17.36226	0.0	7.42204	-0.42297	-0.30845	-0.85203	0.004936	3.214189	0.64297
74		11	*	19.09769	2.19325	5.99694	17.64458	0.0	7.55301	-0.30590	0.67700	0.66940	0.000658	3.138953	0.88292
75		12	*	19.81845	2.13085	6.13643	18.48807	0.0	7.60223	-0.07191	0.60203	0.79523	0.010760	3.358908	2.18778
76		13	*	20.95973	2.03263	6.21539	19.80338	0.0	7.55601	0.01107	0.55435	0.83221	0.011951	3.489580	3.15301
77		14	*	22.40240	1.92678	6.24798	21.45753	0.0	7.43768	0.04143	0.52233	0.85174	0.016122	3.491758	3.67073
78		15	*	24.00360	1.83852	6.22560	23.28661	0.0	7.25374	0.06493	0.48502	0.87209	0.020823	3.367968	3.74950
79		16	*	25.60114	1.77469	6.11573	25.10378	0.0	6.98579	0.10709	0.43396	0.89455	0.022546	3.131994	3.47307
80		17	*	27.03862	1.68638	5.96145	26.73785	0.0	6.69297	0.14367	0.38812	0.91034	0.015895	2.764696	2.94201
81		18	*	28.18015	1.62168	5.82466	28.03258	0.0	6.43695	0.15806	0.35316	0.92211	0.015719	2.338412	2.19527
82		19	*	28.91148	1.62589	5.71483	28.85895	0.0	6.24725	0.17824	0.31733	0.93142	0.014695	1.984590	1.35857
83		20	*	29.16177	1.63104	5.67000	29.14000	0.0	6.17000	0.21157	0.29094	0.93305	0.006306	1.756554	0.46408
84		21	M	29.41631	1.63104	5.67000	29.43172	0.0	6.17000	0.0	0.29309	0.95608	0.0	1.728189	0.46594
SEC	2.TYP=NLIF			1.44000	0.0	6.16000	3.00000	0.0	6.90000						
85	1	1		1.44000	0.00643	6.16123	3.00000	0.19285	6.86682	-0.42309	0.14344	0.89466	0.001006	1.726101	0.17374
86		2		1.44000	0.00968	6.16049	3.00000	0.36318	6.76705	-0.41087	0.45684	0.78897	0.000447	1.722223	0.17160
87		3		1.44000	0.01043	6.15704	3.00000	0.49166	6.61642	-0.39078	0.70527	0.59152	0.000757	1.711767	0.17041

Figure 25. (Continued) Output from the sample case.

CASE TITLE REPORT TEST CASE.TRANS. CALC., 2DSTRIP BL, M-0.6, ALPHAS
PAGE TITLE INPUT PANEL CORNER POINTS AND COMPUTED PANEL QUANTITIES

ALPHA = 1.30 MACH = 0.6000
VISCOUS/INVISCID CYCLE NO. 0

PNL NO	IV	IU	X	XA	YA (DEFINING LINES)	ZA	XB	YB	ZB	NX (NORMALS)	NY	NZ	AVERAGE PROJ.DIST	MAXIMUM DIAGONAL	PROJECTED AREA
88		4		1.44000	0.01034	6.15174	3.00000	0.56079	6.43560	-0.36566	0.87265	0.32368	0.000901	1.697409	0.16635
89		5		1.44000	0.00855	6.14952	3.00000	0.56044	6.23747	-0.33205	0.94321	-0.01005	0.000831	1.679407	0.16568
90		6		1.44000	0.00274	6.15037	3.00000	0.49591	6.05307	-0.29944	0.89093	-0.34145	0.002733	1.658980	0.16069
91		7		1.44000	0.00019	6.14938	3.00000	0.36010	5.91436	-0.25990	0.68514	-0.68047	0.000666	1.639813	0.15903
92		8		1.44000	0.00048	6.14568	3.00000	0.18800	5.81871	0.23695	0.48513	-0.84173	0.001491	1.617753	0.15974
93		9		1.44000	0.0	6.14000	3.00000	0.0	5.76000	-0.22778	0.31623	-0.92093	0.002693	1.606968	0.15882
				3.00000	0.0	6.90000	6.60000	0.0	8.00000						
94	2	1		3.00000	0.19285	6.86682	6.60000	0.37576	7.87556	-0.27766	0.25662	0.92577	0.009384	3.779055	1.10557
95		2		3.00000	0.36318	6.76705	6.60000	0.67208	7.60736	-0.23700	0.60155	0.76287	0.013172	3.766819	1.10104
96		3		3.00000	0.49166	6.61642	6.60000	0.90969	7.28157	-0.20313	0.77640	0.59660	0.004941	3.738248	1.10452
97		4		3.00000	0.56077	6.43560	6.60000	1.07016	6.91110	-0.17698	0.90856	0.37840	0.002809	3.714481	1.09220
98		5		3.00000	0.56044	6.23747	6.60000	1.14071	6.51729	-0.16053	0.98016	0.11624	0.011686	3.697779	1.08704
99		6		3.00000	0.49591	6.05307	6.60000	1.03076	6.13531	-0.13204	0.94731	-0.29183	0.003658	3.686629	1.07619
100		7		3.00000	0.36010	5.91436	6.60000	0.75277	5.84542	-0.09101	0.71643	-0.69169	0.000676	3.668593	1.07681
101		8		3.00000	0.18800	5.81871	6.60000	0.39363	5.66702	-0.06519	0.45749	-0.88682	0.003050	3.644127	1.07826
102		9		3.00000	0.0	5.76000	6.60000	0.0	5.58000	-0.05156	0.24272	-0.96873	0.005625	3.622647	1.08073
[illegible]	TYP	NEIT		6.60000	0.0	8.00000	9.04000	0.0	9.40000						
[illegible]				6.60000	[illegible]	7.88345	9.04000	0.51516	9.14894	0.45840	0.33769	0.82209	0.016216	2.897902	1.32817
[illegible]				[illegible]	[illegible]	7.60637	9.04000	0.79534	8.64626	0.30618	0.76984	0.56000	0.032902	2.890693	1.23567
[illegible]				[illegible]	[illegible]	[illegible]	9.04000	0.75535	[illegible]	0.07511	[illegible]	0.20908	0.079721	2.799046	1.13415
[illegible]				[illegible]	[illegible]	[illegible]	9.04000	[illegible]	[illegible]	[illegible]	[illegible]	[illegible]	[illegible]	2.718345	1.18571
[illegible]				[illegible]	[illegible]	[illegible]	[illegible]	[illegible]	[illegible]	[illegible]	[illegible]	[illegible]	[illegible]	2.699403	1.19198
[illegible]				[illegible]	[illegible]	[illegible]	[illegible]	[illegible]	[illegible]	[illegible]	[illegible]	[illegible]	[illegible]	2.661682	[illegible]
[illegible]				[illegible]	[illegible]	[illegible]	[illegible]	[illegible]	[illegible]	[illegible]	[illegible]	[illegible]	[illegible]	[illegible]	1.18561
[illegible]				[illegible]	[illegible]	[illegible]	[illegible]	[illegible]	[illegible]	[illegible]	[illegible]	[illegible]	0.018047	2.557420	1.18578
[illegible]				[illegible]	[illegible]	[illegible]	[illegible]	[illegible]	[illegible]	[illegible]	[illegible]	0.97955	0.006111	2.512334	1.19831
				[illegible]	[illegible]	[illegible]	[illegible]	0.0	9.44000						
[illegible]				[illegible]	[illegible]	[illegible]	[illegible]	[illegible]	[illegible]	[illegible]	[illegible]	[illegible]	0.002271	2.500998	1.41457
[illegible]				[illegible]	[illegible]	[illegible]	[illegible]	[illegible]	[illegible]	[illegible]	[illegible]	[illegible]	0.027961	2.500796	[illegible]
[illegible]				[illegible]	[illegible]	[illegible]	[illegible]	[illegible]	[illegible]	[illegible]	[illegible]	[illegible]	[illegible]	2.493774	1.21966
[illegible]				[illegible]	[illegible]	[illegible]	[illegible]	[illegible]	[illegible]	[illegible]	[illegible]	[illegible]	0.042989	2.544981	1.41964
[illegible]				[illegible]	[illegible]	[illegible]	[illegible]	[illegible]	[illegible]	[illegible]	[illegible]	[illegible]	[illegible]	2.509122	1.41584
[illegible]				[illegible]	[illegible]	[illegible]	[illegible]	[illegible]	[illegible]	[illegible]	[illegible]	[illegible]	0.004054	2.503214	[illegible]
[illegible]				[illegible]	[illegible]	[illegible]	[illegible]	[illegible]	[illegible]	[illegible]	[illegible]	[illegible]	0.009291	2.505017	[illegible]
[illegible]				[illegible]	[illegible]	[illegible]	[illegible]	[illegible]	[illegible]	[illegible]	[illegible]	[illegible]	0.025681	2.513579	[illegible]
[illegible]				[illegible]	[illegible]	[illegible]	[illegible]	[illegible]	5.70000	[illegible]	[illegible]	[illegible]	0.006255	2.506189	[illegible]
				[illegible]	[illegible]	[illegible]	[illegible]	0.0	9.36000						
[illegible]				[illegible]	[illegible]	[illegible]	[illegible]	[illegible]	[illegible]	[illegible]	[illegible]	0.85686	[illegible]	1.918107	[illegible]
[illegible]				[illegible]	[illegible]	[illegible]	[illegible]	[illegible]	[illegible]	[illegible]	[illegible]	[illegible]	[illegible]	1.911368	[illegible]
[illegible]				[illegible]	[illegible]	[illegible]	[illegible]	[illegible]	[illegible]	[illegible]	[illegible]	[illegible]	[illegible]	1.941457	[illegible]
[illegible]				[illegible]	[illegible]	[illegible]	[illegible]	[illegible]	[illegible]	[illegible]	[illegible]	[illegible]	[illegible]	1.925116	[illegible]
[illegible]				[illegible]	[illegible]	[illegible]	[illegible]	[illegible]	[illegible]	[illegible]	[illegible]	[illegible]	[illegible]	[illegible]	[illegible]
[illegible]				[illegible]	[illegible]	[illegible]	[illegible]	[illegible]	[illegible]	[illegible]	[illegible]	0.12995	[illegible]	1.905747	[illegible]
[illegible]				[illegible]	[illegible]	[illegible]	[illegible]	1.15590	[illegible]	[illegible]	0.85941	0.51006	0.011862	1.888181	[illegible]

[illegible] INTERACTIVE PROGRAM TUESDAY, APR 15, 1986

[illegible] PANEL [illegible] AND [illegible] PANEL QUANTITIES

ALPHA 1.30 MACH = 0.6000
VISCOUS/INVISCID CYCLE NO 0

N	IV	[illegible]	XA	YA	ZA	XB	YB	ZB	NX	NY	NZ	AVERAGE PROJ DIST	MAXIMUM DIAGONAL	PROJECTED AREA
128		8	11.47000	0.60079	5.78511	13.24000	0.59054	5.76977	0.02201	0.36222	0.93183	0.015115	1.875860	1.06266
129		9	11.47000	0.0	5.70000	13.24000	0.0	5.68000	-0.00891	0.14361	-0.98960	0.002010	1.872024	1.06541
SEC 4,TYP NLIF			13.24000	0.0	9.18000	16.42911	0.0	8.93905						
130	1	1	13.24000	0.52532	8.85489	16.42899	0.61149	8.89542	0.02571	0.30844	0.95090	0.073565	3.259525	1.90626
131		2	13.24000	1.09797	8.57140	16.42796	1.17827	8.68256	-0.03222	0.39913	0.91633	0.015605	3.258688	1.98242
132		3	13.24000	1.57874	8.18580	16.43434	1.68705	8.36101	-0.05361	0.58081	0.81227	0.016989	3.255000	1.94343
133		4	13.24000	2.23721	8.19121	16.42644	2.29524	8.29043	-0.04424	0.05105	0.99772	0.019505	3.267667	2.02552
134		5	13.24000	2.76716	7.93642	16.43230	2.47655	7.73081	0.03841	0.75250	0.65747	0.115631	3.240589	1.72568
135		6	13.24000	2.84831	7.28240	16.42848	2.47841	7.11832	0.10646	0.99221	0.06470	0.019095	3.304400	2.03654
136		7	13.24000	2.81141	6.63443	16.42552	2.49155	6.50596	0.10670	0.99411	-0.01899	0.012189	3.298120	2.02043
137		8	13.24000	2.49540	6.08931	16.42842	2.33359	5.93847	0.05229	0.91879	-0.39126	0.038527	3.298285	1.92939
			16.42911	0.0	8.93905	18.83095	0.0	8.93931						
138	2	1	16.42899	0.61149	8.89542	18.83078	0.60159	8.85745	0.00802	0.10290	0.99466	0.009758	2.478961	1.46461
139		2	16.42796	1.17827	8.68256	18.82971	1.18787	8.70162	0.00377	0.30456	0.95249	0.015074	2.477226	1.45376
140		3	16.43434	1.68705	8.36101	18.83574	1.75375	8.52441	-0.04111	0.42102	0.90612	0.038714	2.480636	1.42386
141		4	16.42644	2.29524	8.29043	18.82561	2.25911	8.28493	-0.03338	0.26758	0.96296	0.047514	2.480458	1.38797
142		5	16.43230	2.47655	7.73081	18.83281	2.27115	7.67512	0.05166	0.98520	0.16347	0.043725	2.483909	1.42410
143		6	16.42848	2.47841	7.11832	18.83054	2.27064	7.06799	0.08573	0.99632	0.00067	0.000555	2.496650	1.46989
144		7	16.42552	2.49155	6.50596	18.82838	2.23648	6.46214	0.09553	0.99527	-0.01758	0.011779	2.499723	1.47041
145		8	16.42842	2.33359	5.93847	18.82666	2.19727	5.85649	0.07584	0.98334	-0.16519	0.030680	2.504767	1.43189
			18.83095	0.0	8.93931	20.89867	0.0	8.92897						
146	3	1	18.83078	0.60159	8.85745	20.90590	0.54302	8.88945	-0.00371	0.10548	0.99441	0.008975	2.154803	1.19224
147		2	18.82971	1.18787	8.70162	20.90556	1.07260	8.77251	-0.01413	0.23741	0.97131	0.006077	2.182124	1.19211
148		3	18.83574	1.75375	8.52441	20.90385	1.60524	8.67739	-0.03708	0.24060	0.96991	0.017984	2.193100	1.17364
149		4	18.82561	2.25911	8.28493	20.90700	2.03926	8.39149	-0.01127	0.48804	0.87275	0.018867	2.213748	1.11583
150		5	18.83281	2.27115	7.67512	20.89691	2.04988	7.84653	0.10452	0.99434	0.01925	0.000490	2.206627	1.20337
151		6	18.83054	2.27064	7.06799	20.88712	2.04075	7.30227	0.10975	0.99391	-0.00947	0.002497	2.219181	1.19216
152		7	18.82838	2.23648	6.46214	20.88435	2.03290	6.75777	0.10943	0.99332	-0.03674	0.005957	2.232149	1.19001
153		8	18.82666	2.19727	5.85649	20.89203	2.03806	6.21359	0.09221	0.99532	-0.02900	0.010812	2.252425	1.19125
			20.89867	0.0	8.92897	23.89664	0.0	9.00150						
154	4	1	20.90590	0.54302	8.88945	23.90285	0.50912	8.96561	-0.02433	0.07177	0.99712	0.000305	3.047234	1.58153
155		2	20.90556	1.07260	8.77251	23.90157	1.01434	8.89694	-0.03022	0.17642	0.98385	0.010808	3.055892	1.57577
156		3	20.90385	1.60524	8.67739	23.90172	1.47683	8.68715	-0.01228	0.29292	0.95606	0.032545	3.063270	1.55963
157		4	20.90700	2.03926	8.39149	23.89256	1.72958	8.25443	0.06749	0.72159	0.68903	0.058193	3.061383	1.48997
158		5	20.89691	2.04988	7.84653	23.89417	1.83177	7.75529	0.09140	0.99013	0.10624	0.024152	3.061201	1.57771
159		6	20.88712	2.04075	7.30227	23.88525	1.82139	7.24548	0.07227	0.99719	-0.01974	0.000465	3.056735	1.58502
160		7	20.88435	2.03290	6.75777	23.88583	1.84205	6.73567	0.06836	0.99759	0.01199	0.007271	3.058234	1.58522
161		8	20.89203	2.03806	6.21359	23.89360	1.84257	6.22568	0.06423	0.99791	0.00632	0.001101	3.061844	1.58533
			23.89664	0.0	9.00150	26.97006	0.0	8.95094						
162	5	1	23.90285	0.50912	8.96561	26.97418	0.49796	8.90591	0.01803	0.07990	0.99664	0.002507	3.119032	1.55231
163		2	23.90157	1.01434	8.89694	26.97240	0.96514	8.72838	0.03841	0.24538	0.96867	0.028691	3.115714	1.54140
164		3	23.90172	1.47683	8.68715	26.96544	1.34274	8.40390	0.07793	0.53546	0.84096	0.035610	3.120612	1.53166
165		4	23.89256	1.72958	8.25443	26.95724	1.58263	7.96596	0.08545	0.86788	0.48937	0.003403	3.141261	1.53986

Figure 25. (Continued) Output from the sample case.

3 D VISCOUS INVISCID INTERACTIVE PROGRAM

TUESDAY, APR 15, 1986

REPORT TEST CASE.TRANS CALC , 2DSTRIP BL, M=0.6, ALPHAS
INPUT PANEL CORNER POINTS AND COMPUTED PANEL QUANTITIES

ALPHA = 1.30 MACH = 0.6000
VISCOUS/INVISCID CYCLE NO. 0

			DEFINING XA	YA	ZA	N-LINES XB	YB	ZB	NORMALS NX	NY	NZ	AVERAGE PROJ.DIST	MAXIMUM DIAGONAL	PROJECTED AREA
[illegible]		5	23.89417	1.83177	7.75529	26.95972	1.67389	7.47342	0.06649	0.97928	0.19131	0.002345	3.165515	1.55137
[illegible]		6	23.88525	1.82139	7.24548	26.95723	1.67881	6.97343	0.04836	0.99881	-0.00595	0.003884	3.164968	1.55282
168		7	23.88583	1.84205	6.73567	26.95937	1.69102	6.47266	0.05053	0.99819	0.03260	0.002017	3.172443	1.55508
169		8	23.89360	1.84257	6.22568	26.96979	1.69079	5.97178	0.04928	0.99878	0.00117	0.000152	3.180747	1.55368
			26.97006	0.0	8.95094	28.43298	0.0	8.92383						
170	6	1	26.97418	0.49796	8.90591	28.43552	0.50353	8.83938	0.03150	0.12796	0.99128	0.009598	1.553557	0.73858
171		2	26.97240	0.96514	8.72838	28.43382	0.97184	8.64061	0.04736	0.37291	0.92666	0.004812	1.557402	0.73767
172		3	26.96544	1.34274	8.40390	28.42628	1.33215	8.28244	0.05335	0.67869	0.73249	0.009107	1.564400	0.73594
173		4	26.95724	1.58263	7.96596	28.42099	1.56277	7.82708	0.05058	0.88395	0.46483	0.004036	1.581067	0.73987
174		5	26.95972	1.67389	7.47342	28.42369	1.62768	7.32153	0.03764	0.98725	0.15467	0.007003	1.602433	0.73958
175		6	26.95723	1.67881	6.97343	28.42380	1.62088	6.81054	0.03531	0.99937	-0.00194	0.002899	1.608027	0.74132
176		7	26.95937	1.69102	6.47266	28.42809	1.62782	6.29961	0.04342	0.99887	0.01918	0.001340	1.618658	0.74270
177		8	26.96979	1.69079	5.97178	28.44263	1.61640	5.78917	0.04546	0.99891	-0.01039	0.002722	1.634870	0.74231
			28.43298	0.0	8.92383	30.76100	0.0	8.91839						
178	7	1	28.43552	0.50353	8.83938	30.76100	0.49706	8.82790	0.00382	0.17222	0.98505	0.001758	2.382419	1.18172
179		2	28.43382	0.97184	8.64061	30.76100	0.95524	8.62269	0.00777	0.39969	0.91662	0.002484	2.382488	1.17569
180		3	28.42628	1.33215	8.28244	30.76102	1.30854	8.26553	0.01138	0.70797	0.70615	0.001036	2.389291	1.17767
181		4	28.42099	1.56277	7.82708	30.76100	1.57001	7.83461	0.00404	0.87428	0.48540	0.009718	2.394282	1.18474
182		5	28.42369	1.62768	7.32153	30.76102	1.64727	7.33864	-0.00642	0.99006	0.14052	0.003398	2.393654	1.18289
183		6	28.42380	1.62088	6.81054	30.76100	1.64137	6.83327	-0.00847	0.99989	-0.01250	0.000208	2.396280	1.18786
184		7	28.42809	1.62782	6.29961	30.76100	1.63888	6.32798	-0.00680	0.99997	0.00435	0.002344	2.393211	1.18656
185		8	28.44263	1.61640	5.78917	30.76100	1.62955	5.82297	-0.00493	0.99978	-0.02050	0.000513	2.381105	1.18128
			30.76100	0.0	8.91839	36.00000	0.0	8.89000						
186	8	1	30.76100	0.49706	8.82790	35.99997	0.42667	8.82165	0.00440	0.16946	0.98553	0.002472	5.262889	2.45523
187		2	30.76100	0.95524	8.62269	35.99997	0.82006	8.64235	0.00691	0.41152	0.91137	0.000754	5.269319	2.44759
188		3	30.76102	1.30854	8.26553	35.99997	1.15188	8.36545	0.01054	0.67918	0.73390	0.011086	5.275148	2.44541
189		4	30.76100	1.57001	7.83461	35.99997	1.40774	8.01714	0.01045	0.83307	0.55307	0.010256	5.282365	2.45018
190		5	30.76102	1.64727	7.33864	35.99997	1.53620	7.60670	0.01592	0.97508	0.22131	0.017216	5.288132	2.43503
191		6	30.76100	1.64137	6.83327	35.99997	1.53336	7.17385	0.02144	0.99973	-0.00932	0.000595	5.296791	2.45830
192		7	30.76100	1.63888	6.32798	35.99998	1.49776	6.74338	0.02668	0.99882	-0.04065	0.009025	5.307860	2.45411
193		8	30.76100	1.62955	5.82297	35.99997	1.31294	6.35332	0.06171	0.97541	-0.21158	0.048875	5.320848	2.40371
SEC	5,TYP=NLIF		13.24000	2.49562	6.08937	16.42842	2.33368	5.93854						
194	1	1	13.24000	1.86802	5.99559	16.42966	1.75313	5.83150	-0.04156	0.16378	-0.98562	0.005181	3.285070	1.95443
195		2	13.24000	1.23555	5.95322	16.42834	1.15746	5.78050	-0.05030	0.07576	-0.99586	0.002861	3.273629	1.96647
196		3	13.24000	0.63137	5.75612	16.42856	0.59213	5.61208	-0.04189	0.29804	-0.95363	0.003951	3.270663	1.95509
197		4	13.24000	0.0	5.70000	16.42874	0.0	5.53106	-0.04803	0.11126	-0.99263	0.007266	3.258414	1.9651[illegible]
			16.42842	2.33368	5.93854	18.82666	2.19727	5.85649						
198	2	1	16.42966	1.75313	5.83150	18.83253	1.74812	5.61213	-0.04986	0.32227	-0.94533	0.042979	2.495832	1.30712
199		2	16.42834	1.15746	5.78050	18.82961	1.16044	5.57671	-0.08748	0.07287	-0.99350	0.003692	2.485142	1.43054
200		3	16.42856	0.59213	5.61208	18.83125	0.58211	5.48809	-0.06611	0.21870	-0.97355	0.020159	2.488068	1.4108[illegible]
201		4	16.42874	0.0	5.53106	18.83109	0.0	5.40837	-0.05052	0.13545	-0.98950	0.000016	2.482788	1.4255[illegible]
			18.82666	2.19727	5.85649	20.88670	2.05842	5.69828						
202	3	1	18.83253	1.74812	5.61213	20.87991	1.73170	5.39641	-0.05260	0.57492	-0.81652	0.029500	2.155057	0.975[illegible]

Figure 25. (Continued) Output from the sample case.

CASE TITLE: REPORT TEST CASE,TRANS. CALC., 2DSTRIP BL, M=0.6, ALPHAS
PAGE TITLE: INPUT PANEL CORNER POINTS AND COMPUTED PANEL QUANTITIES

ALPHA = 1.50 MACH = 0.6000
VISCOUS/INVISCID CYCLE NO 0

PNL. NO.	IV	IU	EX	XA	YA	ZA	XB	YB	ZB	NX	NY	NZ	AVERAGE PROJ DIST	MAXIMUM DIAGONAL	PROJECTED AREA
				|<---------- D E F I N I N G		N - L I N E S			---------->|	|<---- N O R M A L S		---->|		
203		2		18.82961	1.16044	5.57671	20.87648	1.15297	5.37175	-0.10178	0.05172	-0.99346	0.002551	2.142554	1.201?8
204		3		18.83125	0.58211	5.48809	20.88133	0.57510	5.33481	-0.08625	0.10709	-0.99050	0.012858	2.147258	1.1955[illegible]
205		4		18.83109	0.0	5.40837	20.87863	0.0	5.28024	-0.06786	0.11517	-0.99103	0.005988	2.138645	1.19619
				20.88670	2.05842	5.69828	23.87218	1.84097	5.54329						
206	4	1		20.87991	1.73170	5.39641	23.85594	1.46304	5.43510	0.02409	0.50225	-0.86440	0.048341	3.039751	1.2181[illegible]
207		2		20.87648	1.15297	5.37175	23.85582	0.96787	5.44572	0.01990	0.01300	-0.99972	0.008531	3.072762	1.599[illegible]
208		3		20.88133	0.57510	5.33481	23.85054	0.48296	5.55211	0.04577	-0.06515	-0.99682	0.037554	3.053928	1.5855[illegible]
209		4		20.87863	0.0	5.28024	23.84995	0.0	5.48019	0.07140	0.11818	-0.99042	0.007054	3.027294	1.5866[illegible]
				23.87218	1.84097	5.54329	26.95326	1.69297	5.52020						
210	5	1		23.85594	1.46304	5.43510	26.94032	1.40435	5.55860	0.01966	0.10326	-0.99446	0.034125	3.107005	1.0346[illegible]
211		2		23.85582	0.96787	5.44572	26.93628	0.92895	5.66865	0.05373	-0.12344	-0.99090	0.025300	3.135004	1.50960
212		3		23.85054	0.48296	5.55211	26.93353	0.47460	5.67155	0.05420	-0.11586	-0.99178	0.024805	3.125156	1.4593[illegible]
213		4		23.84995	0.0	5.48019	26.93349	0.0	5.60617	0.03956	0.14180	-0.98910	0.001319	3.129757	1.4924[illegible]
				26.95326	1.69297	5.52020	28.43810	1.62904	5.62337						
214	6	1		26.94032	1.40435	5.55860	28.42143	1.32829	5.63921	0.05714	0.09434	-0.99390	0.005836	1.517460	0.440[illegible]
215		2		26.93628	0.92895	5.66865	28.41695	0.88051	5.77571	0.05028	-0.25814	0.96480	0.008169	1.581758	0.700[illegible]
216		3		26.93353	0.47460	5.67155	28.41666	0.45097	5.73098	0.05716	0.04699	0.99726	0.012196	1.556878	0.656[illegible]
217		4		26.93349	0.0	5.60617	28.41734	0.0	5.65738	0.03803	0.14842	0.98819	0.002911	1.557929	0.694[illegible]
				28.43810	1.62904	5.62337	30.77306	1.62954	5.82408						
218	7	1		28.42143	1.32829	5.63921	30.77306	1.28273	5.80082	0.07717	0.00943	0.99697	0.009953	2.378035	0.76[illegible]
219		2		28.41695	0.88051	5.77571	30.77306	0.85044	5.89722	0.05394	-0.25570	0.96525	0.008745	2.413509	1.075[illegible]
220		3		28.41666	0.45097	5.73098	30.77307	0.43325	5.78187	0.03780	0.18562	0.98189	0.017911	2.398206	1.01[illegible]
221		4		28.41734	0.0	5.65738	30.77306	0.0	5.71667	0.02367	0.15585	0.98762	0.001395	2.399204	1.054[illegible]
				30.77306	1.62954	5.82408	35.99997	1.31292	6.35329						
222	8	1		30.77306	1.28273	5.80082	35.99997	1.07926	6.03748	0.08801	0.50243	0.86013	0.0[illegible]120	5.260128	[illegible]
223		2		30.77306	0.85044	5.89722	35.99997	0.75934	5.81017	0.01895	0.17143	0.98501	0.00452[illegible]	5.253059	[illegible]995[illegible]
224		3		30.77307	0.43325	5.78187	35.99997	0.38659	5.68140	-0.01325	0.29524	0.95533	0.006481	5.25108[illegible]	2.16090
225		4		30.77306	0.0	5.71667	36.00000	0.0	5.62000	-0.01795	0.15258	-0.98813	0.000841	5.247349	2.1683[illegible]

Figure 25. (Continued) Output from the sample case

CASE TITLE: REPORT TEST CASE,TRANS. CALC., 2DSTRIP BL, M=0.6, ALPHAS

PAGE TITLE: INTEGRATED PRESSURES

ALPHA : 1.30 MACH : 0.600(

VISCOUS-INVISCID CYCLE NO 0

TYPE	SEC	NV	CL	CD	CSF	CPITCH	CROLL	CYAW	ETA	SECTCL	SECTCD	ASTRIP	CIRCULTN
			|<------ BASED UPON	INPUT VALUES	OF AREF,BOV2,CREF			------>|					
LIFT	1	1	0.0045	-0.0003	0.0006	-0.0155	-0.0024	-0.0014	0.8463	0.0284	-0.0018	15.0991	-0.0062
		2	0.0226	-0.0007	0.0020	-0.0700	-0.0075	-0.0042	0.5712	0.0898	-0.0028	24.1940	-0.0175
		3	0.0512	-0.0001	0.0064	-0.1443	-0.0185	-0.0113	0.2759	0.1383	-0.0002	35.5155	-0.0322
SECT. TOT:			0.0784	-0.0011	0.0090	-0.2297	-0.0284	-0.0170					
NLIF	2	1	-0.0008	0.0010	-0.0016	0.0010	0.0005	0.0003					
		2	-0.0029	0.0009	-0.0024	0.0026	0.0014	0.0010					
SECT. TOT:			-0.0037	0.0018	-0.0040	0.0035	0.0019	0.0013					
NLIF	3	1	-0.0019	-0.0000	0.0051	0.0019	-0.0048	-0.0032					
		2	0.0037	-0.0005	0.0092	-0.0051	-0.0112	-0.0074					
		3	0.0023	-0.0000	0.0042	-0.0034	-0.0061	-0.0040					
SECT. TOT:			0.0041	-0.0005	0.0184	-0.0067	-0.0222	-0.0147					
NLIF	4	1	0.0028	0.0001	0.0034	-0.0050	-0.0060	-0.0039					
		2	0.0019	0.0000	0.0011	-0.0041	-0.0023	-0.0015					
		3	0.0027	0.0007	0.0076	-0.0060	-0.0178	-0.0115					
		4	0.0064	0.0009	0.0131	-0.0166	-0.0350	-0.0227					
		5	0.0042	0.0007	0.0083	-0.0125	-0.0251	-0.0163					
		6	-0.0004	-0.0000	-0.0007	0.0012	0.0024	0.0016					
		7	-0.0011	-0.0000	-0.0037	0.0039	0.0133	0.0086					
		8	-0.0013	-0.0001	-0.0031	0.0050	0.0125	0.0081					
SECT. TOT:			0.0153	0.0023	0.0259	-0.0340	-0.0580	-0.0377					
NLIF	5	1	-0.0008	-0.0001	0.0001	0.0014	-0.0002	-0.0002					
		2	0.0011	0.0001	-0.0001	-0.0023	0.0002	0.0002					
		3	-0.0003	-0.0000	-0.0001	0.0007	0.0002	0.0001					
		4	-0.0015	0.0000	-0.0003	0.0041	0.0009	0.0006					
		5	-0.0024	0.0000	0.0000	0.0073	0.0000	-0.0000					
		6	0.0006	-0.0000	0.0000	-0.0019	-0.0001	-0.0001					
		7	0.0030	-0.0001	-0.0000	-0.0107	-0.0000	0.0000					
		8	0.0024	0.0000	-0.0007	-0.0096	0.0029	0.0019					
SECT. TOT:			0.0021	0.0000	-0.0011	-0.0110	0.0038	0.0025					
CONFIG.TOT:			0.0962	0.0026	0.0483	-0.2779	0.0058	0.0657					

Figure 25. (Continued) Output from the sample case.

```
PAGE   18                      3-D VISCOUS-INVISCID INTERACTIVE PROGRAM                         TUESDAY,    APR 15, 1986
                               ----------------------------------------
CASE TITLE:     REPORT TEST CASE,TRANS. CALC., 2DSTRIP BL, M=0.6, ALPHAS                     ALPHA =    1.30 MACH = 0.6000
PAGE TITLE:  INPUT DATA                                                                     VISCOUS/INVISCID CYCLE NO.   2
------------------------------------------------------------------------------------------------------------------------

                                         INPUT FLAGS
                                         -----------

                                         ICYCLE =  2
                                         BOV2   =        12.95500
                                         C1VAL  =         0.0
                                         HGND   =         0.0
                                         IAUTOW =  2
                                         IBLFIT =  1
                                         ICONT  =  1
                                         ICONV  =  1
                                         IOUT   =  0
                                         IPCV   =  1
                                         ITERAT =  1
                                         KUTTA  =  2
                                         IVNSP  =  3
                                         LIFSEC =  1
                                         LINEAR =  0
                                         LIST   =  0
                                         MAXCYC =  2
                                         MPR    =  0
                                         NLR    =  0
                                         NOFF   =  0
                                         NSYM1  =  1
                                         NSYM2  =  0
                                         ORIGNX =         0.0
                                         ORIGNY =         0.0
                                         ORIGNZ =         0.0
                                         RFAREA =        95.90401
                                         REFCHD =         8.29120
                                         RMACH  =         0.60000

                                RUN MODE =  1  ( 0=INITIAL RUN. 1=BLOWING RUN.)

                                         NSORCE =  20
                                         NWAKE  =   1
                                         NSTRIP =   4
                                         IXFLAG =   3

                                         OFF - BODY KUTA CONDITION HAS BEEN SELECTED...
                                           PRINTED CP DISTRIBUTION AND FORCE CALCULATION
                                           WILL USE OFF - BODY PRESSURES

                                INPUT UNIFORM ONSET FLOWS IN DEGS AND COMPONENTS

                        ( 1)  DEG --    1.299999  COMPONENTS --     0.999743    0.0          0.022687

                               INPUT MACH NO. =     0.600000  BETA =  0.800000E+00
```

Figure 25. (Continued) Output from the sample case.

CASE TITLE: REPORT TEST CASE,TRANS. CALC., 2DSTRIP BL, M=0.6, ALPHAS — ALPHA = 1.30 MACH = 0.6000
PAGE TITLE: FUNDAMENTAL FLOW SOLUTION — VISCOUS/INVISCID CYCLE NO. 2

****** WARNING ****** PRINTED CP, VX, VY, VZ AND FORCES ARE COMPUTED AT OFF - BODY POINTS

PNL. NO.	SEC NO.	SEC. TYPE	IV	IU	CONTROL POINTS X	Y	Z	INCOMPRESSIBLE POTENTIAL FL SOLUTN VX	VY	VZ	VT	VISCOUS FLOW SOLUTION CPVISC	DELS	H	CF
1	1	LIFT	1	1	29.24013	10.96359	5.66436	0.93231	-0.01307	0.08559	0.93632	0.12468	0.01364	1.44747	0.00215
2				2	29.03622	10.96347	5.64078	0.98662	-0.01499	0.10140	0.99193	0.01610	0.01122	1.40443	0.00254
3				3	28.64761	10.96357	5.60907	1.02211	-0.01426	0.05038	1.02345	-0.04725	0.00901	1.37516	0.00296
4				4	28.11116	10.96349	5.58675	1.01983	-0.01113	0.02401	1.02018	-0.04061	0.00763	1.37522	0.00314
5				5	27.48058	10.96352	5.56079	1.01973	-0.01228	0.04799	1.02094	-0.04215	0.00627	1.38920	0.00326
6				6	26.81805	10.96350	5.52009	1.03064	-0.01718	0.06576	1.03287	-0.06643	0.00467	1.40574	0.00350
7				7	26.18784	10.96351	5.48367	1.04009	-0.01847	0.03926	1.04099	-0.08304	0.00308	1.43536	0.00392
8				8	25.65141	10.96352	5.46120	1.02644	-0.00792	0.03486	1.02706	-0.05459	0.00160	1.56275	0.00413
9				9	25.26169	10.96329	5.44005	1.07117	-0.03579	0.07396	1.07432	-0.15203	0.00118	2.65748	0.00141
10				10	25.06764	10.97600	5.44348	1.10662	-0.04894	-0.32796	1.15523	-0.32460	0.00056	2.40618	0.00390
11				11	25.05743	10.96301	5.48399	0.77459	0.17063	0.38051	0.87971	0.23075	0.00046	2.46123	0.00507
12				12	25.25879	10.96352	5.52620	1.06502	-0.02358	0.11381	1.07135	-0.14583	0.00086	2.43471	0.00267
13				13	25.64748	10.96352	5.56395	1.02922	0.00116	0.08888	1.03305	-0.06678	0.00154	2.54228	0.00128
14				14	26.18195	10.96349	5.62001	1.03308	0.00266	0.11678	1.03966	-0.08031	0.00194	1.50915	0.00416
15				15	26.81053	10.96356	5.68236	1.07420	-0.01810	0.08719	1.07788	-0.15949	0.00342	1.41828	0.00382
16				16	27.47318	10.96352	5.71222	1.07533	-0.02718	0.00927	1.07571	-0.15494	0.00503	1.40258	0.00339
17				17	28.10471	10.96349	5.70677	1.03977	-0.02277	-0.02585	1.04034	-0.08171	0.00687	1.40091	0.00308
18				18	28.64288	10.96350	5.69308	1.01909	-0.01937	-0.02554	1.01960	-0.03944	0.00865	1.40261	0.00285
19				19	29.03436	10.96348	5.68132	0.99370	-0.01648	-0.03353	0.99440	0.01118	0.01085	1.42634	0.00248
20				20	29.24001	10.96351	5.67272	0.93605	-0.01389	-0.03472	0.93679	0.12377	0.01330	1.47251	0.00205
22	1	LIFT	2	1	29.16090	7.39987	5.66218	0.91564	-0.01339	0.07040	0.91844	0.15867	0.02141	1.44938	0.00192
23				2	28.84059	7.39991	5.62529	0.96203	-0.01540	0.10577	0.96795	0.06342	0.01746	1.40458	0.00224
24				3	28.23080	7.39988	5.56673	1.01934	-0.01629	0.07057	1.02191	-0.04413	0.01333	1.36412	0.00267
25				4	27.38876	7.39995	5.52633	1.03561	-0.01078	0.01658	1.03580	-0.07240	0.01075	1.35239	0.00292
26				5	26.39757	7.39989	5.50779	1.03201	-0.00625	0.00969	1.03207	-0.06479	0.00877	1.35971	0.00307
27				6	25.35545	7.39992	5.48668	1.02821	-0.00451	0.02158	1.02845	-0.05741	0.00675	1.37464	0.00325
28				7	24.36435	7.39990	5.46707	1.01886	0.00109	0.00754	1.01889	-0.03800	0.00473	1.40066	0.00353
29				8	23.52112	7.39990	5.45788	1.00530	0.01013	0.00161	1.00535	-0.01072	0.00266	1.45147	0.00410
30				9	22.90884	7.40013	5.44205	1.03720	-0.00732	0.05109	1.03849	-0.07790	0.00136	2.36798	0.00194
31				10	22.58910	7.39812	5.45092	1.00541	0.01494	-0.27981	1.04373	-0.08866	0.00082	2.48810	0.00259
32				11	22.58403	7.39007	5.51242	0.84744	0.13831	0.39963	0.94709	0.10397	0.00061	2.51505	0.00348
33				12	22.90768	7.40009	5.58819	1.06614	-0.02158	0.15716	1.07788	-0.15948	0.00111	2.46504	0.00193
34				13	23.51645	7.39992	5.65806	1.06370	-0.02201	0.09246	1.06794	-0.13873	0.00161	1.68904	0.00320
35				14	24.35703	7.39992	5.73437	1.07619	-0.02539	0.09736	1.08088	-0.16577	0.00353	1.41164	0.00381
36				15	25.34647	7.39989	5.80141	1.10116	-0.03913	0.05167	1.10306	-0.21255	0.00570	1.38025	0.00334
37				16	26.38838	7.39989	5.81260	1.08644	-0.04081	-0.02645	1.08753	-0.17974	0.00823	1.37638	0.00299
38				17	27.37976	7.39992	5.77294	1.04551	-0.03223	-0.05783	1.04760	-0.09662	0.01117	1.38115	0.00273
39				18	28.22421	7.39990	5.72987	1.02087	-0.02363	-0.04470	1.02212	-0.04455	0.01394	1.38313	0.00256
40				19	28.83855	7.39993	5.69944	0.99281	-0.01870	-0.05043	0.99426	0.01144	0.01786	1.41612	0.00216
41				20	29.16106	7.39991	5.67782	0.91634	-0.01499	-0.06952	0.91909	0.15745	0.02341	1.49192	0.00159
43	1	LIFT	3	1	29.07686	3.57456	5.66122	0.90135	-0.00560	0.05300	0.90292	0.18781	0.02719	1.45170	0.00180
44				2	28.63852	3.57524	5.62328	0.95113	-0.01021	0.07431	0.95409	0.09044	0.02183	1.40367	0.00213
45				3	27.80554	3.59075	5.55483	1.00331	-0.01397	0.06878	1.00576	-0.01155	0.01639	1.36383	0.00254
46				4	26.65736	3.62799	5.50029	1.03838	-0.01597	0.01731	1.03865	-0.07823	0.01256	1.34654	0.00281
47				5	25.30577	3.66661	5.49795	1.03428	-0.01472	-0.02421	1.03467	-0.07010	0.00989	1.34876	0.00302
48				6	23.88484	3.70989	5.53098	1.01736	-0.01250	-0.03422	1.01801	-0.03623	0.00742	1.36786	0.00320
49				7	22.53481	3.76683	5.57135	1.00265	-0.00704	-0.03848	1.00341	-0.00683	0.00475	1.40352	0.00354

Figure 25. (Continued) Output from the sample case.

CASE TITLE: REPORT TEST CASE,TRANS. CALC., 2DSTRIP BL, M=0.6, ALPHAS ALPHA = 1.30 MACH = 0.6000
PAGE TITLE: FUNDAMENTAL FLOW SOLUTION VISCOUS/INVISCID CYCLE NO. 2

****** WARNING ****** PRINTED CP, VX, VY, VZ AND FORCES ARE COMPUTED AT OFF - BODY POINTS

PNL. NO.	SEC NO.	SEC. TYPE	IV	IU	X (CONTROL POINTS)	Y	Z	VX (INCOMPRESSIBLE POTENTIAL FL SOLUTN)	VY	VZ	VT	CPVISC (VISCOUS FLOW SOLUTION)	DELS	H	CF
50	1	LIFT	3	8	21.38661	3.81661	5.60855	0.99272	-0.00028	-0.03998	0.99352	0.01293	0.00203	1.56006	0.00360
51				9	20.55191	3.84817	5.62768	1.00214	-0.00469	-0.01359	1.00224	-0.00449	0.00131	2.46320	0.00174
52				10	20.12907	3.87635	5.66301	0.83159	0.09117	-0.27961	0.88207	0.22642	0.00068	2.49230	0.00337
53				11	20.12923	3.86983	5.75069	0.95051	0.07616	0.41043	1.03814	-0.07719	0.00089	2.42182	0.00257
54				12	20.56233	3.85267	5.86353	1.08542	-0.04040	0.19328	1.10323	-0.21291	0.00153	2.48262	0.00130
55				13	21.38992	3.81062	5.96442	1.10391	-0.06462	0.08515	1.10908	-0.22533	0.00220	1.49197	0.00388
56				14	22.53728	3.75731	6.03259	1.10148	-0.06255	0.04788	1.10429	-0.21517	0.00501	1.40145	0.00337
57				15	23.88872	3.70660	6.06332	1.10401	-0.06082	0.00550	1.10570	-0.21814	0.00790	1.36897	0.00306
58				16	25.30960	3.66691	6.02750	1.08764	-0.05335	-0.05668	1.09042	-0.18582	0.01118	1.36281	0.00279
59				17	26.65891	3.62719	5.93108	1.04836	-0.03743	-0.09349	1.05319	-0.10814	0.01507	1.36786	0.00257
60				18	27.80655	3.58724	5.82587	1.01444	-0.02249	-0.09333	1.01897	-0.03817	0.01918	1.37711	0.00237
61				19	28.64058	3.57153	5.74079	0.97141	-0.01339	-0.10459	0.97712	0.04542	0.02515	1.41573	0.00196
62				20	29.07799	3.57391	5.68655	0.89678	-0.00625	-0.11344	0.90395	0.18590	0.03385	1.50455	0.00139
85	2	NLIF	1	1	2.46411	0.06440	6.63511	0.75468	0.07703	0.38173	0.84923	0.28587	0.0	0.0	0.0
86				2	2.47168	0.18659	6.59474	0.77080	0.22390	0.31014	0.86050	0.26566	0.0	0.0	0.0
87				3	2.47205	0.28618	6.51136	0.79471	0.31750	0.19068	0.87677	0.23612	0.0	0.0	0.0
88				4	2.46727	0.35007	6.39909	0.82226	0.35025	0.05226	0.89527	0.20205	0.0	0.0	0.0
89				5	2.47436	0.37490	6.27388	0.85603	0.31877	-0.07974	0.91693	0.16153	0.0	0.0	0.0
90				6	2.47711	0.35302	6.14681	0.88443	0.24658	-0.17317	0.93435	0.12844	0.0	0.0	0.0
91				7	2.47280	0.28379	6.03986	0.91063	0.14755	-0.21602	0.94746	0.10325	0.0	0.0	0.0
92				8	2.47440	0.18161	5.96121	0.92291	0.08655	-0.22223	0.95322	0.09211	0.0	0.0	0.0
93				9	2.47641	0.06238	5.90800	0.92732	0.04277	-0.22565	0.95534	0.08800	0.0	0.0	0.0
94	2	NLIF	2	1	5.00345	0.14725	7.47020	0.89886	0.08386	0.25269	0.93746	0.12248	0.0	0.0	0.0
95				2	5.00385	0.41482	7.33160	0.92507	0.17022	0.15698	0.95361	0.09137	0.0	0.0	0.0
96				3	5.00467	0.62980	7.11092	0.94500	0.18820	0.07900	0.96679	0.06569	0.0	0.0	0.0
97				4	5.01137	0.78530	6.84464	0.95977	0.18308	0.01148	0.97714	0.04538	0.0	0.0	0.0
98				5	5.00465	0.86400	6.54678	0.97014	0.16587	-0.04871	0.98543	0.02900	0.0	0.0	0.0
99				6	5.00488	0.83868	6.24607	0.98382	0.10714	-0.10447	0.99514	0.00970	0.0	0.0	0.0
100				7	5.00902	0.68681	5.98742	0.99554	0.03233	-0.10223	1.00129	-0.00259	0.0	0.0	0.0
101				8	5.00489	0.44066	5.80510	0.99954	0.00351	-0.07620	1.00245	-0.00490	0.0	0.0	0.0
102				9	5.00645	0.15131	5.69692	1.00081	-0.00223	-0.05834	1.00251	-0.00503	0.0	0.0	0.0
103	3	NLIF	1	1	7.89182	0.22528	8.64750	0.82161	0.22572	0.39664	0.93985	0.11790	0.0	0.0	0.0
104				2	7.88930	0.59265	8.35452	0.98438	0.33180	0.08057	1.04191	-0.08492	0.0	0.0	0.0
105				3	7.89877	0.77934	7.92960	1.04804	0.08741	-0.04195	1.05251	-0.10674	0.0	0.0	0.0
106				4	7.89551	0.97142	7.50561	1.00056	0.17571	0.06801	1.01815	-0.03650	0.0	0.0	0.0
107				5	7.89360	1.19285	7.08127	1.02065	0.17370	-0.04643	1.03636	-0.07355	0.0	0.0	0.0
108				6	7.89500	1.23320	6.60854	1.03699	0.06773	-0.10944	1.04494	-0.09115	0.0	0.0	0.0
109				7	7.89226	1.05357	6.16956	1.03518	-0.02399	-0.06834	1.03771	-0.07632	0.0	0.0	0.0
110				8	7.89304	0.69748	5.84617	1.02804	-0.03618	-0.01388	1.02877	-0.05806	0.0	0.0	0.0
111				9	7.89288	0.24317	5.67151	1.02366	-0.01818	0.01985	1.02402	-0.04840	0.0	0.0	0.0
112	3	NLIF	2	1	10.26125	0.26061	9.29051	1.07871	-0.02324	0.02212	1.07919	-0.16222	0.0	0.0	0.0
113				2	10.25645	0.63987	8.89867	1.07430	-0.04798	0.07313	1.07786	-0.15943	0.0	0.0	0.0
114				3	10.24283	0.85733	8.40572	1.06318	0.03595	0.11801	1.07032	-0.14368	0.0	0.0	0.0
115				4	10.26551	1.13351	7.94864	1.03734	0.10870	0.10739	1.04853	-0.09853	0.0	0.0	0.0
116				5	10.26760	1.36949	7.43462	1.03834	0.08569	-0.00160	1.04187	-0.08484	0.0	0.0	0.0
117				6	10.26759	1.41179	6.85602	1.03155	0.03951	-0.01427	1.03241	-0.06548	0.0	0.0	0.0
118				7	10.26149	1.24667	6.30984	1.02184	0.03644	-0.02743	1.02286	-0.04604	0.0	0.0	0.0

Figure 25. (Continued) Output from the sample case.

PAGE 23   3-D VISCOUS-INVISCID INTERACTIVE PROGRAM   TUESDAY, APR 15, 1986

CASE TITLE: REPORT TEST CASE,TRANS. CALC., 2DSTRIP BL, M=0.6, ALPHAS   ALPHA = 1.30 MACH = 0.6000
PAGE TITLE: FUNDAMENTAL FLOW SOLUTION   VISCOUS/INVISCID CYCLE NO 2

****** WARNING ****** PRINTED CP, VX, VY, VZ AND FORCES ARE COMPUTED AT OFF - BODY POINTS

PNL.	SEC	SEC.			<---- CONTROL POINTS ---->			<INCOMPRESSIBLE POTENTIAL FL SOLUTN>				<------- VISCOUS FLOW SOLUTION ------>			
NO.	NO.	TYPE	IV	IU	X	Y	Z	VX	VY	VZ	VT	CPVISC	DELS	M	CF
119	3	NLIF	2	8	10.26603	0.84292	5.91563	1.01702	-0.00011	-0.02802	1.01740	-0.03499	0.0	0.0	0.0
120				9	10.26438	0.29268	5.72676	1.01421	-0.00976	0.00525	1.01427	-0.02868	0.0	0.0	0.0
121	3	NLIF	3	1	12.34360	0.24696	9.16012	1.01049	-0.14054	-0.10332	1.02543	-0.05127	0.0	0.0	0.0
122				2	12.35182	0.66708	8.81478	1.04388	-0.10325	0.07386	1.05157	-0.10480	0.0	0.0	0.0
123				3	12.36334	1.06277	8.43107	1.04331	-0.02604	0.10303	1.04871	-0.09890	0.0	0.0	0.0
124				4	12.35467	1.38806	7.97498	1.03911	0.04294	0.07992	1.04306	-0.08728	0.0	0.0	0.0
125				5	12.35265	1.51473	7.39872	1.03449	0.04922	0.04605	1.03669	-0.07422	0.0	0.0	0.0
126				6	12.35251	1.49562	6.80041	1.02226	0.05510	0.03178	1.02423	-0.04884	0.0	0.0	0.0
127				7	12.35432	1.30585	6.24793	1.00809	0.04920	0.00862	1.00933	-0.01871	0.0	0.0	0.0
128				8	12.35233	0.87543	5.88525	0.99928	0.02364	-0.01897	0.99974	0.00050	0.0	0.0	0.0
129				9	12.35274	0.29784	5.73324	0.99587	0.00502	-0.01280	0.99596	0.00806	0.0	0.0	0.0
130	4	NLIF	1	1	14.83243	0.28406	8.96744	1.01332	-0.03786	-0.01951	1.01422	-0.02857	0.0	0.0	0.0
131				2	14.81987	0.85290	8.75072	1.01718	-0.02637	0.04250	1.01841	-0.03703	0.0	0.0	0.0
132				3	14.82926	1.38545	8.44981	1.01778	0.01155	0.05396	1.01927	-0.03878	0.0	0.0	0.0
133				4	14.81589	1.94886	8.25629	1.01881	0.04459	0.03807	1.02049	-0.04125	0.0	0.0	0.0
134				5	14.83490	2.44425	8.03695	1.01509	-0.00398	-0.05892	1.01681	-0.03379	0.0	0.0	0.0
135				6	14.81558	2.64464	7.51805	1.00206	-0.10824	0.00814	1.00792	-0.01587	0.0	0.0	0.0
136				7	14.81826	2.65907	6.88611	1.00185	-0.10566	0.08836	1.01127	-0.02262	0.0	0.0	0.0
137				8	14.81548	2.53438	6.29290	1.01401	0.01554	0.16673	1.02774	-0.05597	0.0	0.0	0.0
138	4	NLIF	2	1	17.62799	0.30528	8.90782	1.01609	-0.01046	-0.01159	1.01620	-0.03258	0.0	0.0	0.0
139				2	17.62973	0.89480	8.78426	1.01640	-0.03112	0.00143	1.01688	-0.03394	0.0	0.0	0.0
140				3	17.62886	1.45180	8.56722	1.01595	-0.00679	0.04446	1.01694	-0.03407	0.0	0.0	0.0
141				4	17.61188	1.99848	8.36462	1.01395	0.02477	0.02356	1.01452	-0.02918	0.0	0.0	0.0
142				5	17.63661	2.32518	7.99501	1.00682	-0.05185	-0.00936	1.00820	-0.01643	0.0	0.0	0.0
143				6	17.62924	2.37434	7.39805	0.99670	-0.08586	0.03758	1.00110	-0.00220	0.0	0.0	0.0
144				7	17.62631	2.36945	6.78852	0.98847	-0.09352	0.09261	0.99719	0.00560	0.0	0.0	0.0
145				8	17.63345	2.31426	6.19088	0.98939	-0.04386	0.19010	1.00844	-0.01692	0.0	0.0	0.0
146	4	NLIF	3	1	19.84778	0.28660	8.90368	1.02450	-0.00772	0.00007	1.02452	-0.04943	0.0	0.0	0.0
147				2	19.84860	0.85210	8.80477	1.02681	-0.01447	0.01380	1.02700	-0.05446	0.0	0.0	0.0
148				3	19.85272	1.40577	8.66814	1.03018	0.00341	0.03359	1.03074	-0.06207	0.0	0.0	0.0
149				4	19.85573	1.91566	8.46865	1.03566	0.02156	-0.00339	1.03589	-0.07259	0.0	0.0	0.0
150				5	19.84579	2.15694	8.04858	1.02490	-0.10692	0.00329	1.03047	-0.06153	0.0	0.0	0.0
151				6	19.84290	2.16018	7.47127	1.02741	-0.11163	0.07018	1.03584	-0.07248	0.0	0.0	0.0
152				7	19.83890	2.14716	6.89521	1.03749	-0.10755	0.13700	1.05200	-0.10569	0.0	0.0	0.0
153				8	19.83937	2.12780	6.31944	1.10913	-0.09247	0.22279	1.13506	-0.28096	0.0	0.0	0.0
154	4	NLIF	4	1	22.38484	0.26312	8.94598	1.04788	0.00365	0.02033	1.04808	-0.09760	0.0	0.0	0.0
155				2	22.38852	0.78501	8.88060	1.04862	0.01918	0.02368	1.04907	-0.09963	0.0	0.0	0.0
156				3	22.38708	1.29275	8.75813	1.05153	0.04001	-0.00354	1.05230	-0.10630	0.0	0.0	0.0
157				4	22.39178	1.71345	8.50278	1.04941	-0.02684	-0.07748	1.05261	-0.10694	0.0	0.0	0.0
158				5	22.38063	1.91412	8.06254	1.05108	-0.09434	-0.01369	1.05539	-0.11269	0.0	0.0	0.0
159				6	22.37453	1.93714	7.53778	1.06434	-0.07500	0.01928	1.06715	-0.13708	0.0	0.0	0.0
160				7	22.36932	1.93539	7.01049	1.07669	-0.07225	0.02459	1.07939	-0.16264	0.0	0.0	0.0
161				8	22.37270	1.93994	6.48318	1.10738	-0.06949	0.10274	1.11430	-0.23646	0.0	0.0	0.0
162	4	NLIF	5	1	25.43065	0.25176	8.95608	1.03454	0.01043	-0.02387	1.03486	-0.07049	0.0	0.0	0.0
163				2	25.43256	0.74674	8.87438	1.03418	0.02101	-0.05039	1.03562	-0.07203	0.0	0.0	0.0
164				3	25.43010	1.19996	8.67944	1.03129	-0.01214	-0.09134	1.03540	-0.07159	0.0	0.0	0.0
165				4	25.42825	1.53300	8.32792	1.03249	-0.06128	-0.07411	1.03695	-0.07477	0.0	0.0	0.0

Figure 25. (Continued) Output from the sample case.

PAGE 24 3-D VISCOUS-INVISCID INTERACTIVE PROGRAM TUESDAY, APR 15, 1986

CASE TITLE: REPORT TEST CASE,TRANS. CALC., 2DSTRIP BL, M=0.6, ALPHAS ALPHA = 1.30 MACH = 0.6000
PAGE TITLE: FUNDAMENTAL FLOW SOLUTION VISCOUS/INVISCID CYCLE NO. 2

****** WARNING ****** PRINTED CP, VX, VY, VZ AND FORCES ARE COMPUTED AT OFF - BODY POINTS

PNL. NO.	SEC NO.	SEC. TYPE	IV	IU	<---- CONTROL POINTS X	Y	Z ---->	<INCOMPRESSIBLE POTENTIAL FL SOLUTN> VX	VY	VZ	VT	<------- VISCOUS FLOW SOLUTION CPVISC	DELS	H	CF ------>
166	4	NLIF	5	5	25.42151	1.70469	7.86266	1.03962	-0.06153	-0.04600	1.04245	-0.08603	0.0	0.0	0.0
167				6	25.41881	1.75172	7.36230	1.04612	-0.05009	-0.04329	1.04822	-0.09788	0.0	0.0	0.0
168				7	25.41711	1.75855	6.85720	1.05115	-0.05059	-0.05659	1.05389	-0.10959	0.0	0.0	0.0
169				8	25.42238	1.76684	6.35180	1.03797	-0.05059	0.02418	1.03948	-0.07994	0.0	0.0	0.0
170	4	NLIF	6	1	27.70573	0.25036	8.90493	0.99409	0.00540	-0.03690	0.99479	0.01040	0.0	0.0	0.0
171				2	27.70613	0.73465	8.77844	0.99145	0.00236	-0.05632	0.99305	0.01386	0.0	0.0	0.0
172				3	27.70192	1.15299	8.51363	0.98821	-0.01439	-0.06350	0.99036	0.01922	0.0	0.0	0.0
173				4	27.69508	1.45510	8.11951	0.98601	-0.02706	-0.06094	0.98826	0.02337	0.0	0.0	0.0
174				5	27.69247	1.61170	7.64675	0.98503	-0.02921	-0.05920	0.98724	0.02541	0.0	0.0	0.0
175				6	27.69366	1.65022	7.14436	0.98444	-0.03510	-0.06313	0.98708	0.02572	0.0	0.0	0.0
176				7	27.69446	1.65454	6.63872	0.98637	-0.04194	-0.06506	0.98940	0.02113	0.0	0.0	0.0
177				8	27.70216	1.65640	6.13291	0.99925	-0.04588	-0.03929	1.00107	-0.00214	0.0	0.0	0.0
178	4	NLIF	7	1	29.59558	0.25010	8.87738	0.98785	0.00415	-0.00911	0.98790	0.02409	0.0	0.0	0.0
179				2	29.59525	0.73196	8.73264	0.98705	0.00711	-0.01605	0.98720	0.02548	0.0	0.0	0.0
180				3	29.59332	1.14206	8.45273	0.98534	0.00386	-0.02437	0.98565	0.02856	0.0	0.0	0.0
181				4	29.58984	1.44342	8.05233	0.98261	0.00697	-0.02531	0.98297	0.03388	0.0	0.0	0.0
182				5	29.58868	1.60191	7.58049	0.97873	0.01081	-0.03563	0.97944	0.04084	0.0	0.0	0.0
183				6	29.59019	1.63428	7.07597	0.97395	0.00783	-0.04399	0.97497	0.04965	0.0	0.0	0.0
184				7	29.59125	1.63222	6.56790	0.96798	0.00686	-0.04924	0.96926	0.06086	0.0	0.0	0.0
185				8	29.59599	1.62816	6.06016	0.96105	0.00350	-0.06822	0.96348	0.07218	0.0	0.0	0.0
186	4	NLIF	8	1	33.31235	0.23139	8.86471	0.99270	0.00184	-0.00929	0.99275	0.01446	0.0	0.0	0.0
187				2	33.31532	0.67604	8.72855	0.99251	0.00325	-0.01355	0.99261	0.01475	0.0	0.0	0.0
188				3	33.31471	1.06076	8.47324	0.99208	0.00092	-0.01968	0.99227	0.01541	0.0	0.0	0.0
189				4	33.31329	1.36159	8.11887	0.99159	0.00071	-0.02439	0.99189	0.01618	0.0	0.0	0.0
190				5	33.31270	1.54207	7.69636	0.99085	-0.00976	-0.03303	0.99145	0.01705	0.0	0.0	0.0
191				6	33.31296	1.59096	7.23419	0.98980	-0.02157	-0.03272	0.99058	0.01879	0.0	0.0	0.0
192				7	33.31207	1.57947	6.76468	0.98902	-0.02776	-0.03493	0.99003	0.01986	0.0	0.0	0.0
193				8	33.30974	1.52285	6.30544	0.98450	-0.06499	-0.01540	0.98676	0.02635	0.0	0.0	0.0
194	5	NLIF	1	1	14.81527	2.11342	5.96469	1.00894	0.12577	-0.02604	1.01708	-0.03434	0.0	0.0	0.0
195				2	14.81896	1.50402	5.89102	1.00106	0.05295	-0.05104	1.00375	-0.00752	0.0	0.0	0.0
196				3	14.81444	0.90450	5.77646	0.99856	0.04162	-0.03541	1.00005	-0.00011	0.0	0.0	0.0
197				4	14.81868	0.30595	5.65057	0.99545	0.01609	-0.05097	0.99688	0.00623	0.0	0.0	0.0
198	5	NLIF	2	1	17.59962	2.00868	5.81144	0.99139	0.18477	0.00601	1.00847	-0.01699	0.0	0.0	0.0
199				2	17.62697	1.45485	5.70048	0.97745	0.07718	-0.08565	0.98423	0.03137	0.0	0.0	0.0
200				3	17.62782	0.87312	5.61447	0.98096	0.03946	-0.06274	0.98375	0.03232	0.0	0.0	0.0
201				4	17.62646	0.29358	5.51007	0.98284	0.01370	-0.05315	0.98437	0.03109	0.0	0.0	0.0
202	5	NLIF	3	1	19.83246	1.93489	5.64308	0.98520	0.07253	-0.01727	0.98801	0.02388	0.0	0.0	0.0
203				2	19.85184	1.44836	5.48953	0.99082	0.04634	-0.10395	0.99733	0.00531	0.0	0.0	0.0
204				3	19.85289	0.86769	5.44299	1.00256	0.01755	-0.08983	1.00673	-0.01348	0.0	0.0	0.0
205				4	19.85269	0.28941	5.37808	1.01070	0.00839	-0.07250	1.01333	-0.02677	0.0	0.0	0.0
206	5	NLIF	4	1	22.34166	1.77620	5.51893	0.96990	-0.04276	-0.00205	0.97085	0.05774	0.0	0.0	0.0
207				2	22.32808	1.33181	5.41150	1.01904	-0.03363	0.01518	1.01971	-0.03966	0.0	0.0	0.0
208				3	22.32729	0.79658	5.42419	1.02086	-0.02886	0.04388	1.02221	-0.04472	0.0	0.0	0.0
209				4	22.32355	0.26516	5.40892	1.01996	-0.01835	0.06628	1.02228	-0.04487	0.0	0.0	0.0
210	5	NLIF	5	1	25.32568	1.60299	5.51299	1.03458	-0.03048	0.01250	1.03511	-0.07099	0.0	0.0	0.0
211				2	25.39319	1.19109	5.52680	1.01902	-0.02373	0.05330	1.02068	-0.04164	0.0	0.0	0.0
212				3	25.37105	0.71381	5.58322	1.01594	-0.00179	0.05088	1.01721	-0.03462	0.0	0.0	0.0

Figure 25. (Continued) Output from the sample case.

PAGE 25 3-D VISCOUS-INVISCID INTERACTIVE PROGRAM TUESDAY, APR 15, 1986

CASE TITLE: REPORT TEST CASE,TRANS. CALC., 2DSTRIP BL, M=0.6, ALPHAS ALPHA = 1.30 MACH = 0.6000
PAGE TITLE: FUNDAMENTAL FLOW SOLUTION VISCOUS/INVISCID CYCLE NO. 7

****** WARNING ****** PRINTED CP, VX, VY, VZ AND FORCES ARE COMPUTED AT OFF - BODY POINTS

PNL. NO.	SEC NO.	SEC. TYPE	IV	IU	|<---- CONTROL POINTS X	Y	Z ---->|	|<INCOMPRESSIBLE POTENTIAL FL VX	VY	VZ	SOLUTN>| VT	|<------- CPVISC	VISCOUS FLOW SOLUTION DELS	H	------>| CF
213	5	NLIF	5	4	25.38698	0.23939	5.57731	1.01413	-0.00103	0.03567	1.01476	-0.02965	0.0	0.0	0.0
214	5	NLIF	6	1	27.69252	1.51353	5.58560	0.98902	0.03070	0.04963	0.99074	0.01846	0.0	0.0	0.0
215				2	27.67360	1.13571	5.66022	0.98591	0.02010	0.04173	0.98700	0.02589	0.0	0.0	0.0
216				3	27.66954	0.68392	5.71137	0.98876	0.00774	0.05273	0.99019	0.01955	0.0	0.0	0.0
217				4	27.66939	0.23143	5.66630	0.99183	0.00289	0.03418	0.99243	0.01511	0.0	0.0	0.0
218	5	NLIF	7	1	29.62930	1.46696	5.72402	0.95142	-0.05193	0.06995	0.95540	0.08789	0.0	0.0	0.0
219				2	29.58521	1.08563	5.77759	0.96061	0.01215	0.04671	0.96183	0.07540	0.0	0.0	0.0
220				3	29.59535	0.65382	5.79646	0.96842	0.00182	0.03352	0.96900	0.06136	0.0	0.0	0.0
221				4	29.58678	0.22110	5.72153	0.97199	0.00262	0.01941	0.97219	0.05511	0.0	0.0	0.0
222	5	NLIF	8	1	33.45131	1.32301	6.00874	0.97882	-0.03100	0.07828	0.98244	0.03492	0.0	0.0	0.0
223				2	33.32368	0.99475	5.88553	0.98698	0.03491	0.02059	0.98781	0.02428	0.0	0.0	0.0
224				3	33.34593	0.60794	5.79339	0.98681	0.02723	-0.00987	0.98723	0.02542	0.0	0.0	0.0
225				4	33.33748	0.20518	5.70091	0.98630	0.01035	-0.02095	0.98658	0.02671	0.0	0.0	0.0

Figure 25. (Continued) Output from the sample case.

PAGE 26 3-D VISCOUS-INVISCID INTERACTIVE PROGRAM TUESDAY, APR 15, 1986

CASE TITLE: REPORT TEST CASE,TRANS. CALC., 2DSTRIP BL, M=0.6, ALPHAS ALPHA = 1.30 MACH = 0.6000
PAGE TITLE: INTEGRATED PRESSURES VISCOUS/INVISCID CYCLE NO. 2

TYPE	SEC	NV	CL	CD	CSF	CPITCH	CROLL	CYAW	ETA	SECTCL	SECTCD	ASTRIP	CIRCULTN
			|<------ BASED UPON INPUT VALUES OF AREF,BOV2,CREF ------>|										
****** WARNING ******			PRINTED CP, VX, VY, VZ AND FORCES ARE COMPUTED AT OFF - BODY POINTS										
LIFT	1	1	0.0039	-0.0002	0.0005	-0.0135	-0.0022	-0.0013	0.8463	0.0246	-0.0015	15.0991	-0.0058
		2	0.0207	-0.0006	0.0019	-0.0637	-0.0070	-0.0040	0.5712	0.0820	-0.0025	24.1940	-0.0165
		3	0.0484	-0.0001	0.0062	-0.1354	-0.0178	-0.0109	0.2759	0.1306	-0.0003	35.5155	-0.0310
SECT. TOT:			0.0729	-0.0010	0.0086	-0.2126	-0.0271	-0.0162					
NLIF	2	1	-0.0008	0.0010	-0.0016	0.0010	0.0005	0.0003					
		2	-0.0029	0.0009	-0.0024	0.0026	0.0015	0.0010					
SECT. TOT:			-0.0037	0.0018	-0.0040	0.0035	0.0019	0.0013					
NLIF	3	1	-0.0019	-0.0000	0.0051	0.0019	-0.0048	-0.0032					
		2	0.0037	-0.0005	0.0091	-0.0051	-0.0111	-0.0074					
		3	0.0023	-0.0000	0.0041	-0.0034	-0.0061	-0.0040					
SECT. TOT:			0.0041	-0.0005	0.0183	-0.0066	-0.0220	-0.0146					
NLIF	4	1	0.0027	0.0001	0.0033	-0.0048	-0.0058	-0.0038					
		2	0.0018	0.0000	0.0010	-0.0039	-0.0020	-0.0013					
		3	0.0026	0.0007	0.0073	-0.0057	-0.0171	-0.0111					
		4	0.0062	0.0009	0.0128	-0.0161	-0.0341	-0.0221					
		5	0.0041	0.0007	0.0080	-0.0121	-0.0244	-0.0158					
		6	-0.0004	-0.0001	-0.0008	0.0013	0.0028	0.0018					
		7	-0.0011	-0.0000	-0.0035	0.0039	0.0126	0.0081					
		8	-0.0012	-0.0001	-0.0029	0.0046	0.0115	0.0074					
SECT. TOT:			0.0148	0.0022	0.0251	-0.0330	-0.0564	-0.0367					
NLIF	5	1	-0.0007	-0.0000	0.0001	0.0013	-0.0002	-0.0001					
		2	0.0012	0.0001	-0.0001	-0.0024	0.0003	0.0002					
		3	-0.0002	-0.0000	-0.0001	0.0005	0.0002	0.0001					
		4	-0.0015	0.0000	-0.0003	0.0041	0.0009	0.0006					
		5	-0.0024	0.0000	0.0000	0.0074	0.0000	-0.0000					
		6	0.0005	-0.0000	0.0000	-0.0017	-0.0001	-0.0001					
		7	0.0027	-0.0001	-0.0000	-0.0099	-0.0000	0.0000					
		8	0.0022	0.0000	-0.0007	-0.0089	0.0027	0.0017					
SECT. TOT:			0.0018	0.0000	-0.0011	-0.0096	0.0037	0.0024					
CONFIG.TOT:			0.0899	0.0026	0.0469	-0.2583	0.0040	0.0639					

************ ************ ************

Figure 25. (Concluded) Output from the sample case.

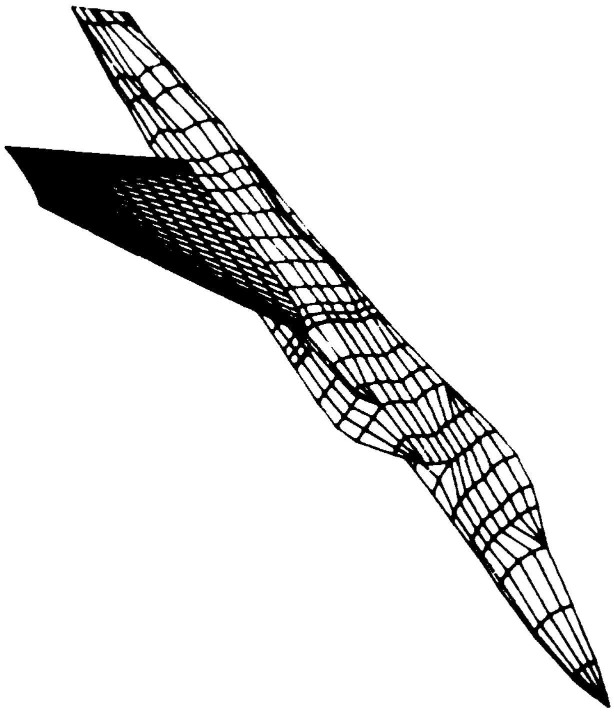

Figure 26. Panel arrangement for test case 1.

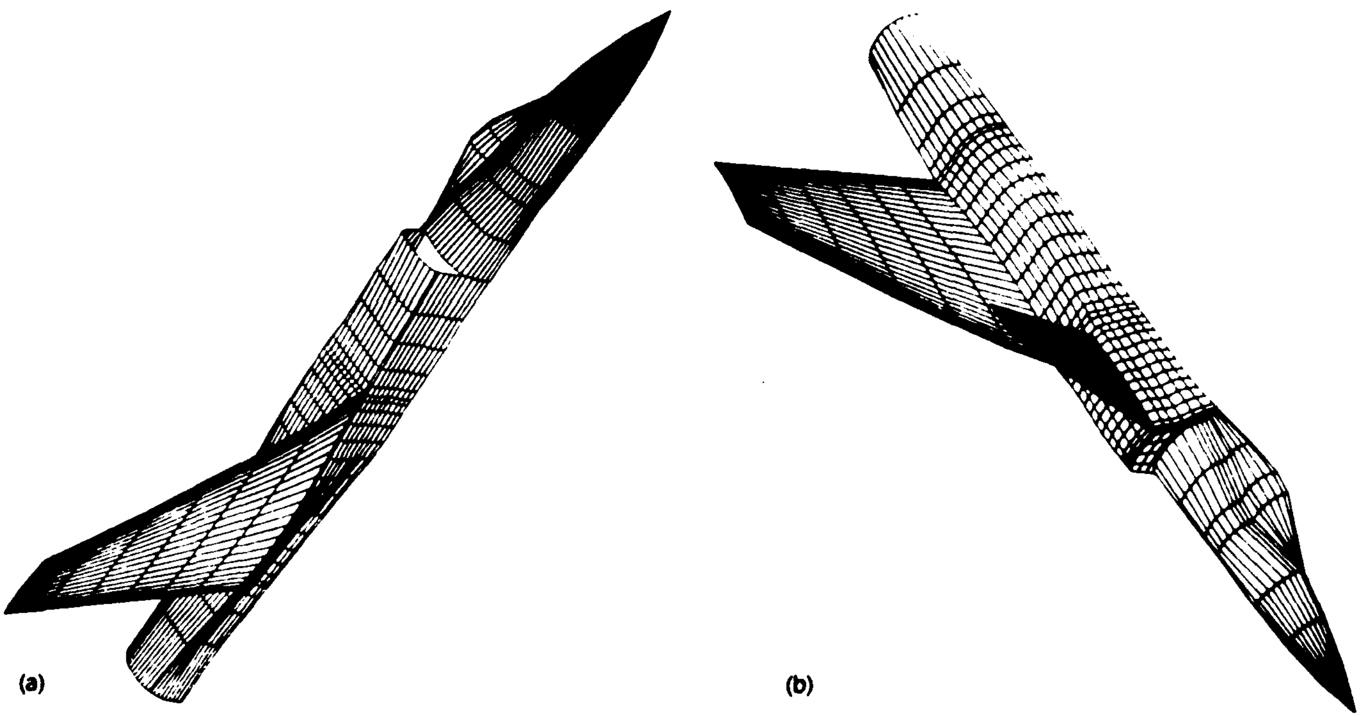

Figure 27. Panel arrangement for test case 2, (a) without canard, (b) with canard.

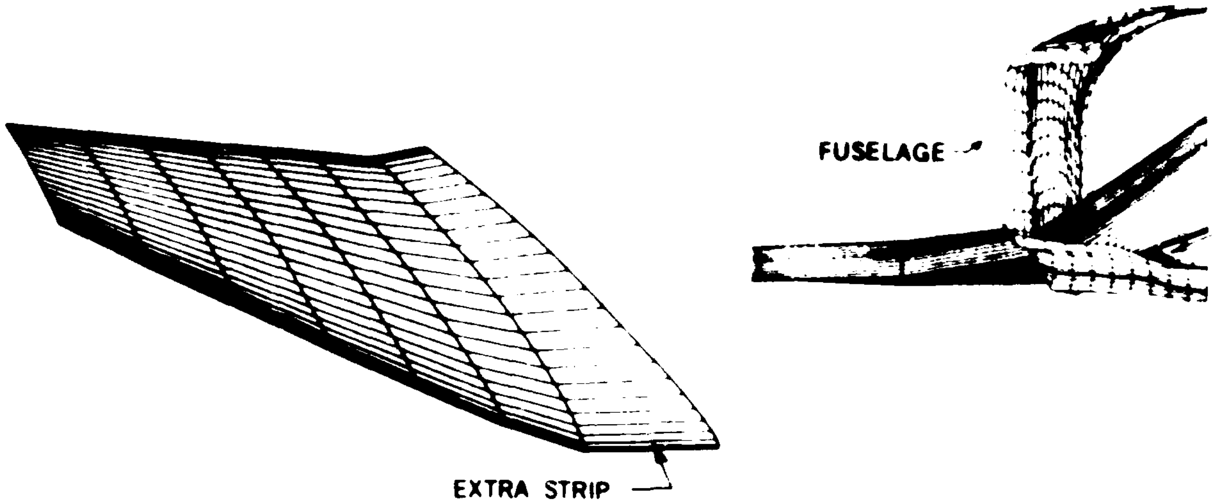

Figure 28. Panel arrangement of the wing for test case 2.

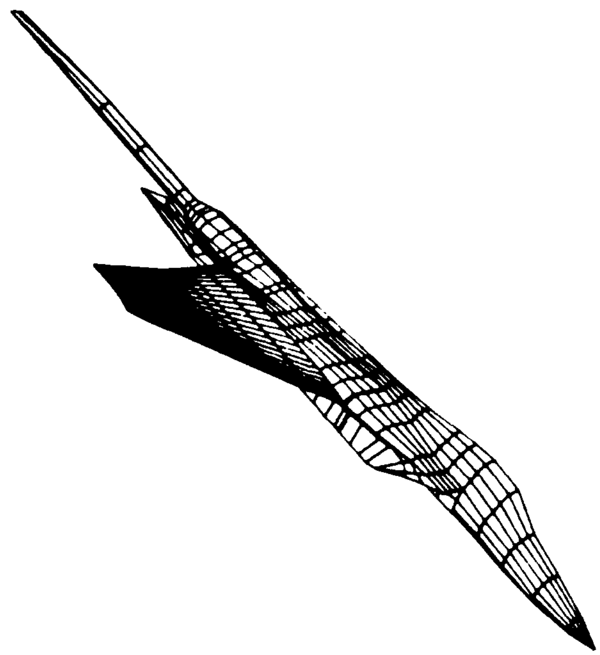

Figure 29. Panel arrangement for test case 3.

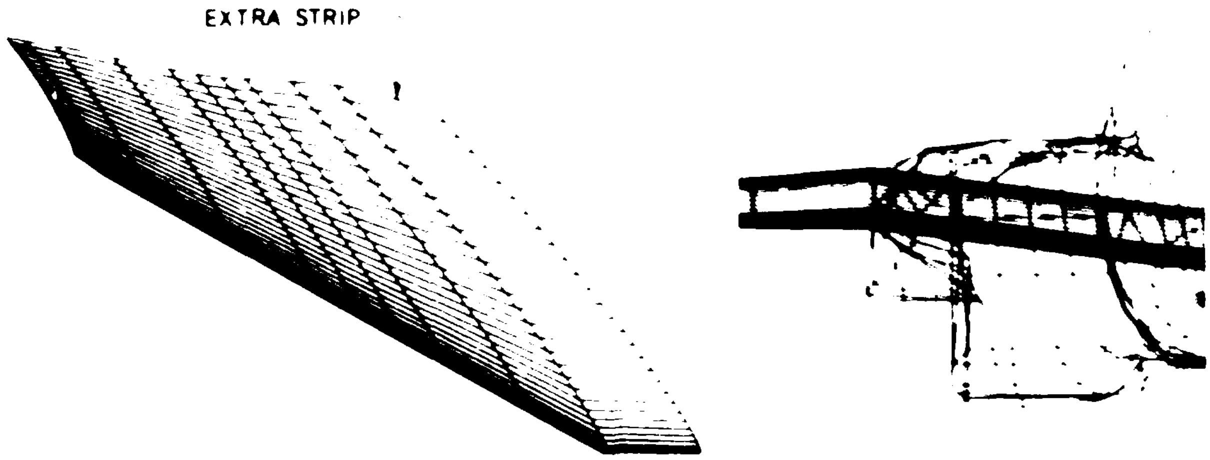

Figure 30. Panel arrangement of the wing for test case 3.

U.S. Government Printing Office 1987 748-061-60751

END

6-8

D